Data assimilation

Application of a particle filter on bathymetry simulations by the morphological model Delft3D

D. Bode

Technische Universiteit Delft

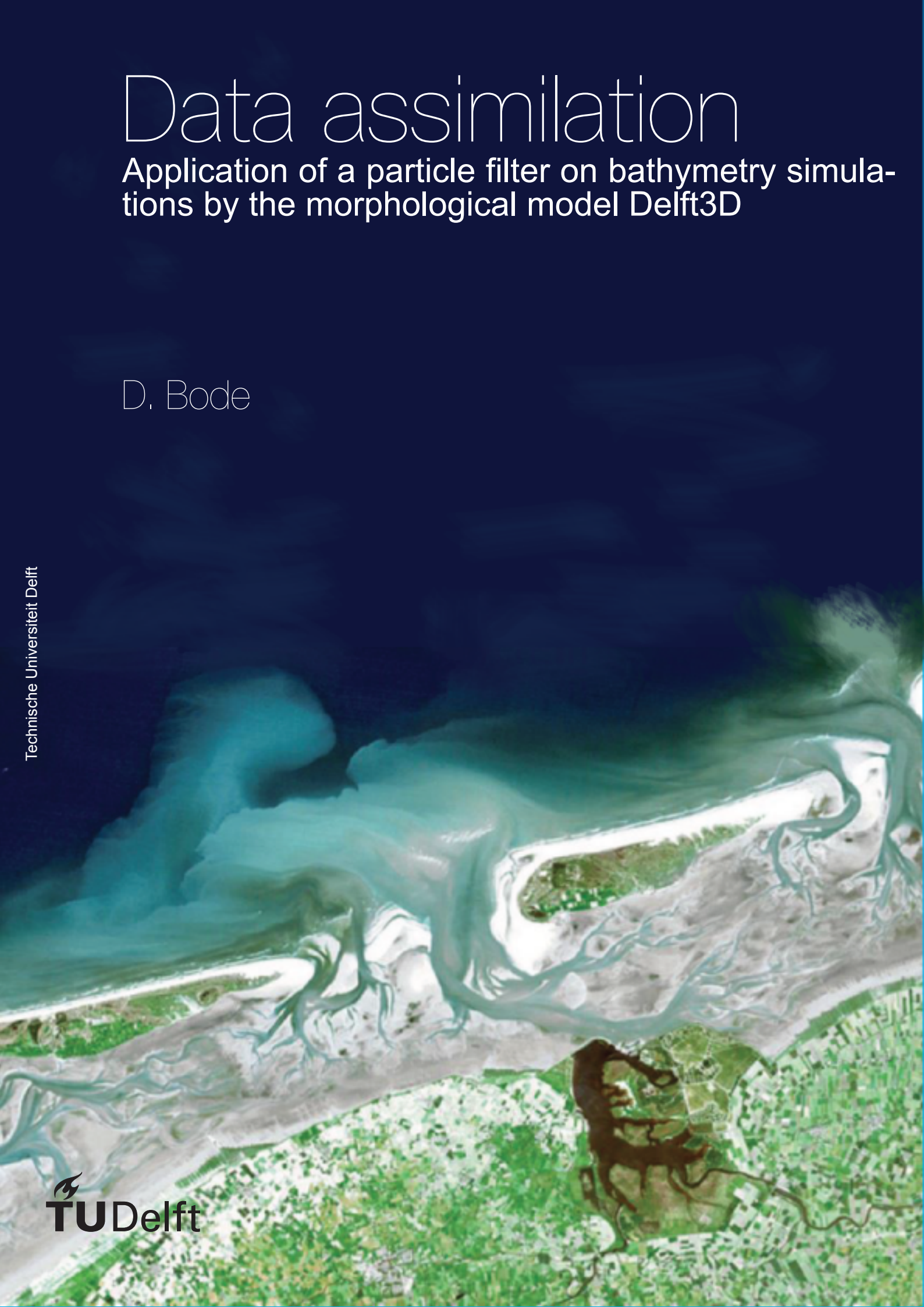

TU Delft

Data assimilation

Application of a particle filter on bathymetry simulations by the morphological model Delft3D

by

D. Bode

to obtain the degree of Master of Science
at the Delft University of Technology,
to be defended publicly on June 19, 2020 at 15:00 AM.

Student number:	4226933	
Project duration:	August 1, 2019 – June 19, 2020	
Thesis committee:	dr. R.E.M. Riva,	TU Delft
	dr. ir. F.C. Vossepoel,	TU Delft
	dr. H. van der Vegt,	Deltares
	prof.dr.ir. Z.B. Wang,	TU Delft and Deltares

An electronic version of this thesis is available at `http://repository.tudelft.nl/`.

TU Delft

Preface

I have written this report to finish my study in Geoscience and Remote Sensing at the University of Technology in Delft. Successfully finishing this project would not have been possible without the help of some people. First of all, I would like to thank my committee; Riccardo Riva, Femke Vossepoel, Helena van der Vegt and Zheng Bing Wang. In every meeting you helped me forward, by asking questions, suggesting new methods and giving your opinions. Femke, thank you for helping to set up the research and for sharing your knowledge on data assimilation. I would like to thank Helena for making time for meetings and helping me to rephrase the focus of my research when needed. And of course for checking up on me to see if I was not crying in the corner of my room during Corona times. (I was not). This thesis marks the end of my time as a student and I would like to thank my friends for making this time so much fun. And for these last months in quarantine times, I want to thank my roommates Jiska, Marjolein and Ellen for being so positive and musical. Lastly, I want to thank my parents and sisters. Thank you, mum and dad, for supporting me, whether it is during my rowing races, my board year or my thesis. And thank you Marieke, Suzanne and Beate for being an example to me, each of you in your own way.

D. Bode
Delft, June 2020

Summary

Predictions of the morphology of coastal areas are used to make decisions on coastal defence and nature conservation. To predict this morphology, simulations made by morphological models are used. To base decisions on this morphology predictions, we want the uncertainties in these predictions to be small. The goal of this research is to get a better insight in the uncertainties in a morphological model. By having a better understanding of these uncertainties, the decisions made using modelled predictions are stronger substantiated. The specific area focused on in this research is the Frisian Inlet, which is located between Ameland and Schiermonnikoog in the Wadden Sea. To achieve the goal of this research, data assimilation is used. Data assimilation combines data with prior knowledge of a model to find the distribution of probabilities of estimates of a true state. In this research, the used data are bed level measurements and the estimates are simulations for the bed level height made by Delft3D.

Data assimilation methods make use of a distribution of model outcomes which should cover all possible outcomes. So, to set up data assimilation successfully, we want to use a parameter that induces a significant change in the bathymetry outcomes of Delft3D. Therefore, a sensitivity study is performed which considers the following six parameters: current related roughness, wave related roughness, wave-related suspended load sediment transport factor, wave-related bedload sediment transport factor, the transverse bed slope and the tidal amplitude. For each parameter, ten values are chosen to simulate. Which of the parameters induces the most change in bathymetry is assessed, using the difference between simulation result and the observation and the mean squared error skill score. The transverse bedload slope (α_{bn}) shows the most variation and is further used in the data assimilation method, which is a particle filter. Hundred uniformly distributed values of α_{bn}, between 0.5-100, are used to create different Delft3D simulations that give a bed level prediction. This initial distribution is used for three different periods: 1970-1975, 1975-1979 and 1979-1982. These epochs are defined by the availability of bed level measurements. After one iteration of the particle filter, a new distribution of the parameter values is found. This is used in the next iteration in the same epoch. In each epoch, three iterations are made.

The methodology as described in this thesis leads to a convergence of the initial distribution. In epoch 1 and 3, the distribution focuses on values of α_{bn} in the high range of the initial distribution. The resulting distribution of epoch 2 focuses on values around α_{bn} of 70.

This study shows that it is possible to get a better understanding of the distribution of α_{bn} values that leads to probable bedlevel predictions by applying a particle filter. The application of this method brings the simulations closer to each other, but the simulations did not get closer to the observations. The contribution to our understanding of data assimilation for morphodynamic models is that it can be used as a calibration tool for a specific parameter.

List of abbreviations

α_{bn} transverse bedload slope. v, ix–xi, 25, 26, 28–31, 33–41, 43–48, 50–55, 57–59

$4D-Var$ four dimensional variational data assimilation. 3

A tidal amplitude. 29

$BedW$ wave-related bedload sediment transport factor. 29–31, 53, 57

DA data assimilation. 1, 3, 10, 30, 31

$KNMI$ Koninklijk Nederlands Meteorologisch Instituut. 22

LOL Landelijk Opslagsysteem Lodingen. 17

MF morphological acceleration factor. 8, 22

MSE mean squared error. 9

$MSESS$ mean squared error skill score. 23, 24, 29, 54, 58, 65, 66

PDF probability density function. ix, 12–16

PF particle filter. 14

RDC current related roughness. 29, 30, 57

RDW wave related roughness. 29–31, 53, 57

$RMSTE$ root mean squared transport error. 58, 66

$SusW$ wave-related suspended load sediment transport factor. 29, 30, 57

List of Figures

List of Tables

Contents

1 Introduction

Morphological models simulate the transport of sediment and the locations where erosion and sedimentation take place. In this way, it is possible to predict what the bathymetry will look like in the future. The prediction of future morphology The input parameters for morphological models have uncertainties, which influence the uncertainty of the model prediction. To use the model predictions for management decisions for coastal areas, it is necessary to know how well the predictions represent the observations. The quantification of the uncertainties in model predictions helps to define the quality of the bed level predictions. Data assimilation is a process to combine observations with dynamic numerical models and is used to quantify the uncertainties in the input and output of a model. The quantification of uncertainties is a first step towards more reliable model predictions. The monitoring and predicting of coastal changes are considered in this research by performing a case study on a tidal inlet in the Dutch Wadden Sea. The Wadden Sea contains the largest tidal flat area in the world [Wang et al., 2018] and is recognized as a UNESCO world heritage area [Wang et al., 2012]. One of the reasons why it is a UNESCO world heritage area is its unique ecology, needed by certain species as living habitat. The unique ecology is vulnerable to external changes in sea level rise [Kirwan and Megonigal, 2013]. Besides its ecological value, the area is of economical importance due to tourism, recreation and salt and gas extraction. The gas extraction causes subsidence and this affects the dynamics of the Wadden Sea region [Fokker et al., 2018]. Since the area is vulnerable to external changes, this could influence the characterizing occurrence of tidal flats.

Research objective

The objective of this research is to find the probabilities of possible outcomes of the morphological model given the model uncertainties, bed level data and data uncertainties. Knowing the probabilities of possible outcomes leads to a view of what model outcomes bear the largest uncertainties and in what outcomes the uncertainty is lower. When the distribution of uncertainties in the model outcomes is better known, possible decisions based on these predictions are better substantiated. The forecast horizon might increase by applying data assimilation (DA), because a prediction further in time is more valuable with uncertainty information. For a user of the morphological model, the model outcome will bear more information. It does not only show the modeller what bed level is predicted, but also if this is a bed level prediction that is in an uncertain range of the possible model outcomes. Data assimilation is used to combine the model with data, given uncertainties in both model and data. By making multiple simulations with different model input, a DA method can steer towards the outcome with a higher probability, relative to the other outcomes, given the model and measurement uncertainties. In this way, the model will be calibrated to find the most probable outcome for the varied setting.
When the objective of this research is achieved, there is a probable outcome of the morphological model and area of interest considered in this report and a method to fine-tune the results in other situations in morphological models as well. In section 1 the research question and sub-questions are defined and these will be used to decide what is the best way to apply data assimilation on the model and data.

Figure 1.1: Satellite image of the Wadden Sea from www.waddensea-worldheritage.org . In the white square is the area of interest of this research.

Case study

Delft3D, an open-source morphological model developed by Deltares, is used to simulate the Frisian inlet in the Wadden Sea. This area is very well studied [Elias et al., 2012, Oost and de Haas, 1996, Van Prooijen and Wang, 2013, Vermeersen et al., 2018, Wang et al., 2018] and there is data available on the bed level in a suitable temporal resolution, which varies from three to five years between measurements. Although the area of the case study is limited to a tidal inlet in the Wadden Sea, the methods used in this area can be applied to other areas and other morphological models as well. The Frisian Inlet is the tidal inlet between the islands of Ameland and Schiermonnikoog. In the South of this basin, there is the Lauwers Lake. The Lauwers Lake used to be the Lauwers Sea, before its closure in 1969. As a result of this closure, the tidal basin became smaller. This perturbed the morphological equilibrium, providing a clear sediment signal. It is expected that this signal continues to evolve until a new morphological equilibrium is reached. Following the rearrangement of the morphology to account for the perturbation makes the period after the closure of the Lauwers Lake an interesting case-study. That is why this tidal inlet is chosen and it will be modelled during the period just after the closure of the Lauwers Sea.

Figure 1.2: Satellite image of the Frisian inlet

Relevant previous research

Data assimilation is used in different fields such as oceanography [Bertino et al., 2007, van Velzen et al., 2016, Vossepoel and van Leeuwen, 2007], geophysics [Van Leeuwen, 2010, 2009] and meteorology [Ghil and Malanotte-Rizzoli, 1991]. These researches will be discussed in a bit more detail in Chapter 2.4.

A very relevant previous research is performed by Garcia et al. [2013]. In this research four dimensional variational data assimilation (4D-Var) is the DA method that is applied on the morphological model Delft3D. The applicability of 4D-Var is assessed, by focusing on the parameters of wave direction, significant wave height and wave peak period. These parameters characterize the nearshore bathymetry of the area of interest of the research, which is Palm Beach located in the Northern area of Sydney.
In the research presented in this report, the Wadden Sea is considered in a case study. The Wadden Sea acts as a buffer between the North Sea and mainland. The fact that the East Frisian part of the Wadden sea plays an important role in this exchange between coastal and open-ocean environment, makes it an interesting research area. In Wang et al. [1995] a first set-up of a dynamic model for morphological development in the Frisian Inlet is made. Since that research, many studies have contributed to an extensive understanding of the morphodynamic behaviour of the Frisian Inlet [Dissanayake et al., 2009, Oost and de Haas, 1996, Stanev et al., 2003, Wang et al., 2018]. However, there are still some knowledge gaps. For example, there is still uncertainty in the future development of sediment volumes and nourishment strategies and a better understanding of sediment fluxes is needed. This can be achieved by performing a morphodynamic analysis of relevant processes and mechanisms in the Wadden Sea. Besides, the monitoring of the morphological and sedimentological development needs further research, which is challenging because sea-level rise and morphological developments both concern slow, long-term processes [Wang et al., 2018].

Research question

The main question of this research is to find the most probable outcome of a morphological model. To find this a distribution of probability for many model outcomes is needed and the methodology to do so is described in this research.

What is the most probable outcome of a morphological model given the model uncertainties, bed level data and data uncertainties?

To find a distribution of the probability of the model outcomes, two subquestions need to be answered. In subquestion 1 the goal is to find a parameter that influences the simulated bathymetry. A parameter that induces a significant change in the bathymetry of a morphological model is needed for the DA. More variation in the model outcomes gives a better set of possible outcomes to work within DA. To answer the first subquestion, a sensitivity study is performed.
Data assimilation is a broad concept and in the answer to the second subquestion it needs to be specified. Which method is applied and how is the parameter of sub-question 1 implemented in this method. Another thing that needs to be answered is in what time frame and in what area the data assimilation will be applied.

1. *Which parameters induce a significant change in the bathymetry of a morphological model?*
2. *How can data assimilation be implemented to optimize a morphological model output based on bed level measurements?*

Thesis outline

To answer the questions stated above, bedlevel data is used. This data is measured in the Frisian inlet in 1970, 1975, 1979 and 1982. During this period the case study is performed, using Delft3D simulations. The DA method used in this research is the particle filter and to apply this one parameter will be varied. This parameter is found by performing a sensitivity study, which answers subquestion 1.
This thesis contains six chapters, which will all contain a part focused on subquestion 1 and a part focused on subquestion 2. Following this introduction, background information that is relevant for this research is given in Chapter 2. In the part dedicated to subquestion 1, the Wadden Sea area and in this region the Frisian inlet are introduced, together with important morphodynamic processes. This information combined with background on morphological models, will help to find possible parameters to use in the sensitivity study. Also, methods to quantify the uncertainties in model predictions are discussed. This is used to determine how the sensitivity study results are assessed. To know how data assimilation can be implemented, the aim of data assimilation is explained in the subquestion 2 part of the Chapter. The process that leads to the results of data assimilation is also discussed.
In Chapter 3 the methodology to get the answers on the subquestions is described. This methodology contains an explanation on the model set-up, the contribution parameters, the quantification methods, DA

methods and how they are applied specifically on the area for this research.
In Chapter 4 the results are presented. These results are further discussed in Chapter 5 and conclusions are drawn and presented in Chapter 6. The conclusion is followed by recommendations, given in Chapter 6 as well.

2

Theory

Subquestion 1

Which parameters induce a significant change in the bathymetry of a morphological model?

An important factor to answer the research question of this thesis is the parameter used in the data assimilation. This parameter should have a significant influence on the evolution of the bathymetry. So, in this chapter an analysis of the sensitivity of the simulation of bathymetry to model parameters is described. The chapter starts with background information on the area of interest and relevant morphological processes.

2.1. The Dutch Wadden Sea

The Wadden Sea is the region of the North Sea at the North Coast of the Netherlands and Germany and the West coast of Denmark, as shown before in Figure 1.1. The Dutch part of the Wadden Sea consists of five islands, which are the barrier islands that separate the Wadden Sea from the North Sea. The barrier islands are part of a bigger coastal system that consists of six different environments: the mainland, back-barrier lagoon, inlet and inlet deltas, barrier island, barrier platform and the shoreface [Oertel, 1985]. In Figure 2.1 this coastal system is shown, where the mainland is named coast and the back-barrier lagoon is the basin. The barrier islands have a protective function for the basin and the mainland. The islands provide protection against storm destruction of the mainland and they protect ecological habitats of the basin and form a protection for the coast of the mainland [Otvos, 2012].

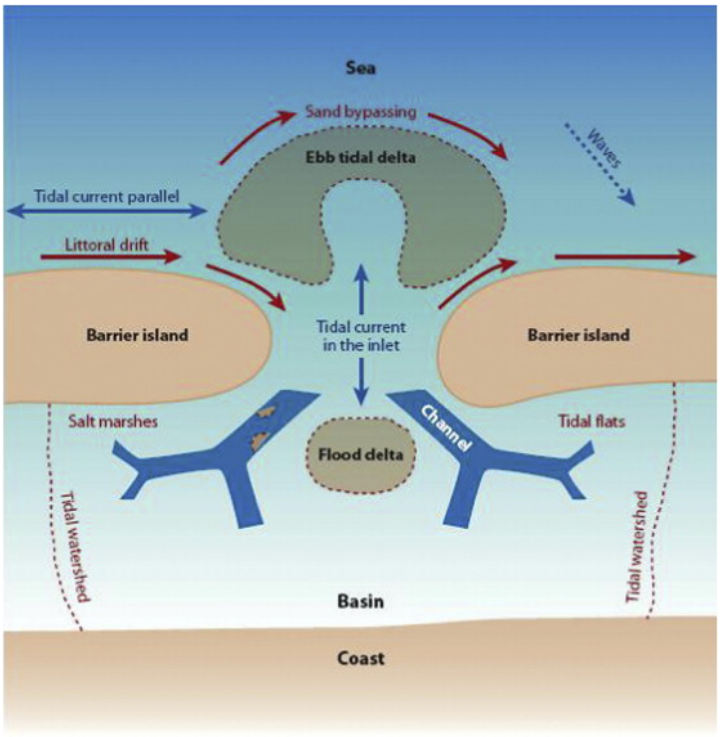

Figure 2.1: Schematic sketch of a tidal inlet system, with different morphological elements and dominant physical processes and phenomena (Source:De Swart and Zimmermann,2009).

Morphological features that are part of the tidal barrier system are the tidal watersheds, tidal channels, tidal flats and salt marshes. A tidal watershed is a topographic high that limits, but does not exclude, the exchange of water between two sub-basins [van de Kreeke et al., 2008]. Sediment can flow between the basin and the sea through the tidal channel. Tidal flats can be defined as a sandy to muddy or marshy flat that emerges during low tide and submerges during high tide [Amos, 1995]. Tidal channels are defined to be below the low tide water level, so this is a part of the basin that is always submerged.
Since the definition of a tidal flat and a tidal channel take the water level into account, a sea-level change influences the distribution of tidal flats and tidal channels. Whether this results in a drowning system or not, depends on the sea-level change and the sediment supply from the sea to the basin. When the sediment supply increases in balance with an increase in sea level, the tidal system will be in equilibrium. When the sea level rise reaches a certain limit where the sediment supply can not increase at the same rate, the system is not in equilibrium anymore. This will lead to the drowning of a tidal inlet system [Van Goor et al., 2003]. The sediment supply to the Wadden Sea comes from the flow from the North Sea through the tidal inlets. The only freshwater influence is from the Ems Estuary and Lake Ijssel at the Texel Inlet, which is the inlet between the mainland and Texel [Wang et al., 2012].
In Wang et al. [2018] it is stated that in a sub-system of a sedimentary system it is desired to reach a dynamic equilibrium between its morphology and the forcing conditions. A distortion of an equilibrium can be natural or man-made and will induce a sediment transport that restores the equilibrium state. Factors that play a part in the equilibrium are accommodation space and sediment supply. Accommodation space is the space that is available for sediment to be deposited. Sediment supply is all the sediment that is delivered to the accommodation space.
A dynamic equilibrium exists when the sediment flux in the basin is balanced by a source or sink term [Zhou et al., 2017]. For example, a net import of sediment in a back-barrier basin can be balanced by subsidence of the bed. Thus, there is an equilibrium between an increase in the accommodation space and an increase in the sediment supply. The time scale on which an equilibrium is restored depends on the spatial scale of a morphological element. An individual channel may find its equilibrium in days to decades, whereas the total Wadden Sea may need centuries to millennia to reach an equilibrium [Wang et al., 2018].
In the Frisian inlet, a dynamic equilibrium between its morphology and the forcing conditions has been disturbed by the closure of the Lauwers Sea. This closure was finished in 1969 and 30% of the former basin area was dammed off, which reduces the volume of the tidal prism from 306 million m^3 to 200 million m^3 [Oost

and de Haas, 1996]. The closure of the Lauwers Sea in 1969 results in changes in sediment transport. These changes will result in a clear sediment signal when simulated in morphological models.

2.2. Morphodynamic processes

Morphology refers to the study on the shape, which in this case is the shape of the bedlevel. Morphodynamics describes how this shape changes over time as a result of sediment transport. Sediment transport is caused by the movement of water which can take sand or mud grains with its stream. The transport can take place as bedload transport or suspended load transport. In a high turbulent flow, there is sufficient upward motion to keep small particles in the moving fluid. This results in transport that takes place in suspension [Nichols, 2009a].

Bedload is larger sediment that is transported in the water by rolling and saltation. When the velocities in water are low, only fine particles and low-density particles can be in suspension [Nichols, 2009a]. This leads to a dominant role for bedload transport when the flow velocities are low and the grain size of the particle is large [Fiechter et al., 2006]. When there are high flow velocities and small grain sizes, the suspended transport becomes more important. When the flow velocity gets too low, the particles will fall out of suspension and settle on the bed [Fiechter et al., 2006]. Bedload that is transported will also settle when the flow velocity decreases. When and where the settling of sediment occurs determines the morphology of the bed.

For sediment to be deposited, it first needs to be eroded from a different location. Erosion is the removal of the loose deposits covering solid rock. The loose material can be moved by gravity when it is at a slope, it can be washed by water, blown away by wind or scoured by ice [Nichols, 2009b]. Multiple processes can influence the sediment transport in rivers, estuaries and tidal inlets. The processes and mechanisms that are dominant in the sediment-sharing system of the Wadden Sea are residual flow, tidal asymmetry and dispersion [Wang et al., 2018]. The explanations about these terms are based on the descriptions given in Wang et al. [2018].

Residual flow is a process where the sediment transport is in the same direction as the tidal flow. So, the sediment transport is strengthened by the tidal waves. It can be caused by meteorological effects, freshwater input and compensation flow caused by Stokes drift. A meteorological effect is caused by wind, which influences hydrodynamics in the Wadden Sea. Freshwater input causes a residual flow towards the sea. Stokes drift causes a landward water flux in the Wadden Sea, which is compensated by a seaward-directed residual flow.

When a tidal wave propagates in shallow water, it can deform. This deformation results in tidal asymmetry, which can form a flood-dominant system or an ebb-dominant system. In a flood-dominant system, the time it takes to reach the maximum flood level is short, whereas it takes relatively long to get to the minimum ebb water level. Therefore the period of flood is longer with a smaller peak velocity than the period and peak velocity of the ebb period. It is the other way around for an ebb-dominant system. The closure of the Lauwers Sea changed the situation in the tidal asymmetry. As seen in Figure 2.2 the flow velocity is decreased after the closure. Furthermore, the velocity during ebb is smaller than the velocity during flood. This change from a symmetric system to an ebb-dominant system causes a sediment import into the basin [Wang et al., 2018].

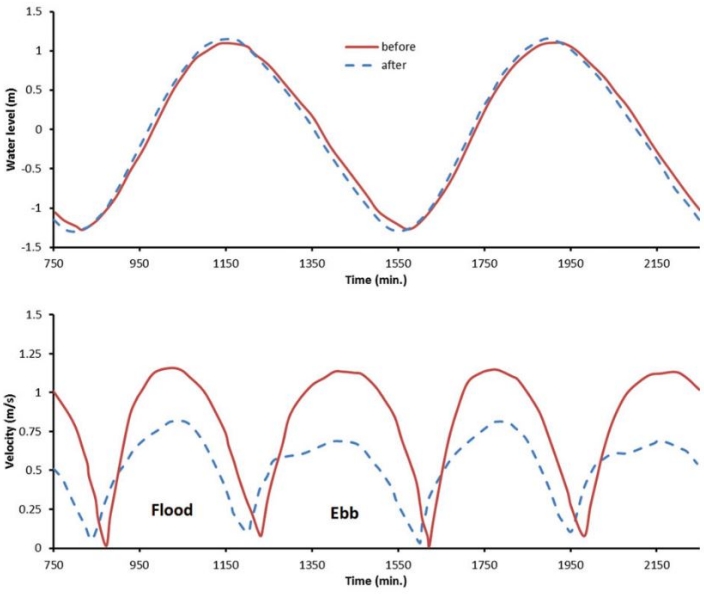

Figure 2.2: The water level and flow velocity in the Frisian inlet and the influence of the closure of the Lauwers Sea, from [Wang et al., 2018]

Two other forms of asymmetry are jet-flow asymmetry and spatial asymmetry. The jet-flow asymmetry is caused by a high velocity of the incoming flow jet, which causes erosion of the inlet. The eroded material is deposited in the far region of the jet. When the tide turns, water is flowing out of the basin through the inlet again. The velocity is more evenly distributed, which means the maximum velocity is smaller. For these

smaller velocities, it is not possible to transport all the far deposited sediments back to the inlet. So there is more sediment coming into the basin than is transported out again. Spatial asymmetry means that within one basin there can be a part ebb-dominated and a part flood-dominated. As a result, a net flux from one side to the other side of a basin occurs. In the Wadden Sea, this happens in the Texel Inlet, where a net flux emerges from the Southern shore. This is a result of flood current dominating the southern part of the inlet while the northern part of the inlet is ebb-dominant.
Dispersion takes place when the tidal flow acts as a mixing agent for dissolved and suspended matters. The result is a residual transport in the opposite direction of the concentration gradient. The decrease in flow velocity after the closure of the Lauwers Sea influences the dispersion. It results in an import of sediment in the tidal basin [Wang et al., 2018].
The timescale on which morphodynamic processes take place depends on the process and the spatial scale of the morphological element. The timescale of a morphodynamic process increases when the size of the morphological element is larger. Some morphodynamic processes occur on timescales of individual storm events. Examples of such processes are waves, currents, sediment transport, and morphological change. Whereas processes like the migration of bars or the evolution of the profile cross-shore can occur on larger timescales [Aagaard et al., 2004].

2.3. Morphological modelling

To get a better understanding of the situation in the Wadden Sea and how the current situation will evolve, a model to simulate the situation have been built. Models can be empirical or process-based and to describe the specific features for both options, an example of an empirical model and an example of a process-based model will be discussed. An empirical model is based on experimental results and observations, whereas a process-based model uses a mathematical representation of physical processes to describe a certain system. An example of an empirical model is ASMITA, which is based on the idea that a tidal basin can be sub-divided into several geomorphologic elements [Townend et al., 2016b]. The state of each element is described by its volume and surface area and empirical relationships define the morphological equilibrium for the elements [Townend et al., 2016b]. ASMITA is limited in the level of detail that it simulates.
For more detailed simulations, Delft3D is suitable. Therefore, the process-based model Delft3D is used in this research to make a representation of the morphodynamic system in the Frisian Inlet. Delft3D uses physical processes to describe hydrodynamics, sediment transport and morphology and water quality for fluvial, estuarine and coastal environments [Deltares, 2018]. The sediment transport can not be modelled grain-to-grain. Thus the sediment transport equations used in the model are derived with a level of empirical modelling. The result is a representation of the morphodynamics which should resemble the reality. It is focused on fast-scale processes and aims to capture the details of the bedlevel change [Townend et al., 2016a]. This research aims to capture details in a restricted area, so Delft3D is suitable.
For the formulation of the exchange between the bottom sediment and the water column, a bottom boundary condition is used in Delft3D. This is derived from an asymptotic solution of the advection-diffusion equation [Townend et al., 2016b]. Information about sediment composition, wave conditions, tidal forcing, time scales and transport models is used as model input. Numerical parameters as input are for example the morphological acceleration factor (MF) or the simulation time. The MF is a scaling factor between the hydraulic and morphological simulation. Hydraulic processes usually take place on a smaller timescale than morphological processes. The MF is used to accelerate the morphological simulation to see changes without having to simulate a very long timescale. When a MF of 10 is used and 1 tidal cycle is simulated, then the morphology at the end of the run is the result of 10 tidal cycles. The MF needs to be as high as possible for the simulation, but still give a model result within an acceptable level of accuracy. So, this critical value of MF needs to be found.
Physical parameters as input need to represent the relevant physical processes well. Physical parameters that are always needed are constants like gravity, temperature, air density, salinity and water density. Furthermore, the bed and wall roughness, the horizontal and vertical eddy viscosity and diffusivity are always needed as input. Other physical parameters that can be added are concerning the temperature process, sediment process, wind process or tidal forces [Deltares, 2018]. In section 3.2.1 a description will be given on what parameters need to be added to perform this research.
Previous studies show that Delft3D can make robust and accurate predictions for hydrodynamic results [Elias et al., 2000, Hsu et al., 2006, 2008]. The ability to do the same with predictions for morphological results is not evaluated or validated yet.

Parameters

From previous sensitivity studies, it is seen that the initial bathymetry, frictional parameterization, sediment transport and bed slope terms influence the determination of the morphodynamic evolution [Zhou et al., 2014]. There are significant effects of slope parameterization on the resulting simulated morphology. When physically correct slope effects are used, it is seen that models show a deep incision and steep morphology. This results in different channel networks than are typically observed in nature. The modelled channel networks have deep and narrow channels and a larger number of channels and shorter bars compared to observations in nature. In nature, channels form when minor perturbations on a flat bed grow. Whether or not these small perturbations grow or decay, depends on the width-to-depth ratio. In Delft3D the slope effect is represented by a parameter that determines the magnitude of the transverse slope effect [Baar et al., 2019]. Besides, the roughness of the bed influences the flow of water in different ways for different areas. For example, in an open-channel flow, an increase in bed roughness leads to the formation of an internal boundary layer [Chen et al., 2003]. In high-gradient streams clasts that are large compared to the stream depth, can act as obstacles to the flow [Wiberg and Smith, 1991]. The flow velocity in rills is seen to be highly slope-dependent [Giménez and Govers, 2001]. In Delft3D there is a parameter that represents wave-induced bed roughness and a parameter that represents current-induced bed roughness.

Mean squared error skill score

Previous studies on morphodynamics use the mean squared skill score as a way to characterize uncertainties when quantifying bathymetry changes [Henderson and Allen, 2004, Ruessink and Kuriyama, 2008, Sutherland et al., 2004, Van Der Wegen et al., 2011, van Rijn et al., 2003]. This skill score uses the mean squared error to measure the relative accuracy of a prediction over a prediction of zero change [Bosboom et al., 2014]. In this study, a prediction is a model simulation and a prediction of zero change would be the observation that is used as an initial bathymetry. E.g. in a simulation that runs from 1970-1975, the prediction of zero change is the 1970 observation. To apply the skill score, first the accuracy measure mean squared error (MSE) is calculated using equation 2.1. For each model grid cell, a weight is determined, using the size of the grid cell. The larger the grid cell, the larger the assigned weight. In each grid cell, the difference between the prediction and the observation is determined, which is the error. In the simulation that runs from 1970 to 1975, the observation is the 1975 observation. The error of each grid cell is squared and multiplied with the weight of that grid cell and divided by the total number of grid points, to obtain the mean squared error. The mean squared error can also be calculated using anomalies, showed as p' and o' in equation 2.1. The anomalies are the differences between the prediction or observation concerning the reference. The mean squared error is calculated for the reference prediction as well, as shown in equation 2.2. The angular brackets indicate the spatial average. The reference prediction used in the calculation of skill score is a zero-change prediction. The skill score is then calculated as the relative accuracy over the reference prediction, as shown in equation 2.3. The value of the skill score can range from -∞ to 1. A score of 0 means that the prediction is as good as the reference. When there is no difference between a prediction and observation the skill score is 1. A skill score between 0 and 1 shows the proportion of improvement over the reference prediction. Negative values are found for predictions that perform worse than the reference prediction. One value for the skill score is found for a prediction.

$$MSE = \frac{1}{n}\sum_{i}^{n} w_i (p_i - o_i)^2 = \langle (p' - o')^2 \rangle \tag{2.1}$$

where:

MSE = mean squared error

n = number of points in the spatial domain

i = ith grid point

w_i = weighting factor by ith grid cell size

p_i = predicted field for the ith grid cell

o_i = observed field for the ith grid cell

p' = difference of prediction with respect to the reference

o' = difference of observation with respect to the reference

$$MSE_{ref} = \langle (r-o)^2 \rangle = \langle o'^2 \rangle \tag{2.2}$$

where:
MSE_{ref} = mean squared error of the reference prediction
r = reference prediction
o = observation
o' = difference of observation with respect to the reference

$$MSESS = 1 - \frac{MSE}{MSE_{ref}} \tag{2.3}$$

where:
$MSESS$ = mean squared error skill score
MSE_{ref} = mean squared error of the reference prediction
MSE = mean squared error

Subquestion 2

How can data assimilation be implemented to optimize a morphological model output based on bedlevel measurements?

2.4. Data assimilation

In Wikle and Berliner [2007] multiple definitions of DA are combined to the working definition: "DA is an approach for fusing data with prior knowledge to obtain an estimate of the distribution of the true state of a process". The goal of DA is to make a more accurate representation of a process. In this research, this process is the evolution of bathymetry and therefore bedlevel data is used. The data is fused with prior knowledge, which is the knowledge about the probability distribution of the model. The combination of the prior knowledge and the bedlevel data should result in an estimate of the bathymetry. Data assimilation is used in oceanography [Bertino et al., 2007, Dobricic and Pinardi, 2008, Tuan Pham et al., 1998, van Velzen et al., 2016, Vossepoel and van Leeuwen, 2007], geophysics [Nakano et al., 2007] and meteorology [Ghil and Malanotte-Rizzoli, 1991]. In Scott and Mason [2007] an optimal interpolation method is applied on a morphological model with success. In this research waterline, movement data is used and the advice is to use data assimilation in other coastal and morphological models as well. Also, in van Dongeren et al. [2008] data assimilation is successfully applied. In this case to make accurate predictions on subtidal bathymetry. The techniques used in these studies are different than the data assimilation technique used in this research, which is the particle filter. In van Dongeren et al. [2008] an optimal least squares estimator approach is used to predict nearshore subtidal bathymetry. In Vossepoel and van Leeuwen [2007] the particle filter is used, but is applied on a global ocean general circulation model. The difficulty in the application on a morphological model is that the morphodynamic changes are cumulative [Cowell and Thom, 1994]. In Bertino et al. [2007] an extension of the Ensemble Kalman filter is presented and applied in a simplified ecological model. In Nakano et al. [2007] a merging particle filter is presented and its application for predicting geophysical processes is demonstrated experimentally. In the papers by Van Leeuwen [2010, 2009] the methodology of the particle filter is discussed, but not so much its applications.
The theory that is used to combine data and prior model knowledge is explained in this section.

Bayes' theorem

Bayes' theorem is used to determine the probability of certain events happening. The explanation of the Bayes' theorem in this section, is based on the explanation of Dekking et al. [2005]. A simple example is used to show how the theorem works. A probability can be in the range of 0-1. When the probability is 0 or 1 this is absolutely certain, uncertainties are any number in between. In Figure 2.3 an illustration is shown of two fundamental rules that are used in the Bayes' theorem. In part a of Figure 2.3 a cube is shown which contains two circles. One circle is blue and the other circle is white. When one of the figures is taken out of the cube, there are two possible events. Event A is that the draw is the blue circle and event B is that the draw is the white circle. Both events have a probability of 0.5. And the probability that the first event happens or the second event equals the sum of the two probabilities. This first rule is the sum rule and is shown in Equation 2.4.

$$P(A \cup B) = P(A) + P(B) \tag{2.4}$$

where:

P = probability

A = Event A

B = Event B

$P(A \cup B)$ = probability of event A or event B occurring

$P(B)$ = probability that event B occurs

$P(A)$ = probability that event A occurs

The second rule that is fundamental for the Bayes' theorem is the product rule, an example is shown in part b of Figure 2.3. In the cube, there is not only the blue and white circle, but there is a blue square as well. Assume the goal of a random draw from this cube is to get the blue circle. To draw a blue circle two events need to happen: event A is that the shape is a circle and event B is that the colour is blue. These two events are independent, the colour and shape do not influence each other. The probability that event 1 occurs, draw a blue item, is 0.5. The probability that event 2 occurs, draw a circle, is also 0.5. The product rule gives their joint probability, so it gives the probability of both events occurring. The product rule is shown in Equation 2.5 and in this case, it would give 0.5*0.5, so a joint probability of 0.25.

$$P(A \cap B) = P(A) \cdot P(B) \tag{2.5}$$

where:

$P(A \cap B)$ = joint probability of event A and event B occurring

$P(B)$ = probability that event B occurs

$P(A)$ = probability that event A occurs

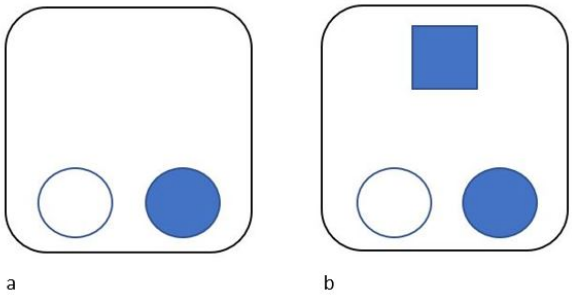

Figure 2.3: Illustration of a) the sum rule and b) the product rule

In the example shown to explain the product rule, the considered events were independent. The joint probability of two events is said to be conditional, when the two events are dependent. The joint probability of two conditional events can be used to find the probability of event A by knowing the probability of event B. In the example that is discussed above, this could be that a person that draws a shape from the cube can feel the shape. The probability that an item from the cube is blue and a circle, can be determined using the joint probability, shown in Equation 2.6. The joint probability of two events is given by the conditional probability of both multiplied with the probability of one of the events.

$$P(A \cap B) = P(A \mid B) \cdot P(B) = P(B \mid A) \cdot P(A) \tag{2.6}$$

where:

$P(A \cap B)$ = joint probability of event A and event B occurring

$P(A \mid B)$ = conditional probability that event A occurs given that event B occurs

$P(B)$ = probability that event B occurs

$P(A)$ = probability that event A occurs

Equation 2.6 can be rewritten to form the Bayes' theorem, which is shown in equation 2.7.

$$P(A \mid B) = \frac{P(B \mid A) \cdot P(A)}{P(B)} \tag{2.7}$$

Assume that event A is that the item is a circle, event B is that the item is blue and event C is that the item is a square. The probability that the item is a circle, not taking into account any other information, is 0.5. So, P(A)=0.5. The probability that the item is blue, is 0.5 as well. So, P(B)=0.5. P(B| A) is the probability that the item is blue, given that it is a circle. This probability is 0.5. P(B| C) is the probability that the item is blue, given that it is a square. This probability is 1. P(C) is the probability that the item is a square, which is 0.5. The probability that the item is blue, not given any information is P(B). This can be found using the product and sum rule: P(B)=P(B| A)P(A)+P(B| C)P(C). This gives P(B)=0.5*0.5+1*0.5=0.75.

Applying Bayes' theorem

The Bayes' theorem as explained before, was applied on probabilities. It can also be applied on probability density functions, which are functions of a continuous random variable. Assume that one sample in the set of possible values of the random variable is chosen. Using the PDF, it can be determined how likely the random variable would equal this sample compared to another sample. This sample is a certain variable in the model, which is referred to as state variable and in this research, these variables are estimated using data assimilation.

The solution to nonlinear data-assimilation problems is based on the Bayes' theorem, which is presented in equation 2.8. The equation shows that the multiplication of the PDF of the observations given the model, with the PDF of the model before the observations, divided by the PDF of the observations, gives the PDF of the model given the new observations. The PDF of the observations given the model is also called the likelihood. In this research the model, represented by m in this theorem, is the morphological model Delft3D and the observations, represented by d, are the bedlevel measurements. A visualization of the theorem is given in Figure 2.4, which shows that the multiplication of the likelihood and the prior PDF gives the posterior PDF.

$$P_m(\psi \mid d) = \frac{P_d(d \mid \psi) \cdot P_m(\psi)}{P_d(d)} \tag{2.8}$$

where:

d = observations

m = model

ψ = state variable of the model

$P_m(\psi \mid d)$ = probability density of the model given the new observations

$P_d(d \mid \psi)$ = probability density of the observations given the model, also called the likelihood

$P_m(\psi)$ = probability density of the model prior to the observations being taken into account

$P_d(d)$ = probability density of the observations

The goal of the data assimilation is to find the posterior model PDF, given the observations. To find this, the model PDF and the observation PDF are needed. First the prior model PDF and observation PDF are described. Then the connection between the distributions gives the model PDF, given the observation. This is called the posterior PDF and is explained using Figure 2.4.
The prior PDF is given by $P_m(\psi)$ in equation 2.8 and is shown in part *b* of Figure 2.4. The prior PDF represents the relative likelihood of possible state variables, without taking any observations into account. The modelled state variable is the simulated bedlevel and the observations are the bedlevel data. So, the prior PDF shows the possibilities of each state variable in the total set of state variables.
The PDF of the observations is given as $P_d(d)$ in equation 2.8 and is in part *a* of Figure 2.4. This shows the probability of different values for the state variable for the observation. This also has a spread, because when a measurement is repeated in the same location at the same time, this might not give the same bedlevel.
The model PDF shows the probability of one model outcome occurring, compared to the other model outcomes, while taking into account the observations. This model PDF is also called the posterior distribution and is shown in part *c* of Figure 2.4.
The posterior distribution, $P_m(\psi|d)$, is the update of the a priori understanding with observations. This update is shown in Figure 2.4. In the prior model PDF shown in part *b* of the figure, the probability of model outcomes is high for high values values of bedlevel. However, in the observation PDF, which is the likelihood, shown in part *a* of the figure, there are no observations in that range of bedlevels. By taking the observations into account to obtain the posterior distribution, the right side of the posterior PDF becomes smaller than in the original prior model PDF. Taking the observations into account, means that the observation PDF and prior model PDF are multiplied to obtain the posterior PDF, see denominator of equation 2.8.
The distribution of the observations given, the state variable, $P_d(d|\psi)$, quantifies the distribution of measurement errors given a simulation of the state variable [Wikle and Berliner, 2007]. This distribution is called the likelihood. Multiplication of the likelihood and the prior PDF gives the posterior PDF.
The difficulty of the Bayes' theorem is in the prior model PDF, because this often depends on a model with many dimensions. This leads to a large number of possible model states that define the PDF. It is impossible to know all the state variables and to know exactly what the prior PDF really looks like.

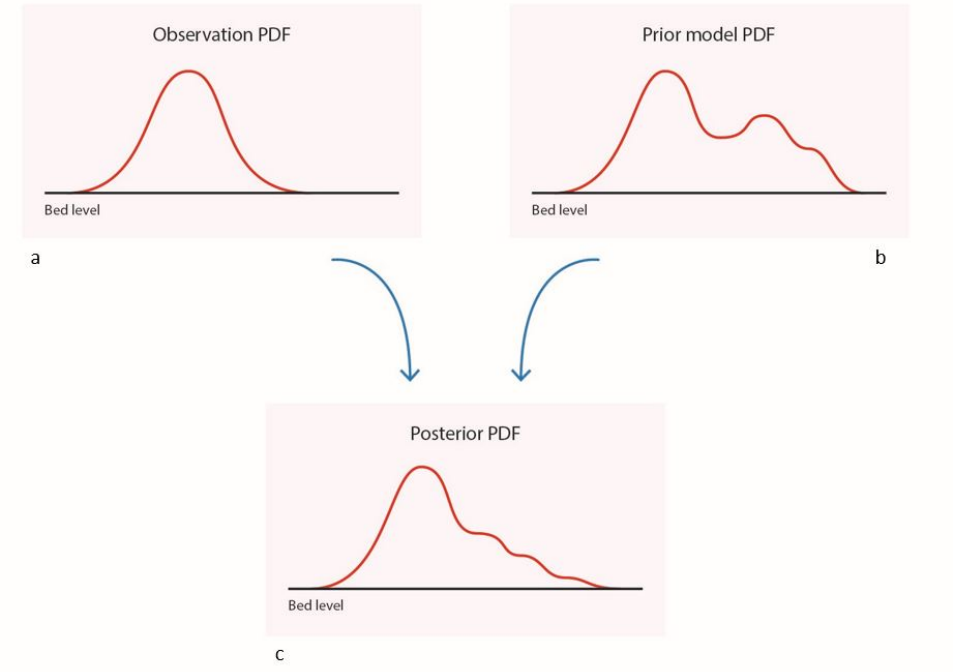

Figure 2.4: The combination of a prior model PDF and an observation PDF to form the posterior PDF.

Particle filter

The concept of a particle filter (PF) as discussed in this section, uses the explanation given by Van Leeuwen [2009] as a guideline.
Since it is impossible to represent the full prior PDF, the particle filter uses a set of model states to represent the prior distribution. In Figure 2.5 an example of a PDF is shown with the model states that represent the PDF. The model states in the set are called particles, which in this case are model set-ups created by changing one parameter between different runs. Because of the varying parameter, typically the model results end up at a different location in the PDF. The target PDF shown in 2.5 is the prior model PDF that is represented by the particles. In this research, the probability of the modelled bedlevels as a result of all different parameter values forms the target PDF. To represent the PDF by the particles a Dirac delta function is used, which is given in equation 2.9. The state variable in the vector is the simulated bedlevel. At each location to evaluate, the difference between the state vector of the observation and the state vector of the particle is calculated. By taking the sum of the differences of all locations, and dividing this by the number of particles, the probability density of the model prior is found and is one number.

$$p_m(\psi) = \frac{1}{N}\sum_{i=1}^{N}\delta(\psi - \psi_i) \tag{2.9}$$

where:

$P_m(\psi)$ = probability density of the model prior to the observations being taken into account

N = number of particles from density $P_m(\psi)$

ψ = the state vector

ψ_i = the state for the i_{th} particle

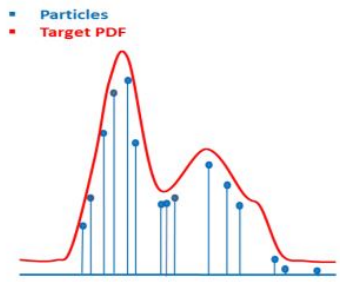

Figure 2.5: A representation of a PDF using particles. Adjusted figure from [Ansari, 2014]

The evolution of the prior PDF is represented by running several simulations. In these simulations, the particles, which form the prior PDF representation, are propagated forward in time. So, from the initial situation, the simulation makes a prediction of the state variable, the bedlevel. The likelihood represents the distribution of the observations, given the model simulations. In this research, the likelihood is the distribution of errors in observing the bedlevel, while taking into account the simulated bedlevels. The likelihood is represented by a chosen distribution function, which can be for example a Gaussian or Lorentz function. It often can be assumed that measurement errors are Gaussian distributed. The representation of the likelihood using a Gaussian distribution is shown in equation 2.10. The equation takes the difference between a simulation of one of the particles and the observation. The standard deviation of the observation, σ, gives the width of the likelihood. The ratio between the difference and the standard deviation determines the value of this expression. This effectively applies a weight to the particles, which results in different probabilities. The standard deviation σ should represent the uncertainty in the data. There are multiple options possible to use as standard deviation and the choice of representation is somewhat subjective. Possibilities are spatial standard deviation and temporal standard deviation. The spatial standard deviation is the standard deviation within one observation in the area. The temporal standard deviation is the standard deviation of observations at different moments in the same area. The consequence of a large value of σ is that the exponent is a smaller negative number. A smaller negative power of e results in a larger value. So, when the standard deviation is larger, the result of equation 2.10 will be larger. This results in a wider spread of the likelihood, $P_d(d \mid \psi)$. In this research it is not possible to choose the temporal standard deviation, since there is only one observation available for each period.
The particle filter is then applied multiple times and therefore it is expected that the difference between simulation and observation decreases. The iteration is performed, because in one update there might not be a good estimate. When iterating the process, more different simulations are started and therefore the chance that a probable bedlevel estimate is found is larger. The coefficient, a, is used, because one observation is used multiple times in these iterations. The standard deviation of this one observation remains the same and might be relatively large when used in the last iteration. Therefore the coefficient can be used to divide the quadratic standard deviation [Emerick and Reynolds, 2013]. It is often chosen equal to the number of iterations.

$$P(d \mid \psi) = e^{-0.5 \frac{(d-m_i)^2}{\frac{\sigma^2}{a}}} \tag{2.10}$$

where:

$P(d \mid \psi)$ = probability density of the observations given the model state

d = observation, in this study: bedlevel measurements

m_i = simulation result of the ith particle, in this study: bedlevel simulation by Delft3D

σ = standard deviation of the observation

a = coefficient

The principle of a standard particle filter is visualized in Figure 2.7. In part 1 of the figure, the blue bars represent ten particles that form a representation of the prior PDF shown in light blue. The bars have equal

lengths to show that the particles have equal weights.
The propagation of the particles forward in time is visualized by the brown arrows towards part 2 of the figure. In this research, this means running the simulation in Delft3D to predict the bedlevel. In part 2, it is shown where the particles end up, together with the observation PDF which is shown in green. In this research, this is the bedlevel observation and the Gaussian distribution around it. When the prior PDF is close to the observation PDF the likelihood is larger. For the bedlevel values with a high likelihood, the assigned weight is high. These weights are used in equation 2.11 to find the particles with their assigned weights, shown as red bars in part 3 of the figure. The concept of assigning weights to particles is called importance sampling. By assigning the weights to the particles, they are not modified, only their relative importance changes. An advantage is that the dynamical balances remain the same, so the solution is consistent with physics. However, the particles are not pulled back when they move away from the observations. Another difficulty in importance sampling is that filter degeneracy occurs. This means that after a few analysis steps, one particle gets all the weight, while the other particles get zero weight. Filter degeneracy means that the statistical information in the particles becomes too low to be meaningful.

In Figure 2.6 the concept of importance sampling for a particle filter is visualized. A bullet represents the particles and the size of the bullet represents the particle weight. A larger bullet is a particle with a larger weight. The vertical axis is the model variable and the x-axis is time. At each tenth time unit, a new observation is available, represented by a vertical line. The particles start at t=0 with an equal weight. At t=10, four particles receive a weight t=10 and at the last time step of the figure, t=20, there are three particles with weight left. This is filter degeneracy, which is seen in part 3 of Figure 2.7. This shows only three particles with a relevant weight. A possible solution for filter degeneracy is resampling, which reduces the variance in the particle weights. This is done between parts 3 and 4 of the figure, where three particles are copied to get ten particles again. When applying resampling, first of all, the particles with a low weight are abandoned. The particles with a high weight are copied until the total number of particles is restored. A particle with a larger weight will be copied more. Multiple identical particles can result in different outcomes when propagating forward in time, when the system is stochastic. However, in a deterministic model, the identical particles will always give identical outcomes. Therefore, in this application, the particles should not be copied, but new particles need to be chosen.

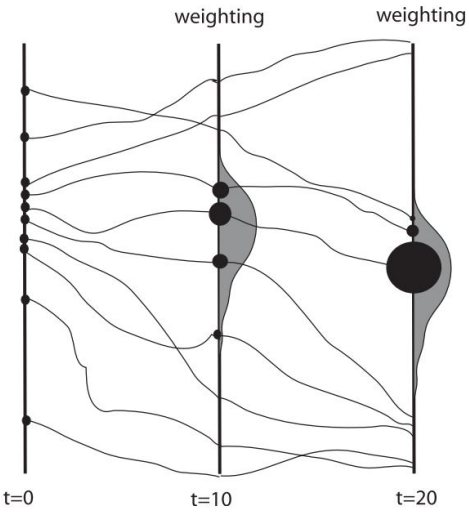

Figure 2.6: Particle Filter, importance sampling, from [Van Leeuwen, 2009]

Different methods exist on how to choose these new particles (Gaussian resampling, localization, merging [Van Leeuwen, 2009]) and the method used in this research is Kernel dressing. Kernel dressing means that for each particle a continuous PDF will be made. The PDF for each particle is made with the same width and height, until it is updated with the weight of the particle. A kernel dress around a particle with a high weight will be larger. This results in more samples drawn from the high weight particle dresses. Often, a Gaussian PDF is chosen, because in that case only two parameters need to be estimated. To set up the Gaussian distributions, a mean and a covariance are needed. As a mean, the particle state is used and as a covariance, a factor smaller than the covariance of the full particle set is used. From the Gaussian distribution that is drawn around each particle, new particles are chosen. The number of particles that are chosen from each particle dress, is determined by the weight of that specific particle.
The particles that are obtained can be used to propagate forward in time and see the evolution of the model PDF. When there are multiple observations available at the first analysis time, the particles can also be used to propagate again from the start time to be analysed when another observation comes in.

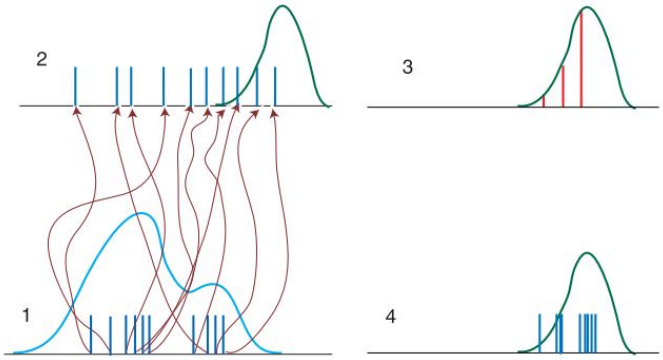

Figure 2.7: The standard particle filter, as visualized in Van Leeuwen [2010]

$$P(\psi \mid d) = \sum_{i=1}^{N} w_i \delta(\psi - \psi_i) \tag{2.11}$$

where:

$P(\psi \mid d)$ = probability density of the model given the new observations

N = number of particles from density $\mathrm{P}_m(\psi)$

w_i = the weight of the i_{th} particle

ψ = the state vector

$$w_i = \frac{P(d \mid \psi_i)}{\sum_{j=1}^{N} P(d \mid \psi_j)} \tag{2.12}$$

where:

w_i = the weight of the i_{th} particle

$P(d \mid \psi_i)$ = probability density of the observations given the model state of the i_{th} particle

$P(d \mid \psi_j)$ = probability density of the observations given the model state of the j_{th} particle

The weights, w_i, are determined using equation 2.12. This equation shows that the assigned weight is high, when the probability that the observations are true given the model state is high. The weights are needed to determine the relative importance of the particle, which is shown in equation 2.11. The larger the weight, the more this particle contributes to the estimate.

Bedlevel data

The data used in this research gives information on the bedlevel in the Wadden Sea and is measured by the Meet- en Informatiedienst Noord-Nederland. Elias and Vermaas [2019] give information on the data availability and the measuring and processing procedures. A summary of this information is presented here.
The measurements are digitally saved by Rijkswaterstaat since 1985. The saved data can be found in the Landelijk Opslagsysteem Lodingen (LOL) database. The depth of the seabed is measured using sonar soundings on a ship that travels in lines which are parallel to each other. The distance between these lines can vary between 200 meters in the Wadden Sea to 1000 meters along stable island coasts. The distance between measurement locations can differ, but is approximately 30 cm. At tidal flats, it is possible to measure with laser altimetry. Each year one of the basins is completely measured, which means that once in the six years there is a complete overview of the bed of the entire Wadden Sea.
The data is delivered at a 20x20 meter grid and this is converted to the model grid. In section 3.1 it is explained how the conversion to model grid is made.

3

Method

3.1. Model set up

A case study is performed using Delft3D on the Frisian Inlet in the Wadden Sea. To be able to do so, the model needs to be set up in this specific area. The set-up for this research is based on the model set-up as used by de Boer [2002]. Model input that is discussed is initial bedlevel, wave conditions, tidal forcing and morphology.

Data conversion

One of the inputs for the model is an initial bed level. The initial bed level for each period is based on the observed bathymetry in the starting year of that period. As explained in section 2.4 the available bed level data is available on a 20x20 meter grid. The data on the 20x20 meter grid is shown in Figure 3.1. It needs to be converted to the grid as it is used in this research. This model grid is shown in Figure 3.2a and consists of 105x82 grid cells. The cells are irregularly spaced, because the area of interest of this study is mostly at the tidal inlet and less at the outer part of the North Sea. Most channels in the bathymetry are located in the Frisian inlet, in the middle of the basin and a small part North and South to the inlet. The time scale for bathymetry change in a tidal channel is smaller than for the more equal bathymetry in the North Sea. To accurately monitor these relative fast changes, the grid is finer at this location. In the grid there are two blanks. The left blank is Ameland and the right blank is Schiermonnikoog. The blank part below Schiermonnikoog is excluded from the modelled area, because in this way the boundary of the area is at the location of the tidal watershed. As explained, there is negligible transport of water and sediment through a watershed. When the complete area at the Eastern boundary is used, this leads to an unrealistic flow of water east from Schiermonnikoog.

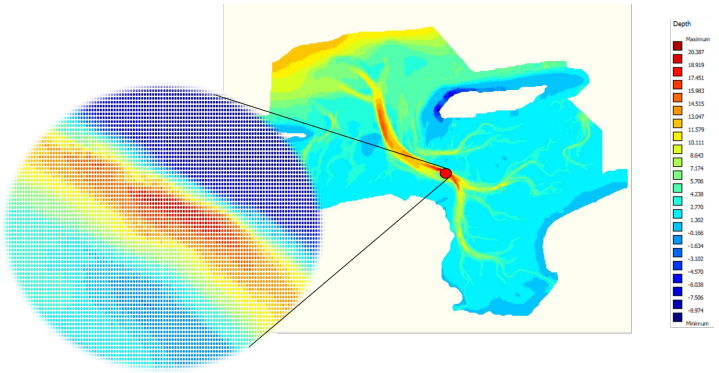

Figure 3.1: The bed level data on the 20x20 meter grid

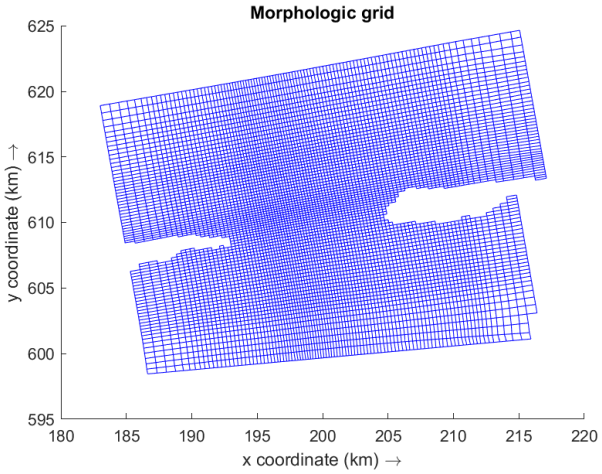

(a) The morphologic grid

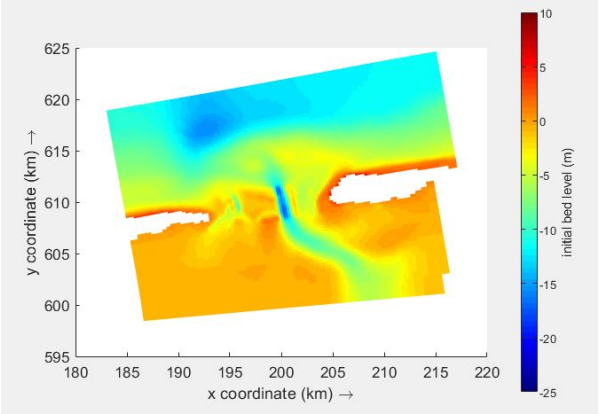

(b) The initial bathymetry from 1970 bed level data

Figure 3.2: Delft3D initial settings Frisian Inlet

The conversion from the 20x20 meter grid to the 105x82 grid is made in the program QuickIn. This is exported to use in Delft3D and the result is shown in Figure 3.2b.
In the model, the boundaries must be defined as either closed or open. An open boundary makes transport of water and sediment through the boundary possible. For a closed boundary, this is not possible. The outer boundaries of the Wadden Sea area are closed because there is negligible transport of water and transport via the Western and Eastern boundaries to the other basins. The south side of the Wadden Sea is the mainland, so this is a closed boundary as well. The islands are confined by closed boundaries and the North Sea boundaries are open.

Subquestion 1

Which parameters induce a significant change in the bathymetry of a morphological model?

Delft3D set-up

In the area given to Delft3D, an initial bathymetry and a model grid needs to be specified. For the area, the boundaries need to be defined as either open or closed. An open boundary means that transport of water and sediment is possible. Through a closed boundary, no transport is possible. An open boundary requires flow and transport boundary conditions, that represent the influence of everything outside the modelled area. The flow through an open boundary can have different boundary conditions. They can be forced by water levels, currents, water level gradients, total discharges, discharges per grid cell, or a combination of water level and current, which is called the Riemann invariant. The hydrodynamic forcing that defines the boundary condition can be prescribed using harmonic components, astronomic components or time-series. When the hydrodynamic forcing type is harmonic, then user-defined frequencies, amplitudes and phases will be used. For the astronomic type, the flow conditions are specified by tidal constituents, amplitudes and phases.
In section 3.1 "Forcings", the processes used in this research are defined. Possible simulated processes in Delft3D are salinity and temperature which influences the density of water and can cause density-driven flows. Other processes are spreading of pollutants and traces, transport of sediment and influence of wind, waves, secondary flows, tidal forces and dredging and dumping. When these processes are used in the model set-up an initial condition for the process is needed.
To simulate the processes some physical parameters are needed. These parameters can be constants like gravity or air density. Water density can also be given as a constant parameter, when a homogeneous simulation is performed. Bed roughness, wall roughness and viscosity are other physical parameters that are defined for each model set-up. What other parameters are needed to set up the model depends on what processes are needed. The possible processes that can be used to describe a situation in Delft3D are a heat flux

model, sediment processes, morphological processes, wind, tidal forces and discharges. What processes are needed to set up the model-specific for this research, is explained in the method.

Forcings

In the model set-up, processes that take place in the Wadden Sea need to be described as good as possible. As described in section 2.2 some of the processes are residual flow, tidal asymmetry and dispersion. Another important factor is the amount of suspended and bedload transport. These processes are influenced by tidal forcing, meteorological effects, freshwater input, flow velocities and grain size. To capture these influences in the model the tidal forces, wind, morphology and sediment processes will be used.

Tidal forcing

The open boundary type used is the water level type and it is forced using harmonic equations. So, the frequency, amplitude and phase for the open boundaries are defined. The frequency is given in [deg/hour], the amplitude in [m] and the phase in [deg]. The largest tidal influence is the moon, which is defined by the lunar constituents M0, M2, M4 and M6. These tidal constituents have a period of 12.42 hours. The solar constituents S2, S4 and S6 are of smaller influence on the tides. The solar constituents have a period of 12 hours. Since this period is easier to work with, a simplification of the tides will be applied [van de Kreeke and Robaczewska, 1993]. The amplitude of the M-constituents and the frequency of the S-constituents are used. To be able to do so, the phase of the M-constituents need to be recalculated using the frequency of S. This is done using equation 3.1. The phase is given in deg, which is converted to hour using the M-frequency [deg/hr]. Then this is converted to phase (deg/hr) again using the S-frequency (in deg).

$$P_{tide} = \frac{M_{freq}}{M_{phase}} S_{freq} \tag{3.1}$$

where:

P_{tide}	= Phase of the tide that will be used in the model	$[deg]$
M_{freq}	= Frequency of M-constituent	$[deg/hr]$
M_{phase}	= Phase of M-constituent	$[deg]$
S_{freq}	= Frequency of S-constituent	$[deg/hr]$

Wave and wind

Wave measurements are made at multiple buoys in the Wadden Sea, of which the locations are shown in Figure 3.3. The data gathered with these measurements is the wave height, wave direction and wave period. The data can be averaged over time to define twelve wave conditions. For each wave condition, a fraction of occurrence is given, which shows how often that type of wave occurs. In one simulated tidal cycle, all twelve wave conditions will be applied in proportion with their fraction of occurrence. The twelve wave conditions are simulated in a certain order, that is not necessarily the order in which they occur in reality. Therefore, the simulation results in between tidal cycles can not be used in data processing. Only the result of a simulation is considered, because a total tidal cycle is completed. The wind data is from statistical data as well,

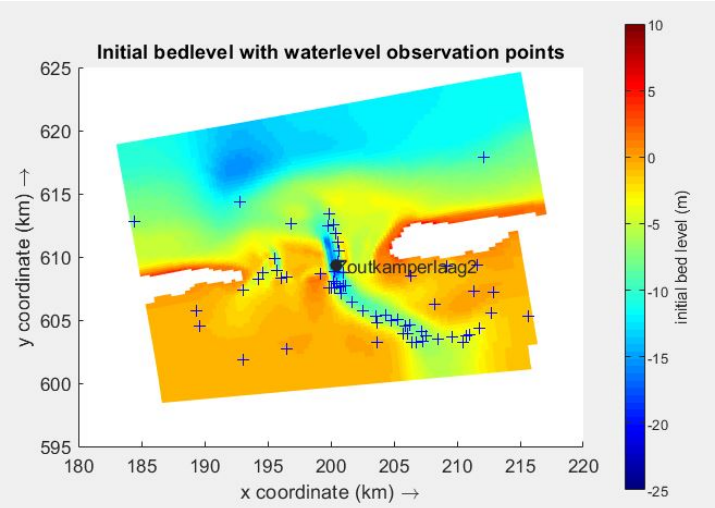

Figure 3.3: The initial bathymetry from 1970 with water level observation locations

measured by the Koninklijk Nederlands Meteorologisch Instituut (KNMI) [de Boer, 2002].

Morphology
In the morphology input, there are a lot of parameters that influence the transport of sediment. For example the gradient along and across a channel. This determines the ease for a sediment particle to travel through a channel or to travel from the channel side to the channel centre. The bed roughness as a result of waves and current is also given in the morphology input. As explained in chapter 2.3 the bed roughness influences the water flow and this can result in changing sediment transport.
Furthermore, the connection between the MF and time is made in this input. The time frame is determined by the availability of the bed level measurements in the inlet. The data that are used are measured in 1970, 1975, 1979, 1982 and 1987. These years will be used as the start time for the simulations that are run up til the year that a new measurement is available. This results in different timeframes for the simulations. For example, the simulation that starts at 1970 will run five years to end in 1975. Whereas, the simulation that starts at 1975 will run four years to end in 1979.
As described in paragraph 2.3 a critical value for the MF is needed. To find this critical value test simulations are performed. In these test simulations, the different simulation times are combined with multiple MF values. The simulation time is varied between three, four and five years, because these are the timeframes between the available bed level observations. The results for erosion/sedimentation and water level are checked for unrealistic scenarios. The water level results of the MF study should be close to the average tidal heights. The erosion/sedimentation results can form an indication that there is an extreme water flow taking place. In comparable model set-ups a value of 200 is found to be the maximum acceptable value as a MF [Baar et al., 2019]. In the multiple runs performed with the model set-up, it is found that an MF of 100 gives realistic simulations that run sufficiently fast.
The simulation time is divided into twelve equal time frames because there are twelve wave conditions. For each of the wave condition, its occurrence is given by a fraction, P. The desired MF is 100, so the MF_i given to each time frame is given by equation 3.2. The last second of each timeframe is set MF to zero.

$$MF_i = n \cdot P_i \cdot MF \tag{3.2}$$

where:
MF_i = the MF of one timeframe
i = number counting from 1 to n
n = number of wave conditions
P_i = fraction of occurrence of ith wave condition
MF = the total MF

Sediment
In the sediment input the specific density, median sediment diameter, dry bed density, initial sediment layer thickness at the bed and the initial suspended sediment diameter is given a value. In this input it is defined if the sediment type is sand, mud or bedload.

3.2. Sensitivity study
When the model is set up, it will be used to perform a sensitivity study. The results will show which parameters have a significant influence on the morphological results. These parameters can be considered to use in the data assimilation.

3.2.1. Parameters
The parameters that will be considered are shown in table 3.1. They are the current related bed roughness, the wave related roughness, the tidal amplitude, the wave-related suspended load sediment transport factor, the wave-related bedload sediment transport factor and the transverse bedload slope. The tidal amplitude. wave-related roughness and current related bed roughness are in meters and the other parameters have no units. Using the values as shown in the table a reference run is performed. This is used as a reference in the

sensitivity study. For each parameter a certain range is known in which the values of the parameters are realistic [Deltares, 2018]. Within these ranges, ten values are chosen for each parameter. For α_{bn} twenty values are used, since the possible range of values is large. These values are shown in appendix C.
The resulting bathymetries will be compared with the reference run and the observation, to see if one parameter has large variations in the outcomes of different input values. The range of the parameters are shown in the last column of table 3.1.
From the results of the runs, shown in appendix A, it is determined if one of the parameters shows more variation in the results than other parameters.

Table 3.1: Parameter names and their abbreviations

Name	Abbreviation	Reference run	Range	Units
Current related roughness	RDC	0.01	0.005 - 1	m
Wave related roughness	RDW	0.02	0.005 - 1	m
Tidal amplitude	A	1.237	0.7 - 1.2999	m
Wave-related suspended load sediment transport factor	SusW	0.3	0.1 - 1	-
Wave-related bedload sediment transport factor	BedW	1	0.5 - 1.4	-
Transverse bed slope	α_{bn}	1.5	0.5 - 100	-

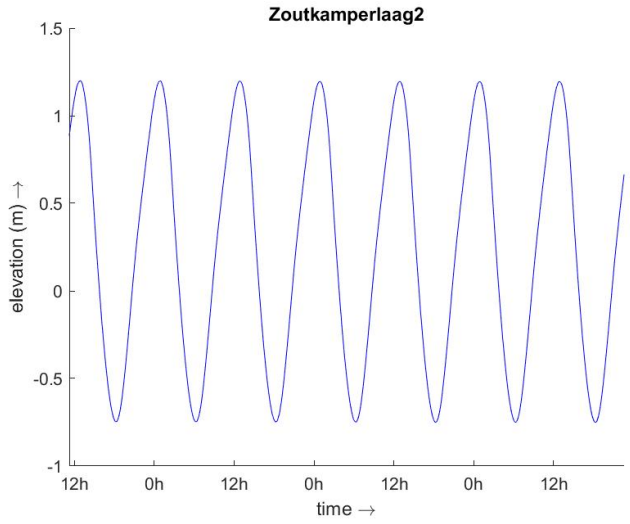

Figure 3.4: The water level at measuring point Zoutkamperlaag2. See Figure 3.3 for location of Zoutkamperlaag2.

The first comparison is performed using the mean squared error skill score (MSESS), which is determined for each simulation. First, it is determined for the whole area. Then, the sub-area is selected and the MSESS is determined using only the sub-area. Next, the sub-area will be divided into tidal flats and tidal channels, which is done using a threshold. In chapter 2.1 the definition for tidal channel is given as the bed that is always submerged. A tidal flat was defined as the bed that is below water level during low tide and above water during high tide. Figure 3.4 shows the water level for a part of the period between 1970-1975 as simulated by Delft3D. The low tide is -0.7 meter and the high tide is 1.1 meter. So, the threshold for tidal channels is set to -0.7 meter. As a threshold for tidal flats, the average of the extreme tides is chosen. So, this is set to 0.2 meter. An example of these thresholds is shown in Figure 3.6. The bed level in each grid cell is compared with the channel threshold to decide which grid cells are tidal channels. The same is done for all grid cells with the tidal flat threshold. The distribution of tidal channels and tidal flats according to these criteria is shown in Figure 3.5. The shown area is a sub-area of the total modelled area. The sub-area is selected, because the North Sea is also defined as a tidal channel. In the sub-area, a large part of the North Sea is discarded, since it is not wanted to take the North Sea into account when evaluating the tidal channel part.

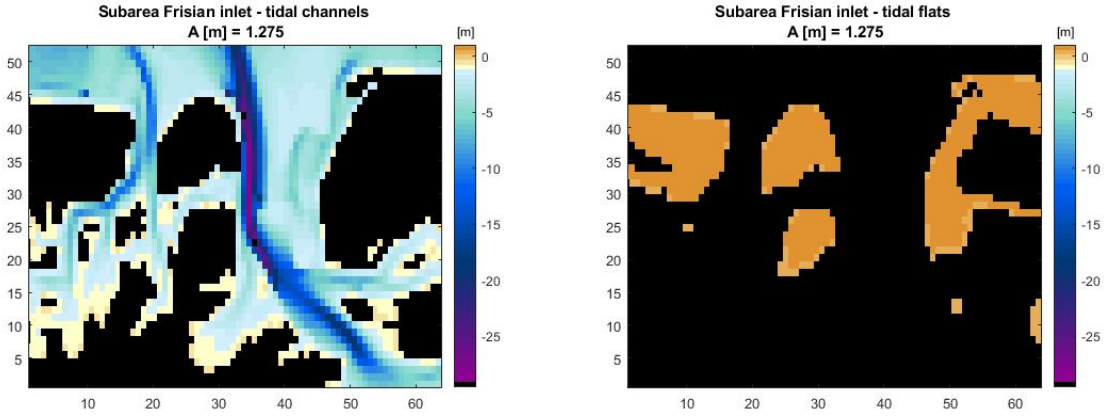

Figure 3.5: The tidal flats and tidal channels in the total area

For each grid cell that is defined as a tidal channel, the volume is calculated. For the grid cells that are defined as a tidal flat, the height from 0.2 to the surface of the flat is calculated. This action is performed for the simulations, the observation and the reference. The MSESS is determined using only the grid cells that are a tidal channel to see the correspondence between observation and prediction, optimized on channel volume. The same is done optimized on the tidal flat grid cells.

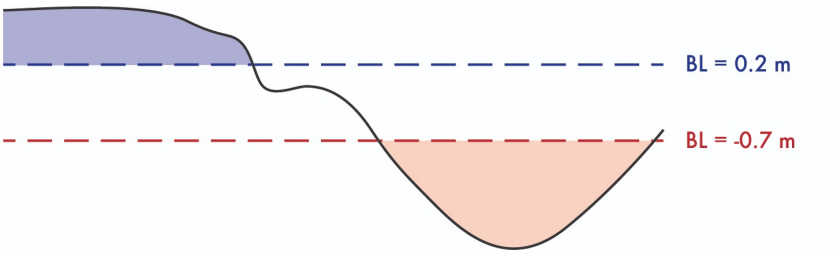

Figure 3.6: Divide tidal channel and tidal flats

To determine the MSESS for each simulation a reference and an observation are needed. As a reference a zero-change model is used, which is the observation made at the start year of the simulation. So, for the period 1970-1975, the reference is the 1970 observation and the observation is the 1975 observation.
Another comparison is performed using the differences between simulations and observation. The difference between simulation and the 1975 observation is determined for the plate height and the channel volume. The mean and median plate height will be determined. For the channel volume, this is the total channel volume and the median channel volume. This difference is in m^3 for channel volume and in m for plate height. To make a comparison between the different simulation easier, the difference is converted to percentages. The results for the MSESS is discussed below. The results of the percentage differences can be found in Appendix A.

Subquestion 2

How can data assimilation be implemented to optimize a morphological model output based on bed level measurements?

3.3. Data assimilation

In this section, the method to apply the particle filter on the specific case study for this research is discussed.

Particle Filter

The parameter that is the result of the sensitivity study is the transverse bed slope, α_{bn}, so this parameter is varied in the particles. In this research, the particle filter is started using an ensemble of 100 particles, which is a small amount for a particle filter. However, the time to perform the simulations for this research is limited, so simulation of more particles is not feasible. With this number of particles, it is expected that the particle filter gives results that optimize the bed level simulations, while the simulation time is manageable. Based on the opinion of experienced Delft3D users and literature, it is chosen to search for α_{bn} values in However, wherein these range is the best value for the particular situation is not known. That is why the 100 particles are chosen by using a uniform distribution. In Figure 3.7 the distribution is shown, which is not a perfectly uniform distribution. When the bins are chosen larger, or when more particles are made, the distribution is more towards a perfect uniform distribution. The different values for the transverse bed slope is the only thing that changes for each particle. The rest of the model settings remain as discussed in the method of subquestion 1. Using this distribution, simulations are started in 1970 and the results from the Delft3D simulations are processed. First of all, an image of the simulated and observed bathymetry is made, which is shown in Figure 3.8a and 3.8b. Figure 3.8c shows a plot of the difference between the simulation bed level result and the 1975 observed bed level. In Figure 3.8d, a plot of the difference between the 1975 observed bed level and the 1970 observed bed level is shown. From these plots, it is decided to select a sub-area for evaluation, because there is not much interest in the North Sea part. Moreover, not very detailed information is given to Delft3D about the waves. So, the quality of the results towards the North Seaside is lower than in the inlet and basin part of the area.

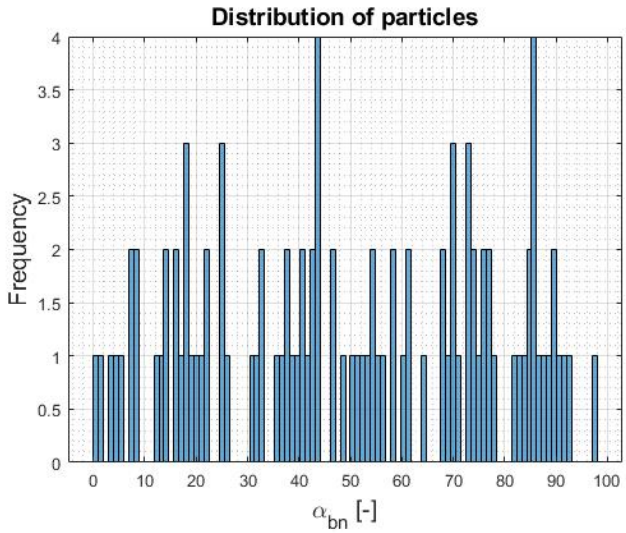

Figure 3.7: Uniform distribution for particles with different α_{bn}, used as a start for all epochs

Areas where changes in the bed level take place, can lead to variation in model outcomes. An area where a lot of sediment transport is taking place is expected to be more difficult to simulate than an area where not much transport is happening. So, the sub-area contains the parts of the area where the bed level differences in this period are large. This means that the simulation predicts a higher bed level than is observed in 1975. In the difference plots between the observation in 1975 and in 1970 positive values at the channel location are shown. This means that in the period 1970-1975 the bed level at that location is increased. There is sediment transport taking place along or in the channel, so it is an interesting part of the area to use in this research. So, two lines across the channel are chosen to evaluate the results on. The first line forms a cross-section through the tidal inlet and the second line forms a cross-section through the channel in the Wadden Sea. The results will also be evaluated on the tidal flat, which is marked as an area. The lines are shown in the bathymetry and difference plots in Figure 3.9.

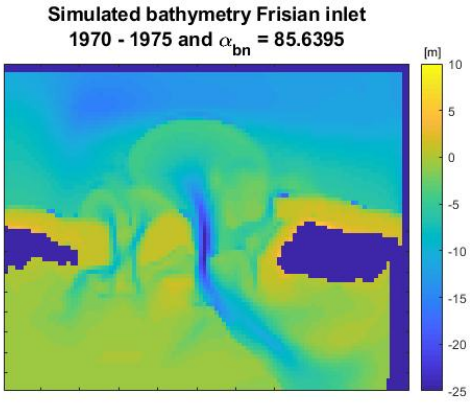

(a) Bathymetry simulation 1975

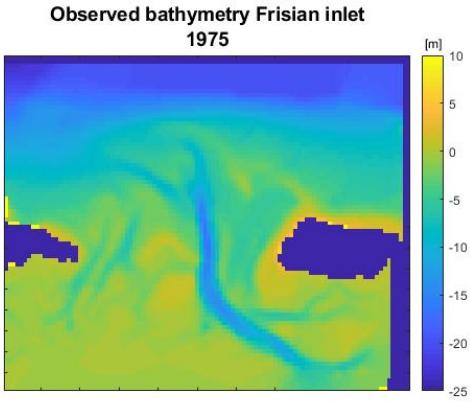

(b) Bathymetry observation 1975

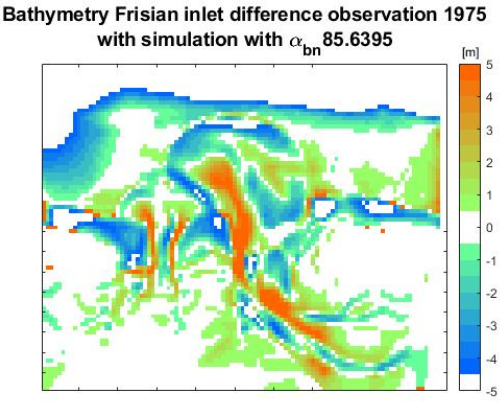

(c) Difference observation and simulation 1975. Positive values show that the simulation predicts a deeper bedlevel than is observed. Negative values show that the simulation predicts a shallower bedlevel than is observed.

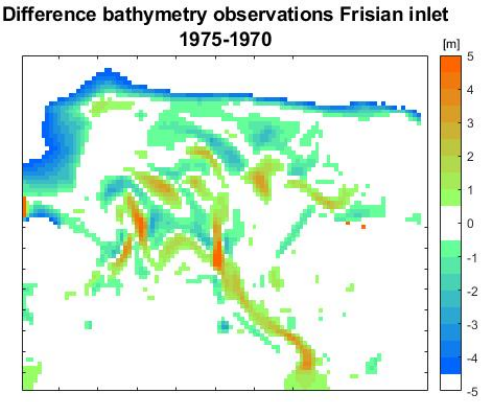

(d) Difference observations 1975 and 1970. Positive values show that in 1970 a deeper bed level is observed than in 1975. Negative values show that in 1970 a shallower bedlevel is observed than in 1975.

Figure 3.8: Example of results: Bathymetry and difference plots in the Frisian inlet - total area

The two channel locations together are used to optimize the model results for channels. A separate optimization is made for the tidal flat area. Using equations 2.10 and 2.12 the weights for the channel optimization and the weights for the flat optimization are calculated. In equation 2.10 the observed bed level in 1975 is used as observation d. One of the 100 simulations is used as m_i. The standard deviation of the observed bed level in 1975, σ, is divided by the factor a as explained in section 2.4. The particle set is expected to reach its optimized values of α_{bn} in three iterations. So the number of iterations and the factor a are set to three. When the period 1970-1975 is simulated three times, the results will be discussed. When the steering by the particle filter is not significant anymore, it is decided to decrease the number of iterations. When the spread of the 100 particles is less than 1 and the particle filter makes it converge more, it is considered not significant.

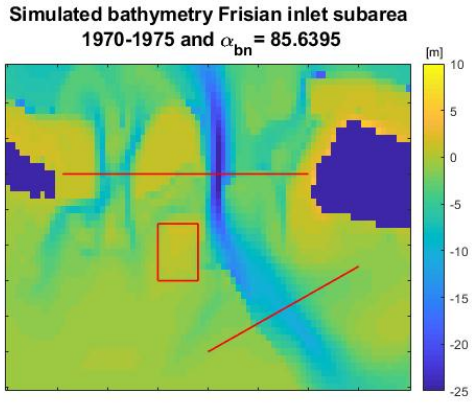

(a) Bathymetry simulation 1975

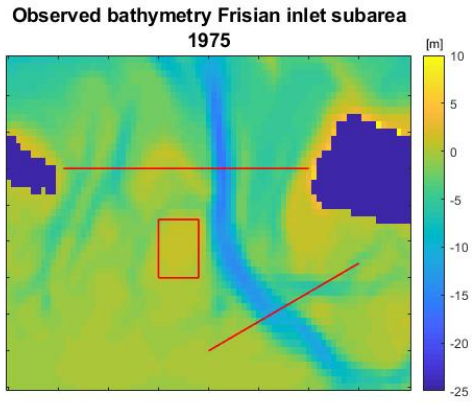

(b) Bathymetry observation 1975

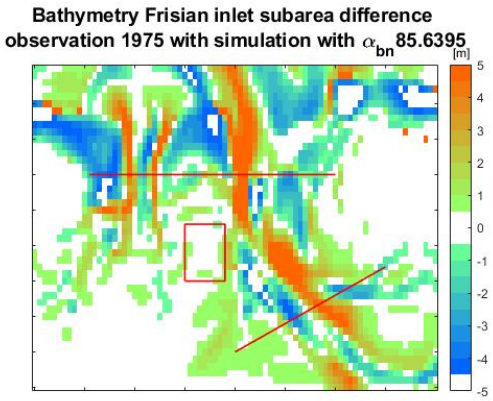

(c) Difference observation and simulation 1975. Positive values show that the simulation predicts a deeper bedlevel than is observed. Negative values show that the simulation predicts a shallower bedlevel than is observed.

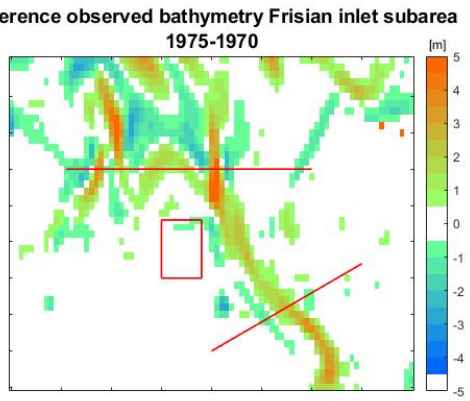

(d) Difference observations 1975 and 1970. Positive values show that in 1970 a deeper bed level is observed than in 1975. Negative values show that in 1970 a shallower bedlevel is observed than in 1975.

Figure 3.9: Example of results: Bathymetry and difference plots in the Frisian inlet with tidal channel cross-section lines and tidal flat area - sub area

Using equation 2.12 a weight is assigned to each simulation, based on the ratio between the probability density of the observations given the model state of one particle and the sum of this probability density of all particles. The two channels are converted to one array, so the processing of the results gives two arrays with weight. One processed on the data of the tidal flat area and one processed on the data of the channel cross-sections. For these weights, it is decided which weights are effective. The effective weight is defined as the ratio between the weight of a simulation and the maximum weight, as shown in equation 3.3. When the effective weight is above 0.5, the considered particle remains in the particle set. When it is below 0.5, the particle is not used again. To be able to start the new simulation with 100 particles again, resampling will be performed on the particles that are above the 0.5 threshold. The number of particles that are discarded, is the number of resamples that need to be produced.

$$w_{eff} = \frac{w_i}{w_{max}} \tag{3.3}$$

where:

w_{eff} = effective weight

w_i = the weight of the ith simulation

w_{max} = the maximum weight of all simulations

The resampling is done using Kernel dressing. Around each remaining particle, a Gaussian distribution will be set up. This distribution uses the particle α_{bn} value as a mean. The standard deviation of the distribution needs to be smaller than the standard deviation of the total particle set. It is chosen to set the standard deviation of one Kernel dress to 0.01 times the standard deviation of the total particle set.
Although it is possible to make an optimization for the channels and the tidal flat, it is decided to proceed further with the channel optimization only. In this project, there is not sufficient time to perform the total optimization for both. So, the resulting particles from the channel optimization are started again in 1970. The results will be processed in the same way.
When three iterations are made in the period 1970-1975, a new set of α_{bn} is found. Then the next epoch will be started, which is the period from 1975 to 1979. The distribution and initial bathymetry for this epoch depends on the outcome of the first epoch. When the α_{bn} distribution still shows significant spread, epoch 2 is started using that distribution to set up the particles. In that case, the initial bathymetry is the weighted bed level average of the last iteration of epoch 1. The weighted average bed level is determined using equation 3.4. The simulated bed level of a grid cell is multiplied with the weight of that simulation. This is done for each simulation and each grid cell. In this way, a combination is made of the 100 simulations. The weights used are the weights optimized on the channels, so one bed level average is found. All the data is processed on the sub-area and not on the total modelled area. The weighted average bed level is also determined for the sub-area only. To make it suitable to use as an initial bathymetry in Delft3D, the weighted average is opened in Quickin, an interpolation tool. In Quickin an interpolation is made, to make the data cover the total model grid again.
When the α_{bn} distribution that results from epoch 1 does not show significant spread, epoch 2 will be started using the same uniform distribution of α_{bn} as was used in epoch 1. As initial bathymetry, the interpolated 1975 observation will be used.

$$\sum_{i=1}^{N} BL_i * w_i \tag{3.4}$$

where:

N = number of simulations

BL_i = the bed level of a gridcell in the ith simulation

w_i = weight of the ith simulation

4

Results

Subquestion 1

Which parameters induce a significant change in the bathymetry of a morphological model?

4.1. Sensitivity study

The MSESS results are shown in Figures 4.1 to 4.4. As explained in section 2.3, the value of the skill score ranges from -∞ to 1. A score of 0 means that the prediction is as good as the reference. When there is no difference between a prediction and observation the skill score is 1. A skill score between 0 and 1 shows the proportion of improvement over the reference prediction. Negative values are found for predictions that perform worse than the reference prediction. The skill score for α_{bn} and wave-related bedload sediment transport factor (BedW) are shown in a separate subfigure, because their values are far from the values of the other parameters. Note that the scaling on the y-axis differs in the figures and subfigures. The α_{bn} and BedW results for the skill score are just below 0, when the total area is processed (Figure 4.1a and 4.1b). However, the optimizations for the sub-area, tidal channel and tidal flat show a further decrease of the negative skill score values. In Figure 4.4a and 4.4b for the tidal flat height optimization the skill score is around -300 for α_{bn} and BedW. It seems that the simulations with varying α_{bn} and BedW perform well over the whole area, but do not perform well when zooming in to specific parts, like the tidal channels and the tidal flats.
The skill score of the other parameters, current related roughness (RDC), wave related roughness (RDW), wave-related suspended load sediment transport factor (SusW) and tidal amplitude (A), is much larger when the total area and sub-area are taken into account, than when it is focused on the tidal flat heights or tidal channel volumes. The order of magnitude of skill score for these parameters and α_{bn} and BedW is equal when optimized on the tidal flat height and channel volume. In Figure 4.1c to 4.4c, the tidal amplitude results are deviated from the other parameter skill score results. The SusW, RDC and RDW only show small variations in the skill score outcomes for the different simulations, whereas the skill score for the tidal amplitude shows more variation. The variation in skill score for tidal amplitude is smallest for the tidal flat height. One of the values of the tidal amplitude is 0.7, which is the minimal tidal amplitude. In the total area, sub-area and tidal channel volume optimization the minimum amplitude scores the best skill score of all tidal amplitude values. For the tidal flat height optimization, this is the other way around. The minimal value for tidal amplitude induces the least changes in water and sediment transport of all used amplitude values. Since the skill score makes use of a zero-change reference the minimal value for amplitude receives a larger skill score than the other tidal amplitude simulations. For the tidal flat height, the situation is different. In the model, there is always sedimentation taking place at the island borders, although this is not the case in reality. In the division between a tidal channel and tidal flat, these parts along the island borders are said to be tidal flats. Since the minimal tidal amplitude does not predict as much sedimentation at the island borders as the other values, this gets a smaller skill score than the other tidal amplitude simulations. It is concluded that the tidal

amplitude does show a lot of variation. However, there is already much knowledge on the tidal amplitude in the area. This makes it a bit obvious that the tidal amplitude that does not occur frequently gives worse values for the skill score. Since it is known which tidal amplitudes are less frequent, it is also known that these amplitudes have larger uncertainty in the bedlevel prediction. Therefore, it is not very useful to use this parameter in the data assimilation. The other parameters considered in the c-part of the figures are RDC, RDW and SusW. SusW and RDC do not show enough variation in their performance to be interesting in DA. Furthermore, the suspended load transport factor, SusW, influences the suspended load which is only a small amount of the total sediment used in the model. So, it only influences the model results locally. The RDW, the wave-induced bed roughness, does show some variation.So, now α_{bn}, BedW and RDW need to be further compared to make a decision.

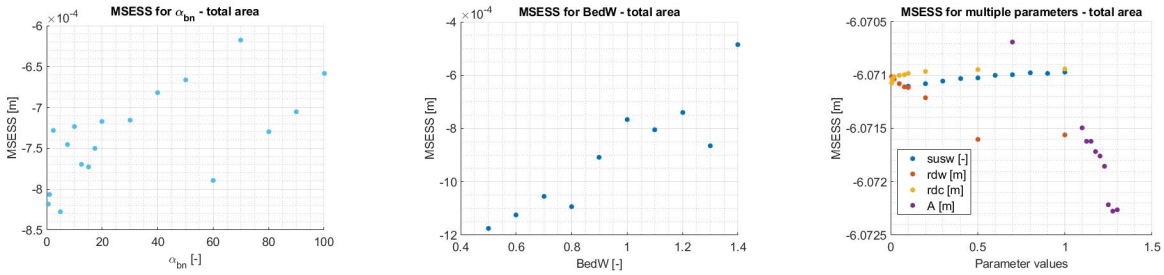

(a) (b) (c)

Figure 4.1: MSESS total area

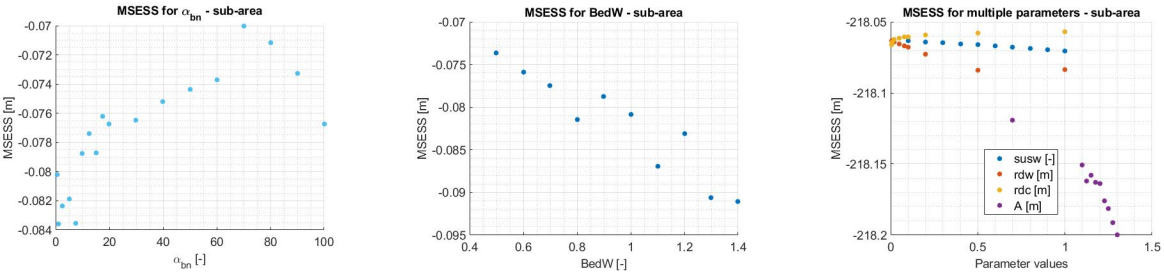

(a) (b) (c)

Figure 4.2: MSESS sub-area

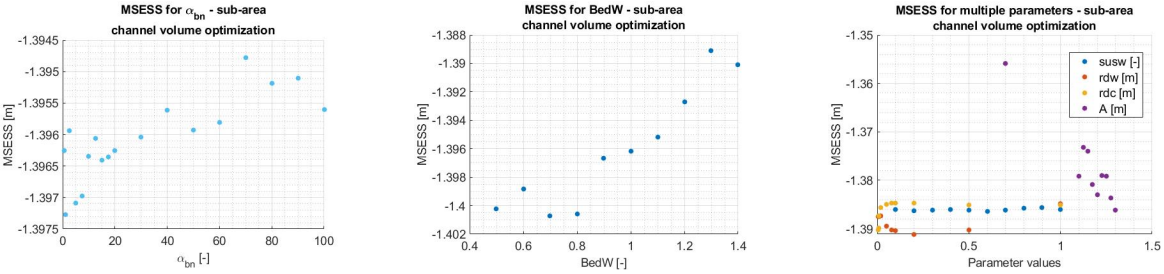

(a) (b) (c)

Figure 4.3: MSESS channel volume

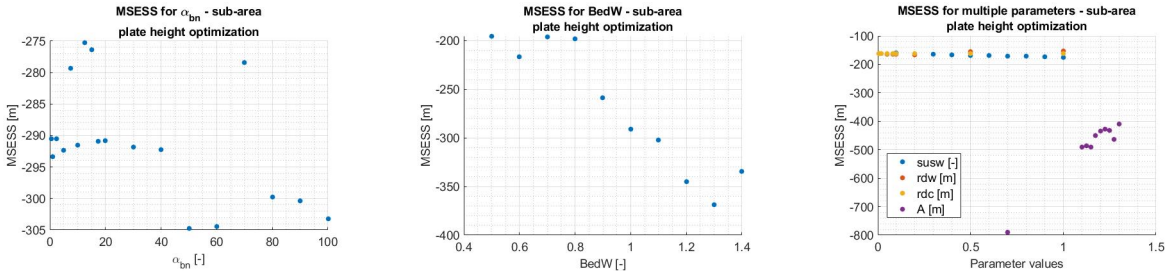

(a) (b) (c)

Figure 4.4: MSESS tidal flat height

In Table 4.1 the variances in the skill score are shown for each processing method for RDW, BedW and α_{bn}. For each processing method, the parameter with the largest variance is shown in bold text. Although the RDW shows variations in the skill score results, in Table 4.1 it is seen that its variation is the largest only for the total area, when compared to the variance in skill score BedW and α_{bn}. The RDW influences parts of the bed that are changed because of waves. However, in the model set-up, a simplified wave scheme is used. So, it might be that this parameter mostly influences the North sea area of the model, where the uncertain wave conditions determine the bed changes. BedW and α_{bn} seem to be better options and since the RDW is mostly concerned with the influence of waves, RDW is not considered any further. As seen from the bold numbers, the BedW has the largest variance when optimized on the flat height and the channel volume. The α_{bn} has the largest variance only when optimized on the sub-area. From these results the BedW would be the most logical choice to work with, when proceeding in DA. However, the choice between α_{bn} and BedW is made using the advice of Delft3D users. The advice is to work further with α_{bn}, because this influences the ease of sediment to travel from the upside of a channel to the centre. In this way, it is an important factor in the bathymetry of the bed everywhere. Whereas, the influence of BedW is limited to areas where bedload plays an important role.

Table 4.1: The variance in the skill score results of the various parameters

Variance	Total	Sub-area	Flat height	Channel volume
BedW	4.5678e-08	3.5798e-05	**4.4715e+03**	**1.8198e-05**
RDW	**4.8718e-08**	6.4182e-05	16.1798	3.9067e-06
α_{bn}	2.9556e-09	**1.4469e-05**	76.2348	4.0232e-07

Subquestion 2

How can data assimilation be implemented to optimize a morphological model output based on bed level measurements?

4.2. Data assimilation

4.2.1. Epoch 1

The results shown in this part of the report are from the simulations performed from 1970 to 1975, started from the uniform distribution of α_{bn} values. In Figure 4.5 the observed and simulated bathymetries of epoch 1 are shown.

In Figure 4.5c the result of the simulation using α_{bn}=12.457 is shown. All simulations show an increase in bed level around the Northern island borders. This is an effect found in each simulation, although it is not seen in any observation. Trouw et al. [2012] show that this effect found in the model can be avoided by setting bedload and suspended load factors to zero. Since the simulations are started with an observation of the bed level as an initial bathymetry, the simulations make a good representation of the bed level. In the simulation, there are two small channels at the Ameland side of the tidal inlet. In the observations, these are seen as

well, but they look not so sharp as in the simulation. The same is seen, when comparing the main channel in the inlet. It seems that the channels in the observation are wider and not as deep as the channels in the simulation.
In Figure 4.5f the differences between the simulated bed level in 1975 and the observed bed level in 1975 are shown in a plot. This plot would show zero differences when the simulation perfectly predicts the 1975 bed level as it was observed. When there are positive values in the difference plot, shown in orange, this means that the observed bed level in 1975 is larger than the simulated bed level in 1975. Figure 4.5f shows positive values at the channel location, which means the bed level of the channel is predicted deeper than it was observed. In Figure 4.5d the evolution of the bed level according to the observations is shown. Positive values in this figure indicate sedimentation at that location in the period 1970-1975, whereas negative values indicate erosion. At the location of the channel, a line of erosion and a line of sedimentation is seen. This could indicate lateral movement of the channel. A channel moving towards the East, results in a deeper bed level at the East side of the original channel location. The West side of the new channel will be larger than before the channel movement, because it is now the side of the channel. So in this area, it could be that the channel was located at the location shown in orange in Subfigure 4.5d and moved to the location shown in blue in Subfigre 4.5d.
Figure 4.5e shows the difference between the 1975 simulation result and the 1970 observation. So, this is the evolution of the bed level in the period 1970-1975 according to the model. This figure would be the same as Figure 4.5d when the simulation perfectly predicts the 1975 bed level as it was observed.
To see the difference in bed level and their locations better, the cross-sections marked as A-A' and B-B' in the figures are made. The cross-sections for the prior iteration in epoch 1 are shown in Figure 4.7.

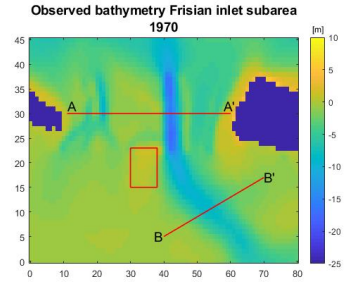

(a) 1970 observation

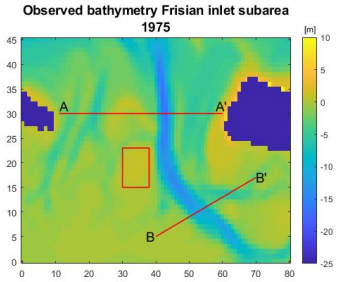

(b) 1975 observation

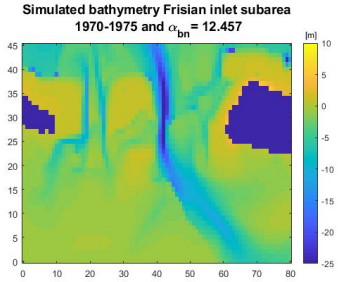

(c) 1975 simulation

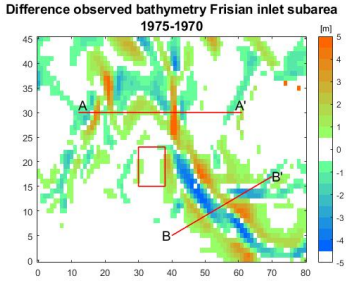

(d) Difference 1975 and 1970 observations.
Positives: deeper bedlevel observed in 1970 than observed in 1975.
Negative: shalsmaller bedlevel in 1970 than in 1975.

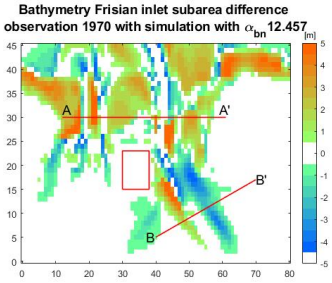

(e) Difference 1975 simulation and 1970 observation.
Positive: deeper bedlevel in simulation than observed in 1970.
Negative: shalsmaller bedlevel in simulation than observed in 1970.

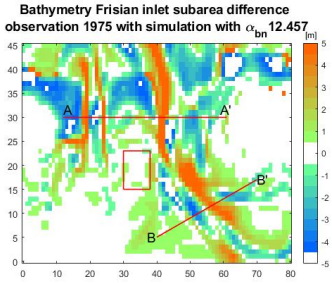

(f) Difference 1975 observation and simulation.
Positive: deeper bedlevel in simulation than observed in 1975.
Negative: shalsmaller bedlevel in simulation than observed in 1975.

Figure 4.5: Bathymetry and difference plots for epoch 1 - subarea

Prior

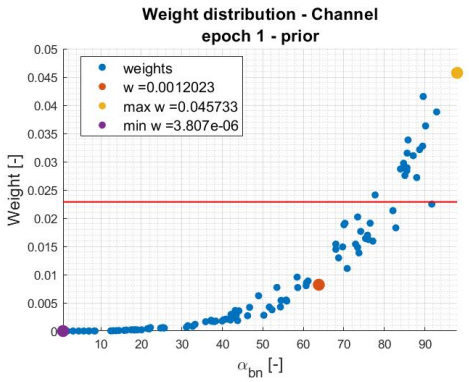

Figure 4.6: Weight as a function of the α_{bn} value for each particle. Each blue dot represents a particle. The red line represents the threshold between particles considered relevant (above the line) and particles that are discarded (below the line).

In figure 4.7a and 4.7b the 1970 and 1975 observations are shown in purple and green dots, respectively. The lines represent the 100 simulations. The simulations are close to the observations and the variation between the simulations is limited to a few locations. In the tidal inlet cross-section, the variation between simulations is found between x-location 15 and 28. At x-location 42 a channel is found in both, the simulations and in the observations. However, the predicted bed level of this channel is almost -35 meter, whereas the observed bed level is -16 meter at its deepest point. In Figure 4.7b the variation between the simulation is seen at y-location 48 to 53 and y-location 62 to 67. The depth of the predicted and observed channel in cross-section B is closer to the observation than is shown in cross-section A. The 1970 and 1975 observed bathymetry in Figure 4.5a and 4.5b show that the channel is smaller and deeper in the tidal inlet than in the Wadden area. So, the steepness of the channel in the tidal inlet, might make the bedlevel prediction more difficult. The location that shows variation in the simulations will influence the weight distribution. In Figure 4.6 the weights that are assigned to the particles are shown. The red line represents a threshold: all particles above the line are considered relevant and all particles below the line are discarded. In other words, the effective weight of the particles above the line is above 0.5. By discarding these particles, new particles are needed which are created by resampling. In the figure, the particle with the maximum weight is shown in yellow and the particle with the minimum weight is shown in purple. The particle that is shown in red, is a particle with α_{bn} value 63.826. In Figure 4.7c and 4.7d only these three particles are shown in the cross-section. This shows that the simulation with the maximum weight is closer to the observations than the simulation which received the minimum weight. The simulation in yellow was simulated using an α_{bn} of 97.9678 and was assigned the maximum weight. The difference in the simulation results between these two is found between x-location 16 and 23 in cross-section A and between y-location 60 and 68 in cross-section B. These are only small variations between the red and yellow simulations, which lead to a significant difference in their assigned weight. A weight is larger when the probability that the observation is true given the model state is large. So, apparently the small difference in prediction of the bedlevel results in a change in the probability of the observation being true. A larger weight means that this particle contributes more to the estimate. The yellow particle is the maximum weight, while the red particle is below the threshold of relevant particles. In this prior iteration, the maximum weight is assigned to the maximum α_{bn} value in the distribution and the minimum weight is assigned to the minimum α_{bn} value in the distribution. So, the purple line in Figure 4.7c and 4.7d is the minimum weight and minimum α_{bn} value and the yellow line is the maximum weight and maximum α_{bn} value.

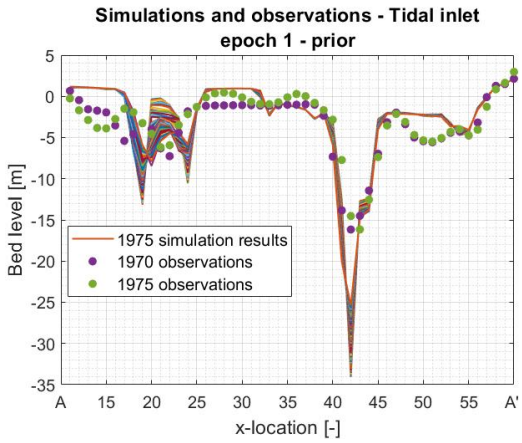

(a) Cross-section through the tidal inlet for all simulations and the observations in 1970 and 1975.

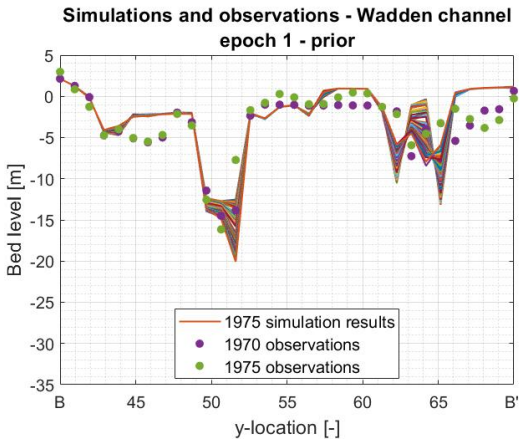

(b) Cross-section of three simulations and the observations in 1970 and 1975.

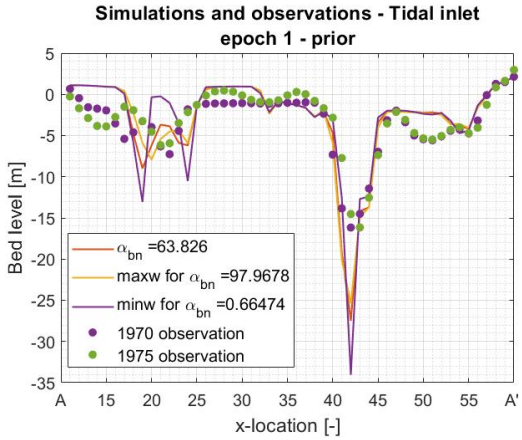

(c) Cross-section through the tidal inlet for three simulations and the observations in 1970 and 1975.

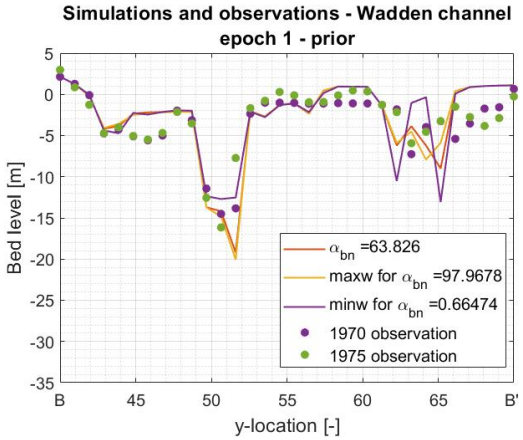

(d) Cross-section through the Wadden channel for three simulations and the observations in 1970 and 1975.

Figure 4.7: Cross-section Wadden channel 1970-1975

In Figure 4.9 the resulting distribution of α_{bn} after resampling is shown. In Figure 4.9a and 4.9c the result optimized on the channel cross-sections is shown. In Figure 4.9a the original uniform distribution is shown in blue and the new found distribution in pink. However, the new distribution is in only a small range so it is not clearly visible. Therefore, it is also shown separately in Figure 4.9c. In this figure, the largest frequency is around an α_{bn} of 98. But some smaller values are found between 84 and 91. And one α_{bn} just below 78 and one of approximately 93. So, the particle filter clearly steers the model towards larger values of α_{bn}, all values below 78 are not considered anymore in the next iteration. Note, that the maximum α_{bn} value for the next iteration is larger than the maximum α_{bn} in the original uniform distribution. By shifting the upper boundary up, it is possible for resamples to have a larger value for α_{bn}. This means that the value of α_{bn} that leads to a probable bedlevel estimate might be out of the original chosen range for α_{bn}. In Figures 4.9b and 4.9d the resulting distribution for the tidal flat is shown. It was stated before that it is expected that this area will not steer the distribution, because no changes take place in the tidal flat area. Apparently, the selected area

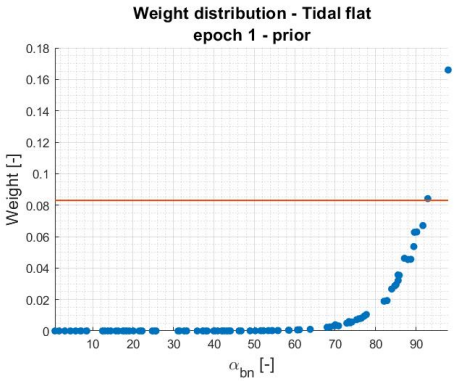

Figure 4.8: Weight as a function of the α_{bn} value for each particle. Each blue dot represents a particle. The red line represents the threshold between particles considered relevant (above the line) and particles that are discarded (below the line). After processing prior simulations of epoch 1.

does have some sediment transport taking place, which could be a small amount or on a limited location. This change in bed level does steer the distribution even more extreme towards values an α_{bn} of around 98. The weight distribution that leads to this distribution of α_{bn} is shown in Figure 4.8. The distribution of α_{bn} values as a result of the channel optimization, as shown in Figure 4.9c, is used in the next iteration in epoch 1.

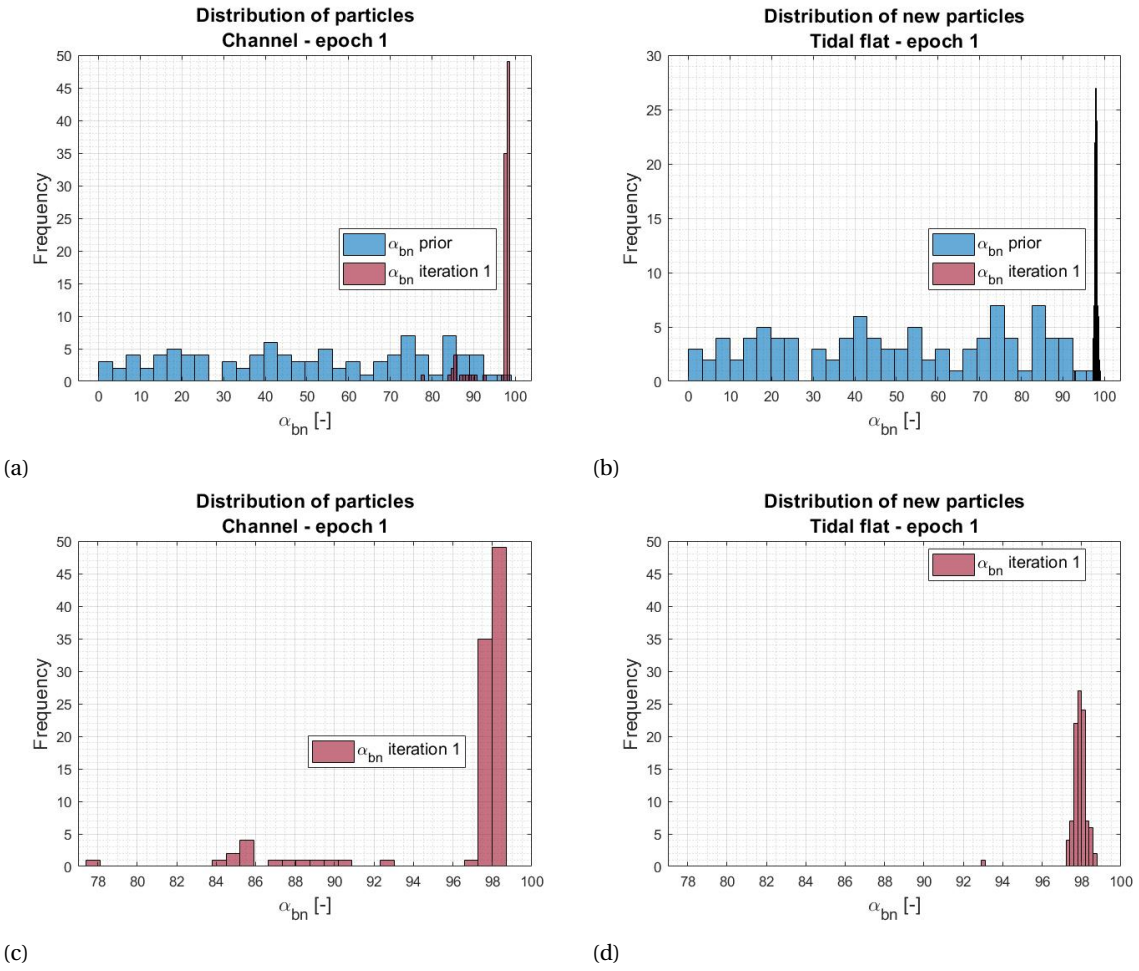

Figure 4.9: The frequency of α_{bn} values in the prior distribution (blue) and the distribution used in first iteration (pink). In a) for optimization on tidal channels and in b) for optimization on tidal flats. Only the distribution for iteration 1 is shown in c) optimized on tidal channels and d) optimized on tidal flats.

Iteration 1

In Figure 4.11 the cross-sections after the first iteration are shown. A result of the iteration is that the hundred simulations are now closer to each other. It seems that by the resampling the worst performing simulations are filtered out. However, when considering the deep channel in cross-section A, the simulations did not get any closer to the observations. Again in Subfigures 4.11c and 4.11d the cross-sections for the particles with the minimum weight, maximum weight and the particle with an α_{bn} value close to that of the maximum weight particle are shown. From Figure 4.10 it is seen that the particle shown in red has an α_{bn} value very close to the particle with the maximum weight, shown in yellow. The big difference in their assigned weights is a result of the small variation in the predicted bed level as seen in Figures 4.11c and 4.11d. In the assigning of weights, the difference between simulation and observation is taken into account. So, a simulation can predict the bedlevel well, but shifted it a bit towards the right. This then results in a small weight and a small relative importance for that simulation. So, a simulation that is subjectively seen as a good prediction of the bedlevel, can be seen as a poor prediction by the particle filter. In the prior iteration, it was seen that the maximum weight was assigned to the particle with the maximum α_{bn} value. In this iteration, this is not the case.

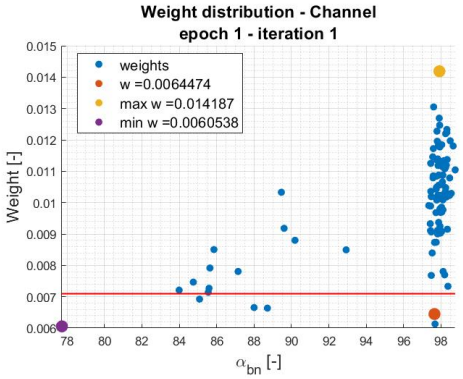

Figure 4.10: Weight as a function of the α_{bn} value for each particle. Each blue dot represents a particle. The red line represents the threshold between particles considered relevant (above the line) and particles that are discarded (below the line). After processing first iteration simulations of epoch 1.

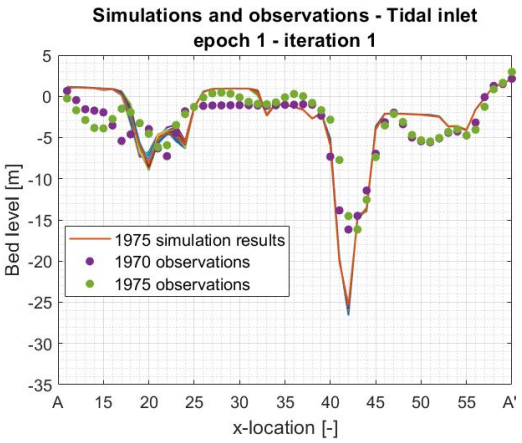

(a) Cross-section through the tidal inlet for all simulations and the observations in 1970 and 1975.

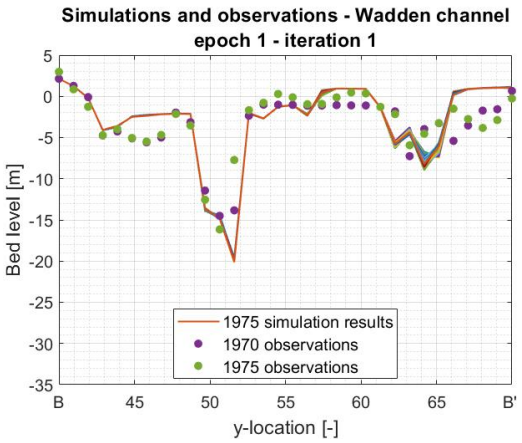

(b) Cross-section through the Wadden channel for all simulations and the observations in 1970 and 1975.

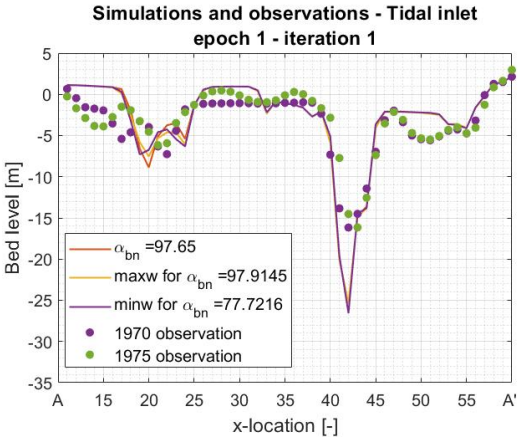

(c) Cross-section through the tidal channel for three simulations and the observations in 1970 and 1975.

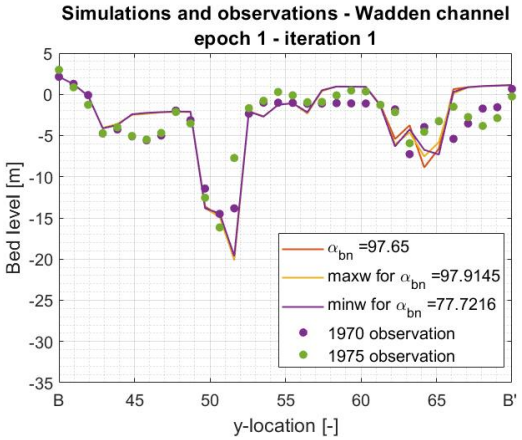

(d) Cross-section through the Wadden channel for three simulations and the observations in 1970 and 1975.

Figure 4.11: Cross-section Wadden channel 1970-1975

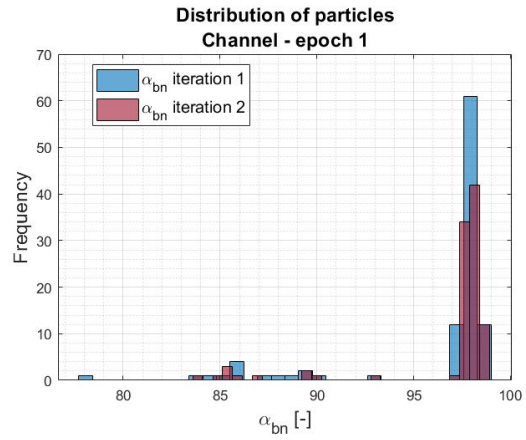

(a)

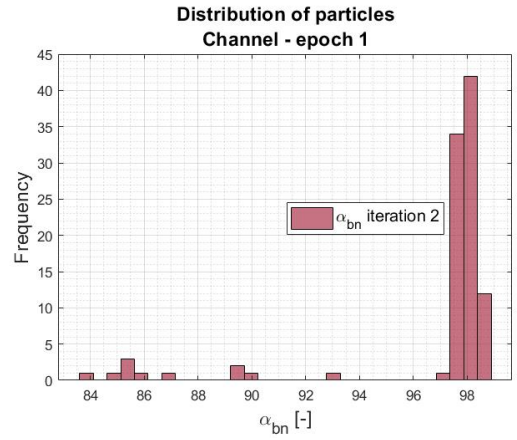

(b)

Figure 4.12: The frequency of α_{bn} values in the first distribution (blue) and the distribution used in the second iteration (pink) for optimization on tidal channels. In a) both distributions, in b) only the distribution for iteration 2.

Iteration 2

In iteration 2 the maximum weight is assigned to the particle with α_{bn} 98.3111. In iteration 1 the particle that is assigned the maximum weight has α_{bn} value 97.9145. In previous iterations, the particle with the minimum α_{bn} value got the minimum weight. This is different in this second iteration, where the minimum weight is assigned to the particle with α_{bn} 98.1383. This is a value that is very close to the value of the relevant particles that have an effective weight above 0.5. When considering the maximum and minimum weight particles in Figure 4.14c and 4.14d, it is seen that the minimum weight particle simulates two peaks. One peak is located in the A cross-section at x-location 17 and the other peak is located in the B cross-section at y-location 67. Since this simulated peak is not seen in the observed bed level, this particle receives a small weight. In general the spread of the weights is decreased in the iterations, which can be seen in the weight distribution shown in Figures 4.6, 4.10 and 4.13. This is a result of the 100 simulation results that are closer together. This evolution can be seen when comparing the cross-sections showing all simulations.

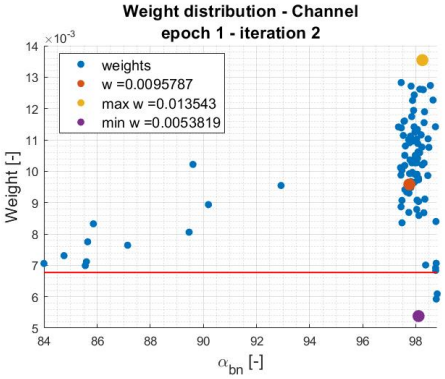

Figure 4.13: Weight as a function of the α_{bn} value for each particle. Each blue dot represents a particle. The red line represents the threshold between particles considered relevant (above the line) and particles that are discarded (below the line). After processing second iteration simulations of epoch 1.

In Figure 4.15 the previous and new distribution of α_{bn} values over the particles is shown. This shows that there is only a small evolution of the distribution of weights in this iteration. One particle moves to a larger α_{bn} range. This distribution will not be simulated anymore, because the number of iterations for the processing of simulations is set to three times within one epoch. The processing to obtain this new distribution was the third iteration. The number of iterations can not be exceeded, since the factor a, as used in equation 2.10, to process the results was set to 3.

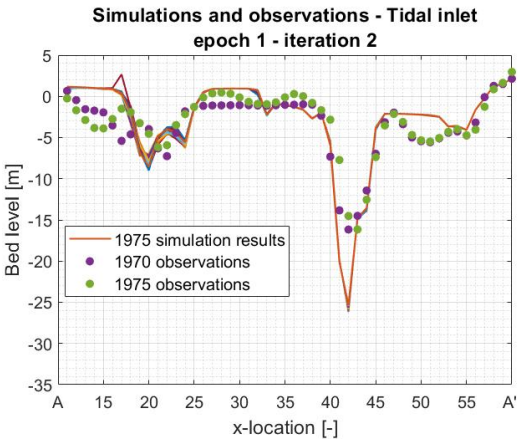

(a) Cross-section through the tidal inlet for all simulations and the observations in 1970 and 1975.

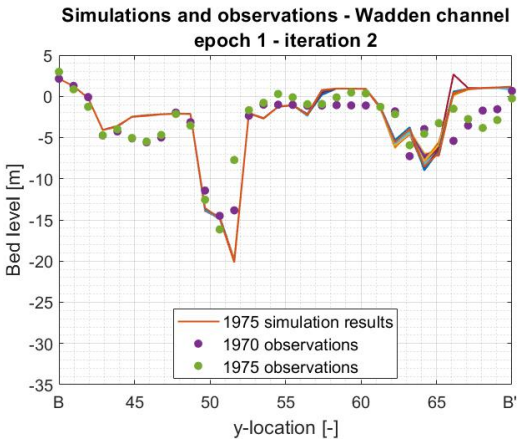

(b) Cross-section through the Wadden inlet for all simulations and the observations in 1970 and 1975.

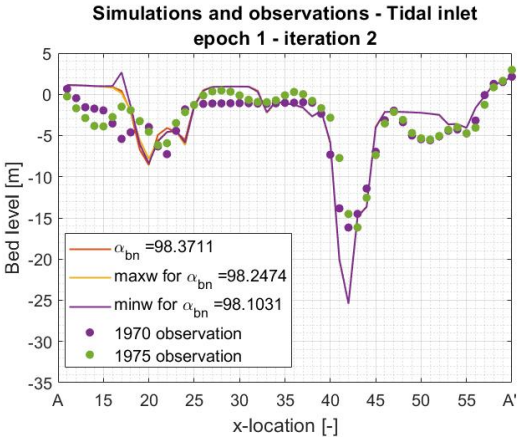

(c) Cross-section through the tidal inlet for three simulations and the observations in 1970 and 1975.

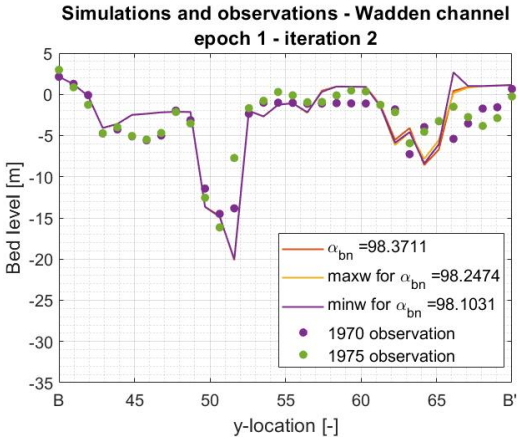

(d) Cross-section through the Wadden inlet for three simulations and the observations in 1970 and 1975.

Figure 4.14: Cross-section channels 1970-1975

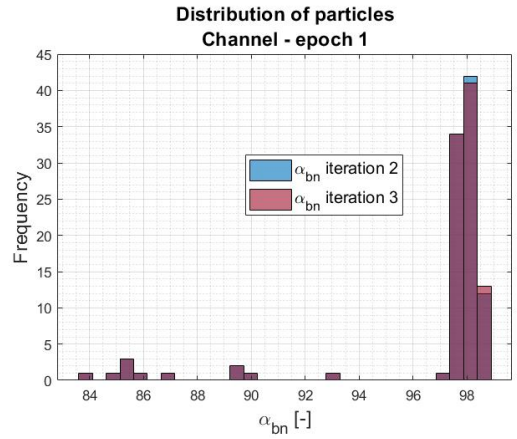

(a)

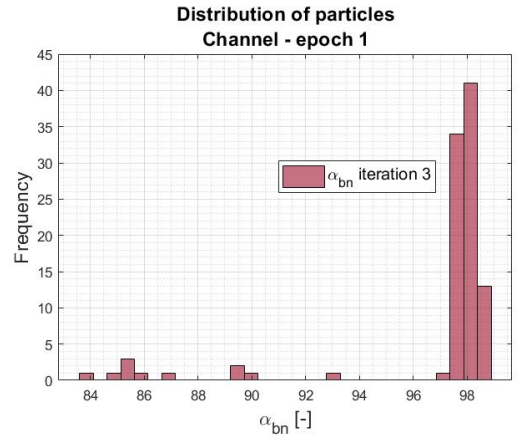

(b)

Figure 4.15: The frequency of α_{bn} values in the second iteration distribution (blue) and the distribution used in the third iteration (pink) for optimization on tidal channels. In a) both distributions, in b) only the distribution for iteration 3.

End epoch 1

In epoch 1 the results show a convergence of the distribution for α_{bn} values, which is shown in Figure 4.16. From the distribution in a range between 0.6647 and 97.9678, it converges in three iterations to a distribution between 83.9910 and 98.5992. So, by applying the particle filter the distribution converges towards the large values of the initial distribution. The smaller boundary of the distribution moves up considerably in one iteration, whereas the upper boundary does not change a lot throughout the iterations. In the cross-sections of the prior simulation, (Figure 4.7), the simulations are far off from the observations at locations of tidal channels. The combination of the grid resolution with the steep slope, could be a cause of the difficulty to predict the bed level at these locations. Though, a finer grid is not ideal, because this will increase the computational cost significantly.

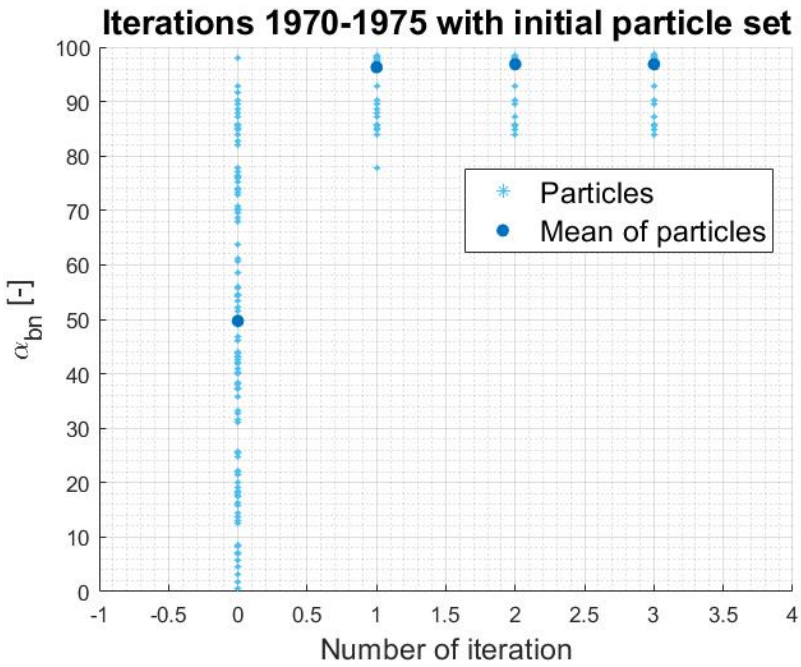

Figure 4.16: The distribution of particles (light blue start) over α_{bn} values (on the vertical axis) for the iterations in epoch 1 (horizontal axis). The blue dots are the mean of particles.

Table 4.2: Values for α_{bn} in epoch 1

	Minimum α_{bn}	Maximum α_{bn}	Mean α_{bn}
Iteration 0	0.6647	97.9678	49.7111
Iteration 1	77.7216	98.5538	96.2933
Iteration 2	83.9910	98.5877	96.8567
Iteration 3	83.9910	98.5992	96.8610

At the end of the epoch, a weighted average bed level is visualized, which is shown in Figure 4.17a. The difference between the weighted average bed level and the 1970 observation is shown in Figure 4.17b. This represents the evolution of the bed level between 1970 and 1975 according to the weighted average bed level of the simulations at the end of epoch 1.

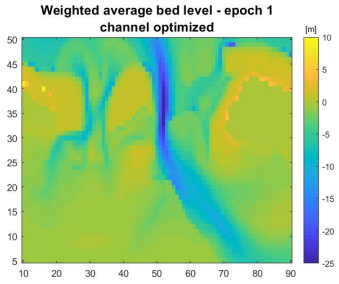

(a) 1975 weighted average bed level

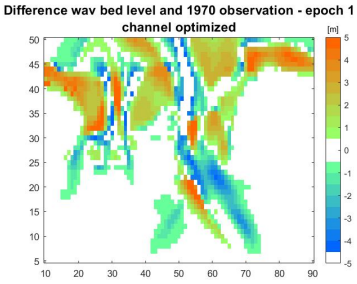

(b) Difference 1975 weighted average simulation and 1970 observation. Positive values indicate a deeper bedlevel in the 1970 observation.

Figure 4.17: Bathymetry and difference plots for epoch 1.

4.2.2. Epoch 2

The second epoch is started using the same initial uniform distribution of α_{bn} values as is used in epoch 1. By doing so, a comparison between the different epochs is possible. The initial bathymetry given to the simulation is the 1975 bed level measurements.

Prior

In Figure 4.20 cross-section A and B are shown for the prior simulation in epoch 2. The prediction of the deep channel in cross-section A is closer to the observation than was seen in the prior simulation of epoch 1. The difference between the simulations and observations is around 2 to 6 meter at the location of the deep channel in cross-section A. The simulations predicted the depth of the deep channel quite close to the observed depth in both cross-sections, A and B. In the observed bathymetry of 1979 (Figure 4.19) the width and depth of the channel are similar in the tidal inlet (cross-section A) and in the Wadden Sea (cross-section B). This might result in the predictions performing well for the deep channel in both cross-sections. The channel is in both cross-sections not extremely narrow or deep, as seen in the tidal inlet in the first epoch. The variation in the simulations is largest at the locations with the smaller channels, which was seen in epoch 1 as well. In cross-section A the simulations are much closer to the observations at x-location 50 and A' than in the prior of epoch 1. The same is the case for y-location B to 48 in cross-section B. At these locations all simulations predict the observed bed level very well. The cross-sections do not show one simulation that is performing much better than others, which is also seen in the weight distribution shown in Figure 4.18. This figure shows that the weights assigned over the particles are quite evenly spread. The weights being more evenly spread than was the case in the prior iteration of epoch 1 could be a result of less variation in bedlevel prediction of the simulation. Another cause can be the fact that the simulations are closer to the observations at the location of the deep channel. Since, the difference between simulation and observation is small, the probability density of the observations given the model state is large (see equation 2.10). And the difference of a simulation with the observation will be close to the difference of another simulation with the observation, because the simulation results are close to each other. This leads to a probability density of observation given the model state to be close to the probability density for other simulations. In the calculation of the weights (equation 2.12) this leads to evenly spread weights over the particles. In almost the whole range of the initial distribution, particles are relevant, except for the values larger than α_{bn} 70. The larger values are all discarded in the new distribution. This is an unexpected result, after seeing that in epoch 1 the probability distribution for α_{bn} was focused around the largest values in the initial distribution.

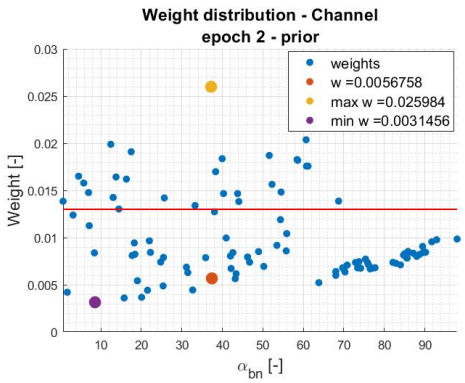

Figure 4.18: Weight as a function of the α_{bn} value for each particle. Each blue dot represents a particle. The red line represents the threshold between particles considered relevant (above the line) and particles that are discarded (below the line). After processing prior simulations of epoch 2.

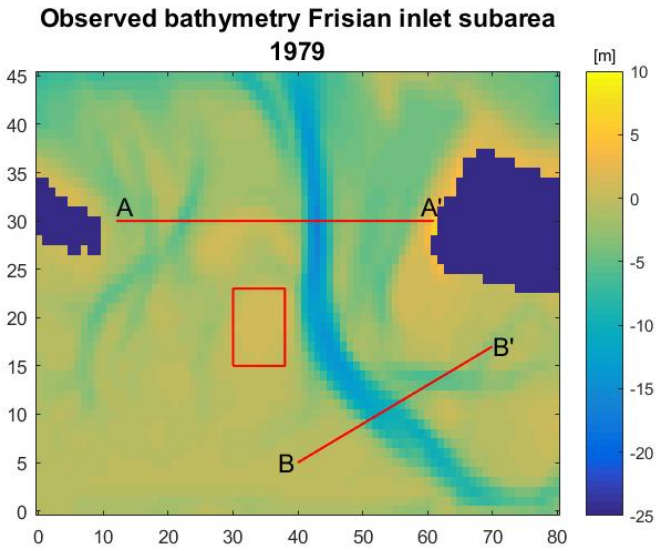

Figure 4.19: 1979 observation

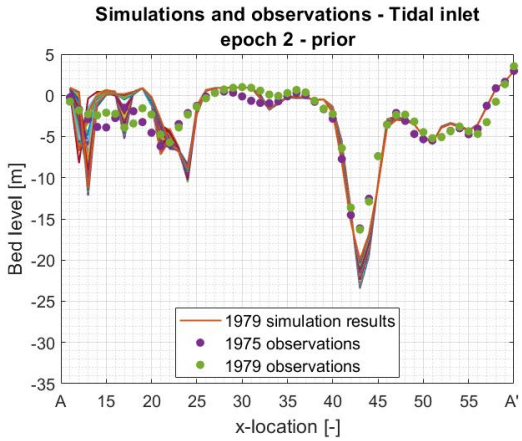

(a) Cross-section through the tidal inlet for all simulations and the observations in 1975 and 1979.

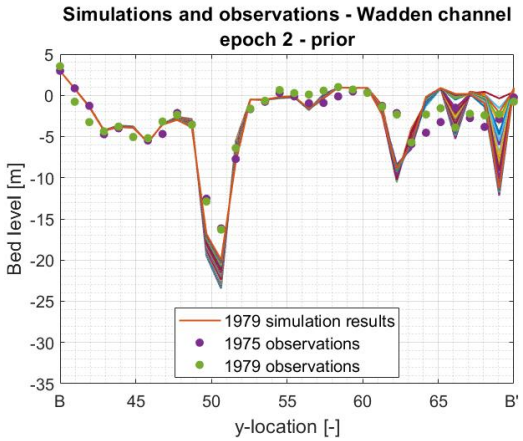

(b) Cross-section through the Wadden inlet for all simulations and the observations in 1975 and 1979.

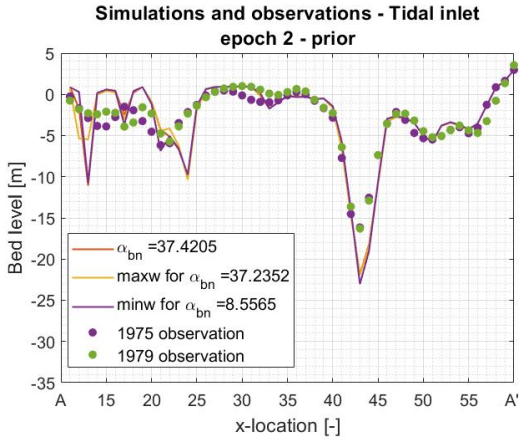

(c) Cross-section through the tidal inlet for three simulations and the observations in 1975 and 1979.

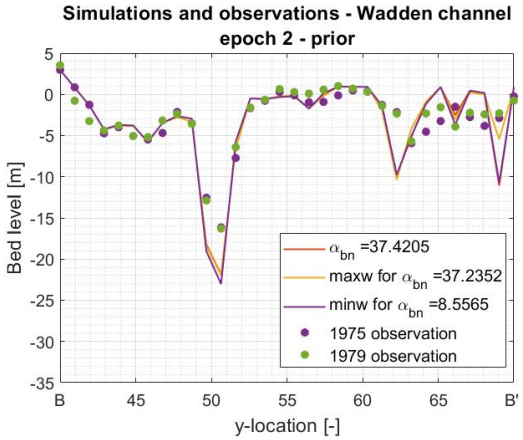

(d) Cross-section through the Wadden inlet for three simulations and the observations in 1975 and 1979.

Figure 4.20: Cross-section channels 1975-1979

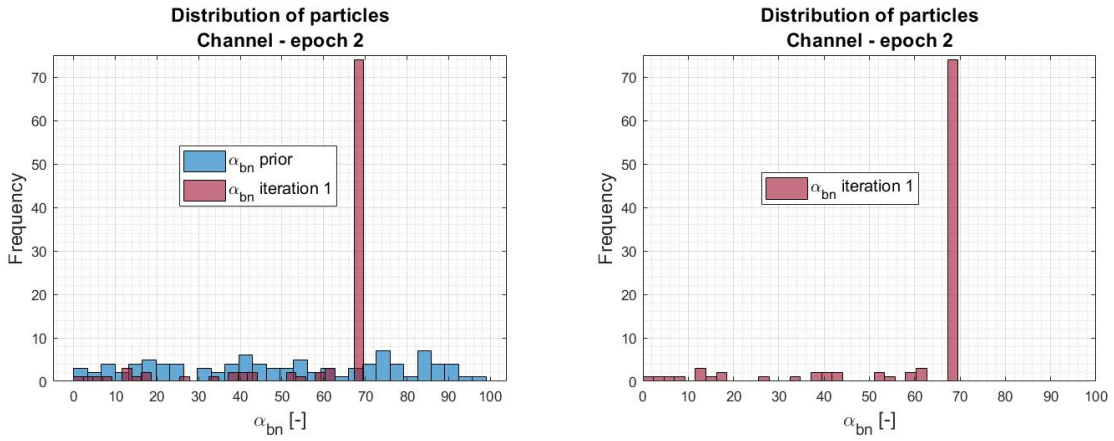

(a) (b)

Figure 4.21: The frequency of α_{bn} values in the prior distribution (blue) and the distribution used in the first iteration (pink) for optimization on tidal channels. In a) both distributions, in b) only the distribution for iteration 1.

Iteration 1

In the cross-sections shown in Figure 4.23 there is less variation in the simulation shown at the location of the deep channel, when compared to the simulations shown in Figure 4.20. There is also a difference between the prior and iteration 1 of this second epoch, when comparing the locations with the smaller channel, which is x-location A to 20 and y-location 65 to B'. In this first iteration, there is a gap between simulations that predict very shalsmall channels and simulations that predict very deep channels. This is best seen between y-location 67 and B'. So, the large values of α_{bn} that are thrown out in the previous iteration, were responsible for simulating that bed levels. In Figure 4.22 it is seen that most particles with an effective weight above 0.5 are found in the values for α_{bn} above 60. The old and new distribution for α_{bn} are shown in Figure 4.24.

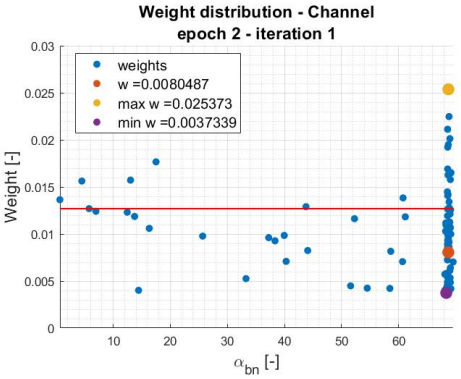

Figure 4.22: Weight as a function of the α_{bn} value for each particle. Each blue dot represents a particle. The red line represents the threshold between particles considered relevant (above the line) and particles that are discarded (below the line). After processing the first iteration simulations of epoch 2.

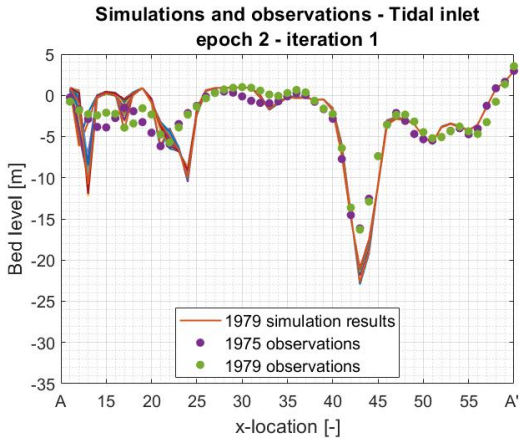

(a) Cross-section through the tidal inlet for all simulations and the observations in 1975 and 1979.

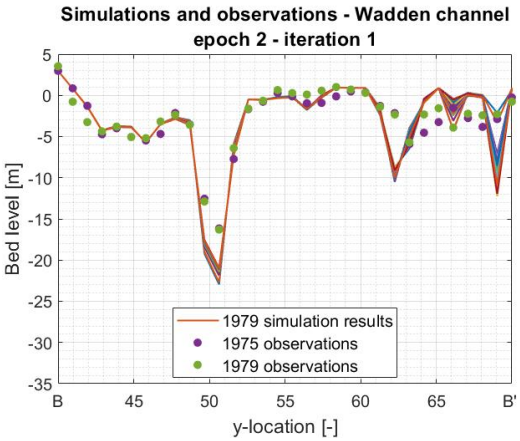

(b) Cross-section through the Wadden channel for all simulations and the observations in 1975 and 1979.

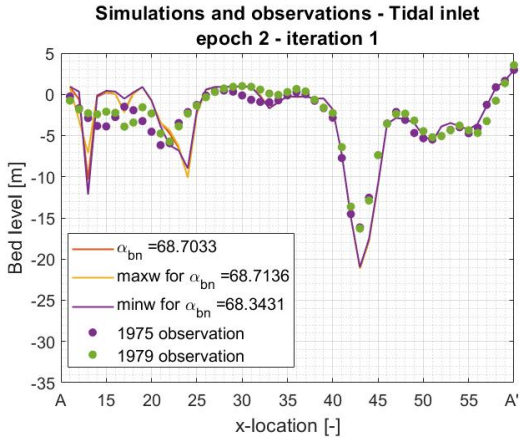

(c) Cross-section through the tidal inlet for three simulations and the observations in 1975 and 1979.

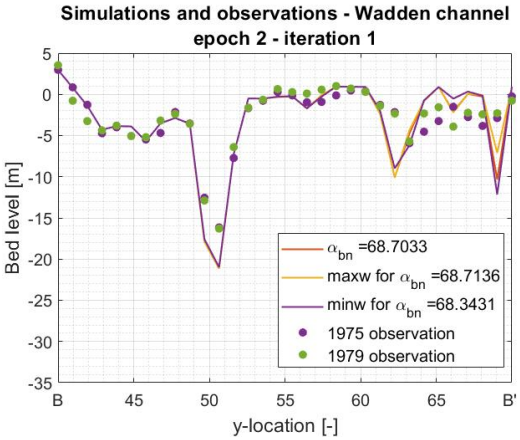

(d) Cross-section through the Wadden channel for three simulations and the observations in 1975 and 1979.

Figure 4.23: Cross-section channels 1975-1979

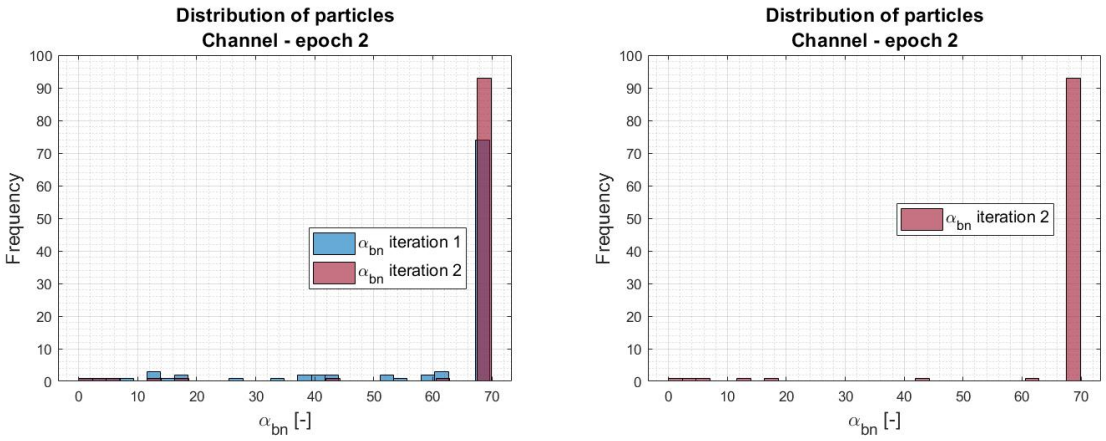

(a) (b)

Figure 4.24: The frequency of α_{bn} values in the first iteration distribution (blue) and the distribution used in the second iteration (pink) for optimization on tidal channels. In a) both distributions, in b) only the distribution for iteration 2.

Iteration 2

In the cross-sections in Figure 4.26 the simulations that predicted shalsmall channels at the location of the small channels are not seen anymore. Besides, there is negligible variation in the prediction of the depth of the deep channel. The shift towards the larger values in the α_{bn} distribution is continued in this iteration. In Figure 4.25 it is shown that the resulting distribution only contains the α_{bn} values of around 69. This results in the distribution shown in Figure 4.27, which is spread between 68.9670 and 69.9083.

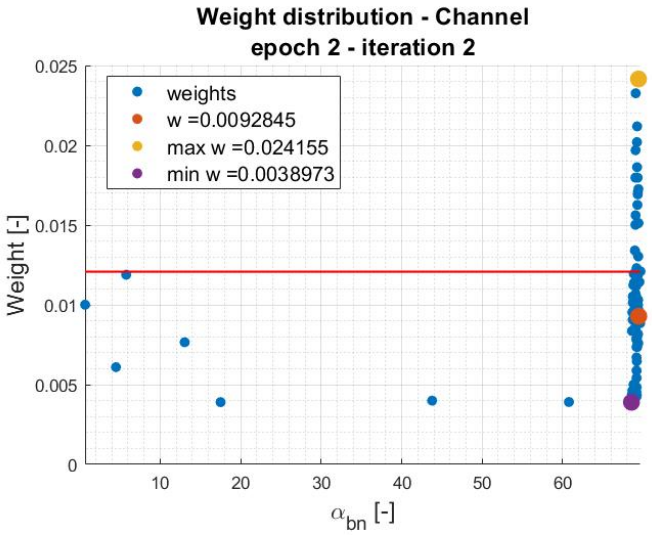

Figure 4.25: Weight as a function of the α_{bn} value for each particle. Each blue dot represents a particle. The red line represents the threshold between particles considered relevant (above the line) and particles that are discarded (below the line). After processing the second iteration simulations of epoch 2.

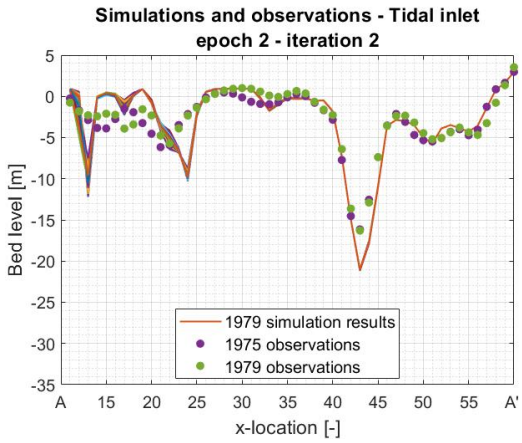

(a) Cross-section through the tidal inlet for all simulations and the observations in 1975 and 1979.

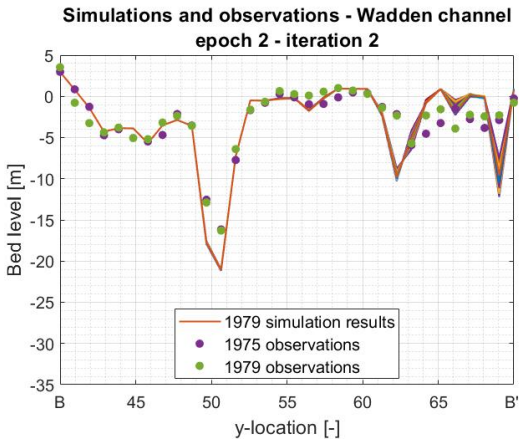

(b) Cross-section through the Wadden inlet for all simulations and the observations in 1975 and 1979.

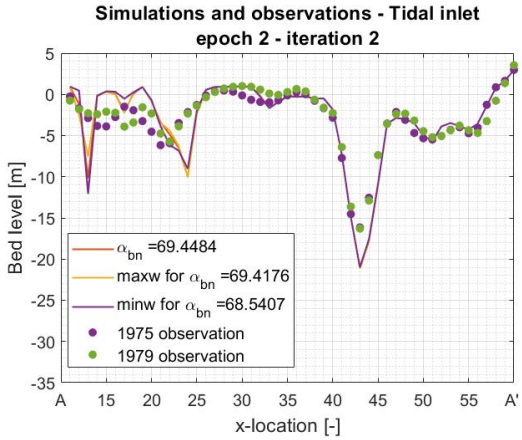

(c) Cross-section through the tidal inlet for three simulations and the observations in 1975 and 1979.

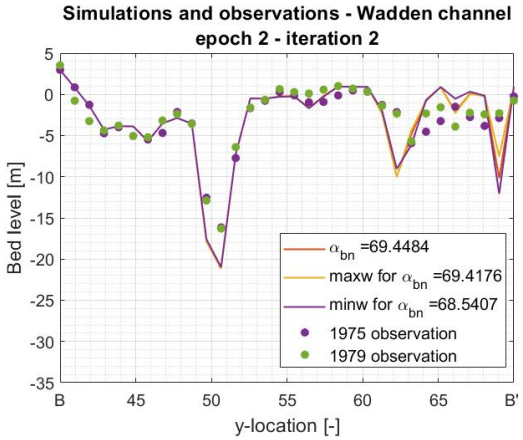

(d) Cross-section through the Wadden inlet for three simulations and the observations in 1975 and 1979.

Figure 4.26: Cross-section channels 1975-1979

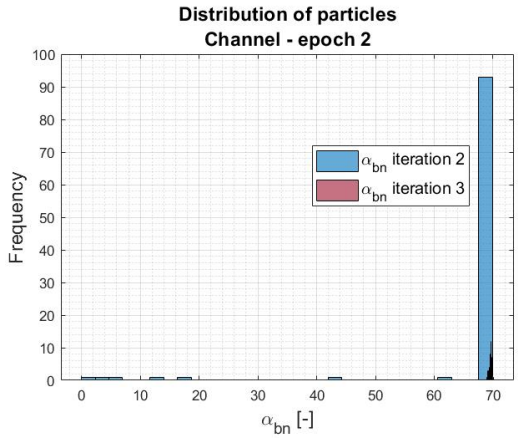

(a)

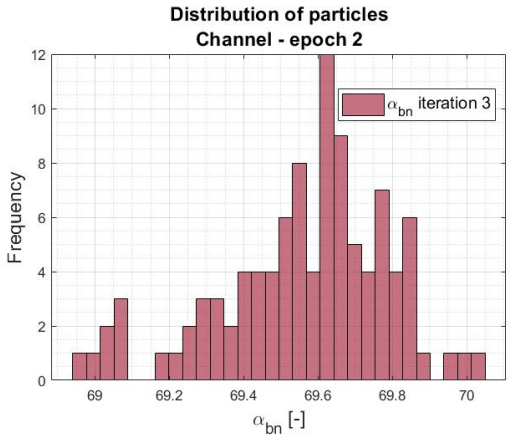

(b)

Figure 4.27: The frequency of α_{bn} values in the second iteration distribution (blue) and the distribution used in the third iteration (pink) for optimization on tidal channels. In a) both distributions, in b) only the distribution for iteration 3.

End epoch 2

To have a closer look on the evaluation of the distribution during epoch 2, the α_{bn} distributions of each iteration is shown in Figure 4.28. This figure and Table 4.3 show that the smallest α_{bn} value of the distribution remains the same until the last iteration. Whereas the largest α_{bn} value in the first iteration jumps towards 69.5563 and in the next iterations the change of this largest value is negligible.
Epoch 2 shows a convergence of the distribution for α_{bn} values as well. However, it converges to different α_{bn} values than was seen in epoch 1. The main difference between the first and second epoch is found at the location of the deep channel in cross-section A. The difference between the simulations and observation at this location is smaller in epoch 2 than in epoch 1. From the distribution in a range between 0.6647 and 97.9678 it converges in three iterations to a distribution between 68.9670 and 69.9083. The smaller boundary of the distribution did not move until the last iteration. Whereas the upper boundary moved towards 69 in the first iteration and did not change a lot after that. The evolution of the boundaries of the distribution in epoch 1 was very different. The upper boundary was large and even ended above the original upper boundary of the initial uniform distribution. The smaller boundary made a big shift to larger values in the first iteration in epoch 1. The cause of this difference might be less variation in simulation and a smaller difference between simulations and observation in epoch 2.

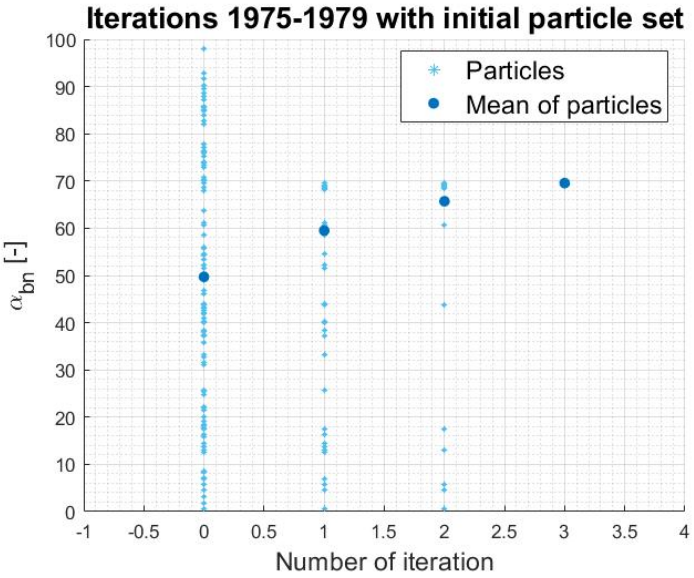

Figure 4.28: The distribution of particles (light blue start) over α_{bn} values (on the vertical axis) for the iterations in epoch 2 (horizontal axis). The blue dots are the mean of particles.

Table 4.3: Values for α_{bn} in epoch 2

	Minimum α_{bn}	Maximum α_{bn}	Mean α_{bn}
Iteration 0	0.6647	97.9678	49.7111
Iteration 1	0.6647	69.5563	59.4988
Iteration 2	0.6647	69.6624	65.7250
Iteration 3	68.9670	69.9083	69.5622

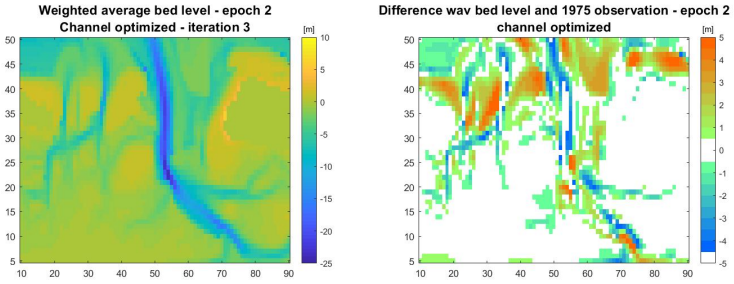

(a) 1979 weighted average bed level

(b) Difference 1979 weighted average simulation and 1975 observation

Figure 4.29: Bathymetry and difference plots for epoch 2

4.2.3. Epoch 3

Only two iterations are performed in the third epoch, due to limited time. Note, that factor a in the likelihood equation 2.10, which equals the number of iterations, is still set to 3. This is done, because the goal was to perform this epoch also with three iterations. And in this way, though only two iterations are performed, the results of these first two iterations can be compared with the first two iterations of the previous epoch.

Prior

The locations that were predicted very well in the prior of epoch 2, are predicted worse in this iteration. These locations are x-location 50 to A' in Figure 4.32a and y-location B to 48 in Figure 4.32b. The prediction of the deep channel in both cross-section is similar to the prediction made in epoch 2. Again in Figure 4.31 the bedlevel observation made in 1982 is shown. This shows that the main channel is a bit smaller in the tidal inlet than in the Wadden Sea. However, the channel in the tidal inlet is not as narrow and deep as seen in the 1970 and 1975 observation for epoch 1. In the simulations of this iteration, again there is not one particle that clearly performs better than the others. However, there is a distribution of weights found, where larger weights are assigned to the large values of α_{bn}. The weight distribution shown in Figure 4.30 is very similar to the distribution found in the prior of epoch 1. The difference is that the weights in this distribution are smaller than the weights found in the prior of epoch 1. In epoch 1 the maximum weight was close to 0.05, whereas in this distribution the maximum weight is close to 0.03. In Figure 4.33 the old and new distribution of α_{bn} are shown. This shows that the frequency of the largest peak decreases from 59 to 49 and the smallest α_{bn} value is discarded. The distribution of values changes a bit, but in general the distribution for the next iteration does not change a lot.

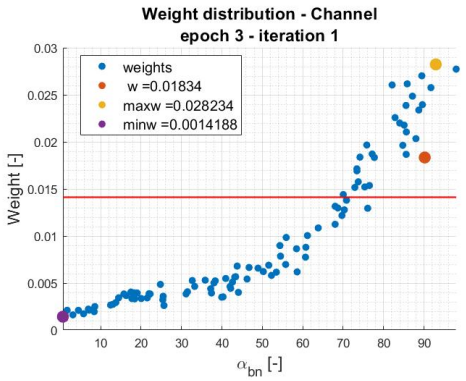

Figure 4.30: Weight distribution after prior

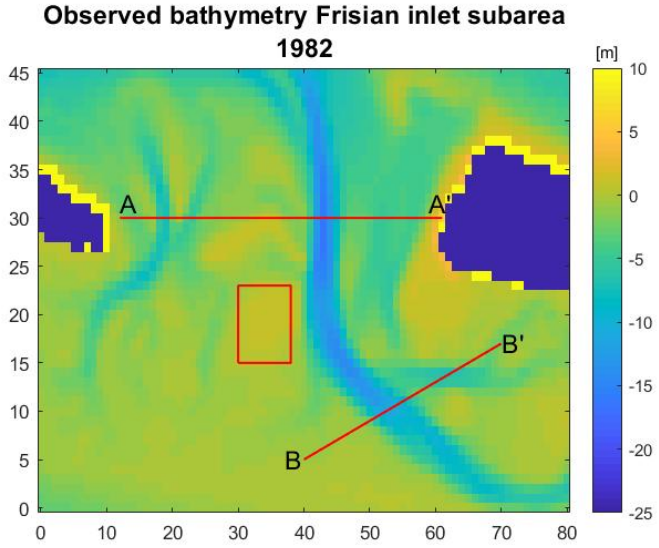

Figure 4.31: 1982 observation

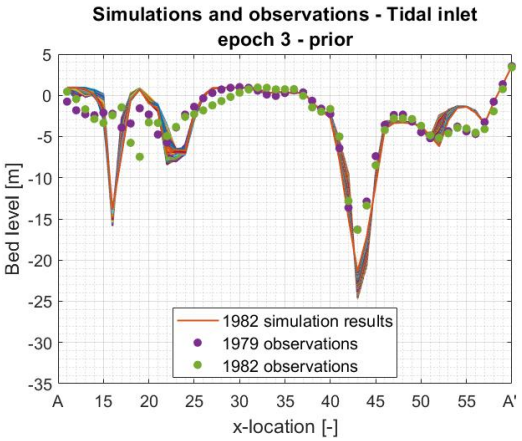

(a) Cross-section through the tidal inlet for all simulations and the observations in 1979 and 1982.

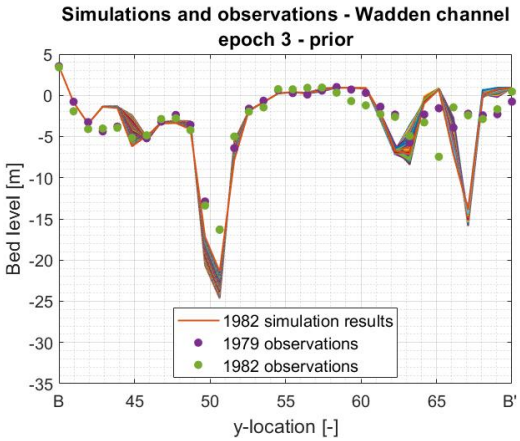

(b) Cross-section through the Wadden inlet for all simulations and the observations in 1979 and 1982.

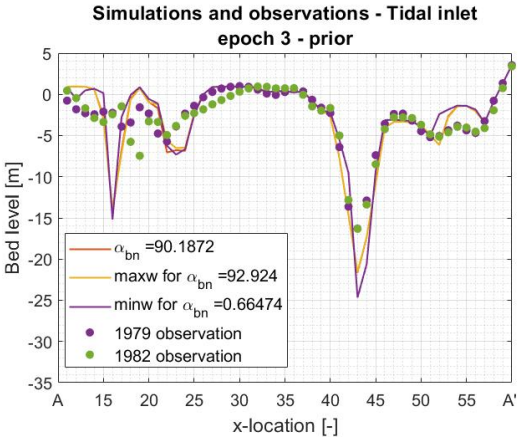

(c) Cross-section through the tidal inlet for three simulations and the observations in 1979 and 1982.

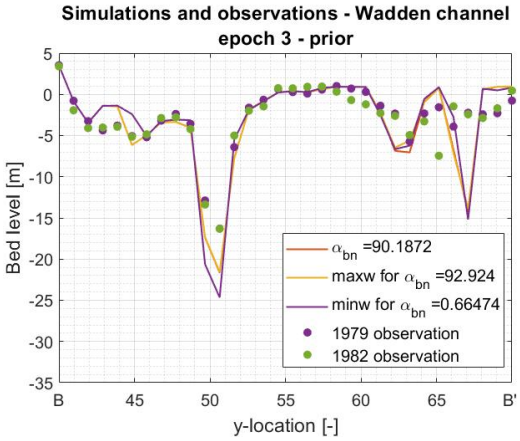

(d) Cross-section through the Wadden inlet for three simulations and the observations in 1979 and 1982.

Figure 4.32: Cross-section channels 1979-1982

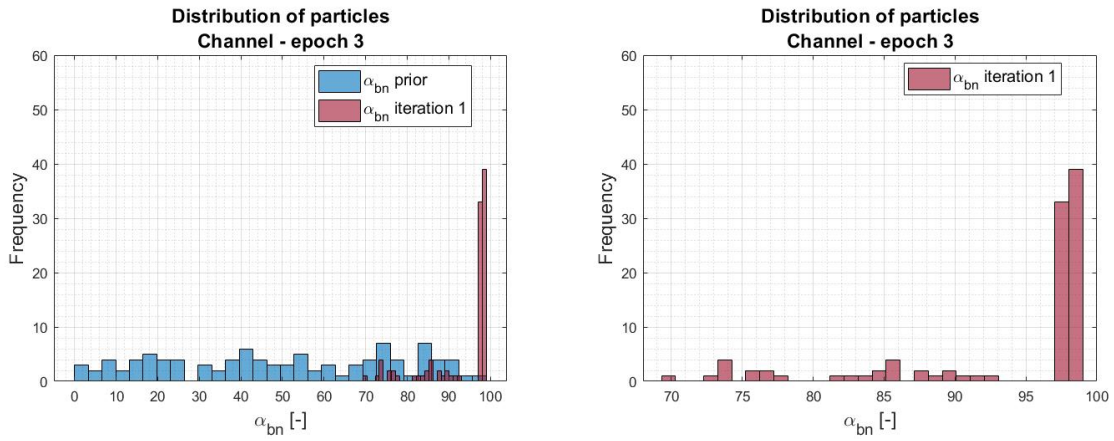

(a) (b)

Figure 4.33: Distribution of α_{bn} values over new set of particles - prior

Iteration 1

In this iteration, it is seen that using the new distribution the predicted bed levels are closer together. However, the simulations did not move towards the observations. The weight distribution in Figure 4.34 shows that all particles below 95 are relevant, except for the particle with the smallest α_{bn} value. A part of the particles with the largest α_{bn} values is discarded. The resulting distribution is still focused on the particles with a α_{bn} value close to 100. Nevertheless, there are also smaller value particles left. The largest weight was assigned to the particle using a α_{bn} value of 77.1714. So, in the new distribution, there are values found around 77 as well.

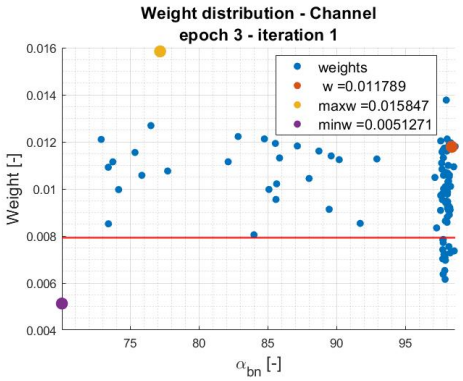

Figure 4.34: Weight distribution after iteration 1

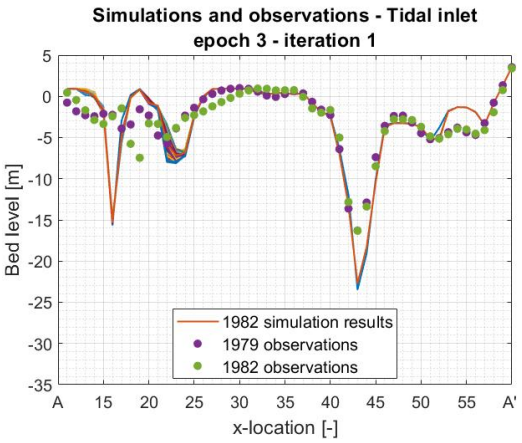

(a) Cross-section through the tidal inlet for all simulations and the observations in 1979 and 1982.

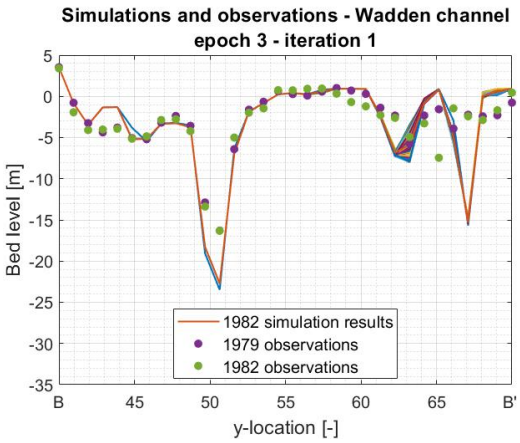

(b) Cross-section through the Wadden inlet for all simulations and the observations in 1979 and 1982.

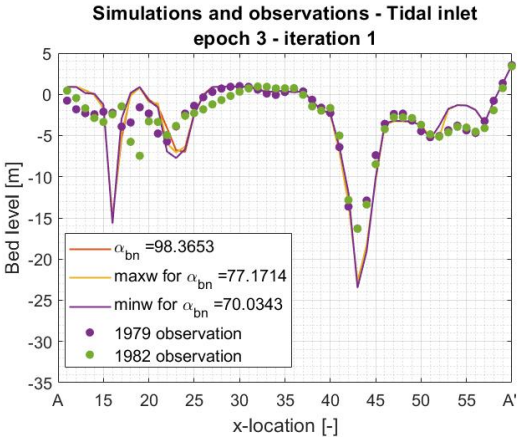

(c) Cross-section through the tidal inlet for three simulations and the observations in 1979 and 1982.

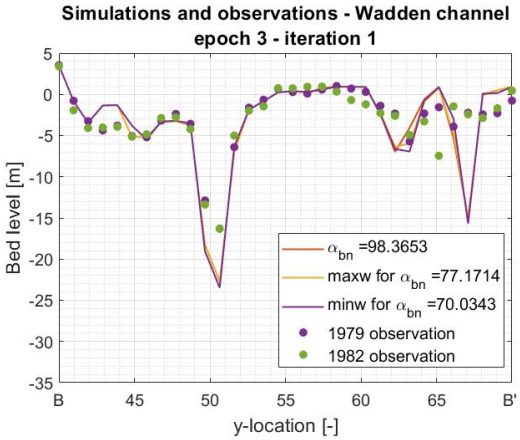

(d) Cross-section through the Wadden inlet for three simulations and the observations in 1979 and 1982.

Figure 4.35: Cross-section channels 1979-1982

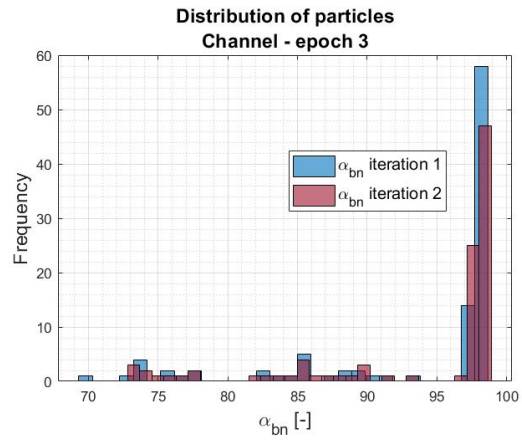

(a)

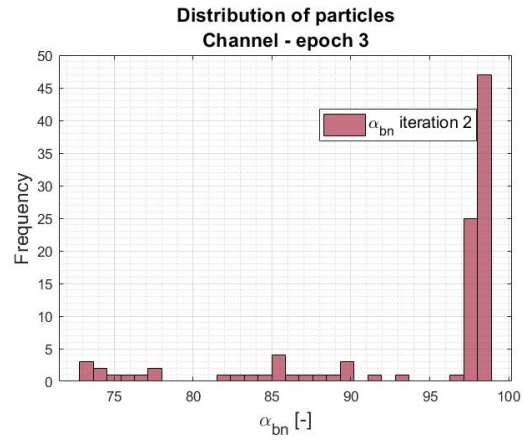

(b)

Figure 4.36: Distribution of α_{bn} values over new set of particles - iteration 1

End epoch 3

The convergence shown in the results of epoch 3, resembles the convergence seen in epoch 1. The evolution of the distribution of the α_{bn} values is shown in Figure 4.37. The smaller boundary of this distribution makes a big jump towards 70. The upper boundary of the distribution moves a bit up, but does not make a big change. The evolution looks like the evolution seen in epoch 1. There it was observed that the smaller boundary moved up immediately and the upper boundary increased a bit in the first iteration and remained steady in further iterations. The mean of epoch 3 is approximately 93.5 and in epoch 1 this was approximately 96.8. The evolution of the distribution seen in epoch 2, was very different.

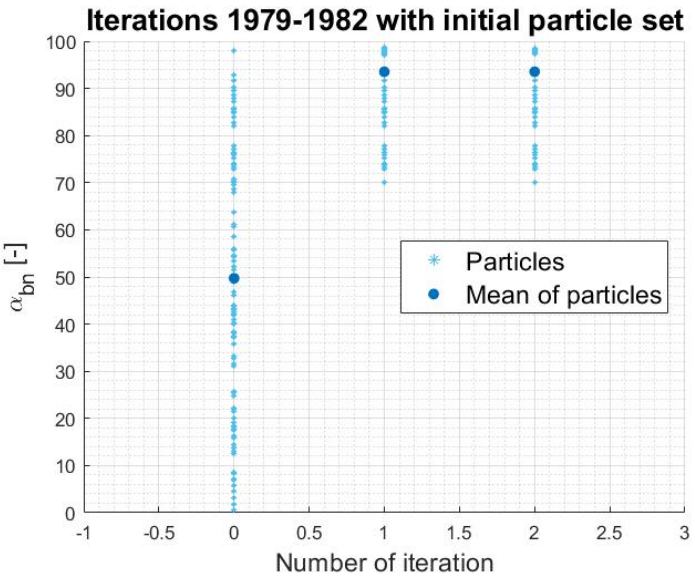

Figure 4.37: Distribution of α_{bn} for iterations in epoch 3

Table 4.4: Values for α_{bn} in epoch 3

	Minimum α_{bn}	Maximum α_{bn}	Mean α_{bn}
Iteration 0	0.6647	97.9678	49.7111
Iteration 1	70.0343	98.6184	93.529
Iteration 2	70.0343	98.5311	93.5462

5

Discussion

In this chapter, the main findings for both subquestions are discussed, together with possible explanations for these findings. Furthermore, some limitations in the method to answer the questions are mentioned.
In subquestion 1 the main finding is that the considered parameters RDW, BedW, α_{bn} and tidal amplitude induce a change in the simulated bedlevel.
In subquestion 2 the difference in the resulting α_{bn} distribution in epoch 2 with respect to epoch 1 and 3 is discussed. The fact that the simulations never perfectly predict the bedlevel is also discussed.

Subquestion 1

Which parameters induce a significant change in the bathymetry of a morphological model?

Findings

The sensitivity study shows that RDW, BedW, α_{bn} and tidal amplitude induce a change in the simulated bedlevel. The α_{bn} and BedW simulations perform well over the whole area of interest, but the performance decreases when zooming in to a specific part, like tidal channel volume or tidal flat height. This result can be used to find similar parameters in other models, which might be an important influence on bedlevel results in other morphological models as well. The transverse bed slope, α_{bn}, influences the ease for a sediment particle to travel from the upside of a channel towards the lower centre of a channel. So, this parameter influences the locations where a slope is present. These locations are the tidal flats and tidal channel locations. This could be a reason why the skill score gives a worse value for the processing of the plate height and channel volume. In those areas, changes are taking place in the bed slope, so when the α_{bn} is not the ideal value this induces wrong predictions at these locations.

Limitations

In the performance of the sensitivity study there were some limitations, that should be considered when drawing conclusions from the results. So, these limitations are discussed here. To make it possible to perform sensitivity studies and apply data assimilation within the time limit of the project, the model set-up represents a simplified version of the Frisian inlet. An increase in detail in the model, for example by using a higher grid resolution, can lead to more details in the prediction of the bed level. This can make an important difference on locations where slopes are steep in bedlevel results. However, this will increase the run time and the data generated as well. So, a trade-off between an investment in time and data storage on the one hand and more detailed results on the other hand, should be considered before implementing any extra detailed information in the model.
Examples to make the model more realistic is by giving real data of oceanic conditions, like ERA5, as input to the model. ERA5 is the latest version of the ECMWF (European Centre for Medium-Range Weather Forecasts) ReAnalysis by Hersbach [2016], which can be used for wave boundary conditions, wind speeds and atmospheric pressure. Another possibility is to make the bed roughness and sediment composition vary through the area instead of giving one constant initial value for the total area.
The mean squared skill score was the best suitable option for this research, although there are some dis-

advantages to using the MSESS on morphological results. Some important disadvantages of the MSESS are discussed in Bosboom et al. [2014] and Bosboom and Reniers [2018]. In this report, a description is given of the disadvantages in Appendix A. The first disadvantage of MSESS is the "double penalty". This occurs when a morphological feature is present in the measurements and is also predicted in the simulation result but at the wrong location. A second pitfall is the fact that it uses a zero change model as a reference, which results in better scores for simulations that predict no or small amounts of change. Lastly, the skill score tends to give higher skill scores with time, which is a result of small spatial scale process that are dominant at the start of a simulation.
For each of the parameters, ten values within a realistic range are simulated to investigate. The realistic ranges are known from previous testing or by knowledge about physical processes. The best insight in the sensitivity of the model is gained, when a lot of simulations with different values within the realistic range are performed. The ten values that are chosen in this research, is a low number of simulations.
Whether the ten values are enough to capture the sensitivity of the model to the parameter, depends on the range of possible values. For example, the range for α_{bn} in which the ten values are chosen, is large. Therefore, sensitivity to the parameter can be missed, because of the gap between two chosen values.
The channel volumes and plate heights were calculated for ten simulations of α_{bn}. The results in appendix A show a significant difference between the simulation with α_{bn}=10 and α_{bn}=20. For the calculation of the MSESS extra simulations are performed in this area. The same would be useful in other parameters. For example, the suspended load shows a big difference between the 0.2 and 0.3 simulation and between the 0.6 and 0.7 simulation. Although the values for the suspended load is chosen in a smaller range, extra simulations in these sensitive ranges might give new and more information on the sensitivity. The quality of this study would benefit from a more thorough sensitivity study to build on, because this gives variable simulation results to the particle filter. When there are 100 simulations given to the particle filter, but they only cover two possible outcomes the filter can only use those two outcomes as information. When there are also possible outcomes between the two options that were considered before, this results in a more nuanced view.

Subquestion 2

How can data assimilation be implemented to optimize a morphological model output based on bed level measurements?

Findings

This study shows that it is possible to get a better understanding of the distribution of α_{bn} values that leads to probable bedlevel predictions by applying a particle filter. The application of this method brings the simulations closer to each other, but the simulations did not get closer to the observations. The finding that the distribution of α_{bn} values over the 100 simulations changed over multiple iterations, shows that the application of the particle filter on a morphological model has an effect. In this research, this was used to calibrate on the α_{bn} parameter and to draw conclusions on a most probable simulation from a set of bedlevel simulations. As long as the parameter to calibrate influences the state variable that it is optimized on, I expect it is possible to use a particle filter as a calibration tool.
The three epochs showed different results for the bedlevel prediction and for the resulting distribution of α_{bn}. A striking difference is the value of α_{bn} in epoch 2 that the distribution converges to. The large values for α_{bn} are discarded in epoch 2 after the first evaluation. In epoch 1 and 3 these large values are the main focus of the found α_{bn} distribution. So, there should be a difference in the cross-sections of epoch 1 and 3 compared to epoch 2 that could explain this difference in the α_{bn} distribution. One thing that is different in the bedlevel predictions made in epoch 2, is the bedlevel at location 50-A' in cross-section A and at location B-45 in cross-section B. In epoch 2 the bedlevel at these locations is predicted perfectly, whereas this is not the case in epoch 1 and 3. Since this is the one thing that is different in epoch 2 when compared to epoch 1 and 3, this might be a cause of the different α_{bn} distribution in epoch 2. This possibility can be tested, by making the evaluation more detailed on location. An evaluation on sub-parts of the cross-sections will also give more insight into why the simulations never make a perfect prediction.
Although it was not the purpose of the research to make a perfect bedlevel prediction, a closer look in this matter can increase the understanding of the parameter α_{bn} and its influence on the performance of the particle filter. The fact that the simulations never predict the observed bedlevel exactly, might be caused by a

different α_{bn} value being suitable for different locations at the cross-section. To find out if this is the case, the division of the area can be made more detailed. For example, the optimization on the tidal channels can be divided in an optimization on the small channels and an optimization on the main channel. The two optimizations might lead to a different distribution of α_{bn} and this can explain why it is difficult to perfectly predict the bedlevel over a larger area with more different morphological elements.
In epoch 1 and 3 of this research, the difference between observations is larger than in epoch 2, mainly at the location of the small channels. So, another explanation for the difference in α_{bn} distribution can be that for periods with more change between the end and initial bed level will lead to larger values of α_{bn} in the resulting distribution. To test this, the method as used in this research can be performed, using synthetic data. A number of synthetic data can be produced with different bedlevels. Using these data, experiments can be performed for periods that are exactly the same, except for the initial and end bathymetry. The results can show if the period with a large difference between initial and end bedlevels lead to high α_{bn} values and the period with a small difference between initial and end bedlevels lead to lower α_{bn} values.
The method applied in this study calibrated the model mostly towards the higher α_{bn} values of the initial distribution. It should be taken into account that this can be influenced by the number of particles, which is 100 in this research. However, the distribution is not perfectly uniform (Figure 3.7), which leads to underrepresented ranges of α_{bn}. For example, around α_{bn}=28, α_{bn}=80 and α_{bn}=94 there are no particles. When an α_{bn} value in these ranges would lead to a highly probable bed level outcome, it might not be found by the particle filter. When more particles are used, the distribution is more towards a perfect uniform distribution, which leads to coverage of all values in the range between 0.5 and 100. This gives a more evenly distributed particle set to the particle filter to start with. So, by increasing the number of the particles, the chances of missing a probable parameter value decreases.
Furthermore, the results suggest that a wide and shallow channel is easier to predict than a narrow deep channel. The simulations in epoch 1 for the deep channel in cross-section A were not predicting the channel bedlevel well. The observed channel was deep and small. Whereas, in all other cross-sections, this bedlevel prediction was better and the channel to be predicted was wider and shallower. However, to be certain of this more experiments should be performed. To test this, again synthetic data could be used. Simulating equal situations and only varying the width or depth of the channel to be simulated will show what channels are best predicted by the morphological model.

Limitations

In the particle filter, the difference between the simulated and observed bed level is used to determine the weights (Section 2.4). In this research, the location where this difference is calculated is not necessarily the location where the observation is performed. The bed level was interpolated first to use as initial bathymetry. However, the interpolated values are also used in the observations of the particle filter. So, by using this interpolated value in the calculation of the likelihood (Equation 2.10), this uncertainty is introduced in the process. When the exact location of the observation is used, this uncertainty is not introduced. Therefore, the only uncertainty in the process is that of the simulations and the deviations in the Gaussian uncertainties of the observation. This makes the added value of the bedlevel observation to the resulting distribution more valuable.

6

Conclusions and recommendations

In this chapter first for both subquestions, the conclusions are presented. These conclusions are followed by recommendations to further expand or improve this research.

Subquestion 1

Which parameters induce a significant change in the bathymetry of a morphological model?

It can be concluded that the tidal amplitude, RDW, BedW and α_{bn} induce a change in the bathymetry simulated by Delft3D. The change observed for different values of RDC and SusW is too small to be significant. The parameters that are used in model set-ups in other models than Delft3D might be different. Though, comparable parameters, that influence bed roughness, tidal amplitude, bedload or bed slope, can be searched for to set up a sensitivity study. This research is not sufficient to draw conclusions if changes are induced in other morphological models as well.

Subquestion 2

How can data assimilation be implemented to optimize a morphological model output based on bed level measurements?

This study tells that it is possible to make a finer selection of α_{bn} from a distribution for the modelling of morphodynamics using a particle filter. The range of α_{bn} of the finer selection depends on the period that is simulated. By applying this method, the simulations are brought closer to each other, but the simulations did not get closer to the observations.
The contribution to our understanding of data assimilation for morphodynamic models is that it can be used as a calibration tool for a specific parameter. This study shows that by applying a particle filter, it is possible to find a bedlevel outcome with a high probability relative to other bedlevel outcomes, given the model and observation uncertainties. So, it is possible to calibrate the model in a certain period and area to find the most probable outcome for the varied setting. The study presents a method that possibly can be used to fine-tune the bedlevel results in other situations in morphological models as well.
Furthermore, the use of data assimilation in morphodynamic studies can be extended to focus more on the uncertainties and the evolution of uncertainties in the predictions of bedlevel.

6.1. Recommendations

1. Delft3D is a model that uses many input parameters to start a simulation and each parameter influences the end result of the simulation. The fact that only six of the parameters are considered in the sensitivity study of this research, is a simplification to keep the estimation problem tractable. The sensitivity study as performed in this research can be expanded, to have a better insight into the morphological model that is considered. For example, more parameters can be taken into account and more values for these parameters can be used to simulate the bed level. Furthermore, it might be possible to replace the MSESS by the root mean squared transport error (RMSTE). The RMSTE deals with some of the disadvantages found using the MSESS. So, making use of this, the quality of the assessment of the sensitivity results will be better. The RMSTE was not used in this research, because it is just introduced [Bosboom, 2020].

2. Considering the data assimilation, it would be very useful to conduct research on this topic using a synthetic experiment as the truth instead of using the observations. Synthetic data is produced by running simulations. Since it is known what settings are used to produce the synthetic data, it is known what distribution should be the result of the particle filter. In this way, a better understanding of the particle filter is obtained, before applying it on actual observations for which it is not known what model settings would give the result. By first testing the method using synthetic experiments, the conclusions that are drawn from the process with actual observations will be better understood.

3. The bed level measurement used as the initial bed level is interpolated from a 20x20 meter grid. However, the measurements are not performed on this 20x20 grid, so these are already an interpolation of the original measurement location. In each interpolation, uncertainties come in. When the measurements used in data assimilation have lower uncertainties, the posterior uncertainty in the data assimilation results are lower as well. The contribution of the measurements is most reliable and valuable when they are used at the location where they are measured

4. Baar et al. [2019] show that the high values for α_{bn}, as found in my study, do result in a better prediction of the bedlevel, but are not realistic. To improve the predictions in these areas using more realistic values for α_{bn}, a recommendation is to change multiple parameters or to change both the parameter, α_{bn}, and the state variable, the bed level. In this way, it is easier to bring model predictions and data closer, because there will be more variation in the simulations. This will result in a distribution of possible bed levels and their probability of occurrence. However, it will be difficult to detect which model settings led to each model outcome in this distribution because the α_{bn} and bed level are both varied.

5. This research has used a particle filter as a data assimilation method, because it is suitable for nonlinear systems and it is relatively easy to implement. To achieve the objective of this research, other data assimilation methods can be used as well. It can lead to better insights when the same research is performed using multiple data assimilation methods. For example, a particle filter and an Ensemble Kalman filter can be applied to this model. When the prior densities are assumed to be Gaussian distributed, the Ensemble Kalman filter can be used to solve the general Bayesian problem as well [Evensen and van Leeuwen, 2002]. Two different methods might indicate different probabilities for the possible model outcomes. By understanding the differences between the used data assimilation methods, a better insight in the probability distribution of the predicted bed levels can be obtained.

6. In this study, it seems that the tidal flats are also able to give information to the particle filter to steer towards certain simulations. So, it could be interesting to process both, the optimization on tidal channels and the optimization on tidal flats. In that way, the understanding of the influence of α_{bn} can be expanded.

7. In this research Kernel dressing is chosen as a resampling method to resample the α_{bn} particles between consecutive iterations. However, this is not the only possible resampling method. Examples of other resampling methods are a guided particle filter, a merging particle filter, Gaussian resampling, localization and a maximum entropy particle filter [Van Leeuwen, 2009]. A study can be performed to see if there are significant differences in resulting particles when using Kernel dressing compared to other methods.

8. The last recommendation is to execute the study on other coast types as well. It might be that α_{bn} in another range works better at coastal areas that do not have a barrier island setting. The way that the particle filter will steer in areas with other coast types will give an insight into the connection of α_{bn} with the bedlevel morphology.

The application of the particle filter in this research, presented some interesting results in the ability of Delft3D to model tidal channels and on the ability of a particle filter to find simulations with a high probability. This research is a valuable step towards more research on the possibility to use data assimilation to find morphological simulations with low uncertainties. Further research can give more insight in these possibilities by applying other data assimilation methods and by using other morphological models.

Bibliography

Aagaard, T., Davidson-Arnott, R., Greenwood, B., and Nielsen, J. Sediment supply from shoreface to dunes: Linking sediment transport measurements and long-term morphological evolution. *Geomorphology*, 60 (1-2):205–224, 2004. ISSN 0169555X. doi: 10.1016/j.geomorph.2003.08.002.

Amos, C. L. Chapter 10 Siliciclastic Tidal Flats. In *Developments in Sedimentology*, volume 53, pages 273–306. Elsevier, jan 1995. ISBN 9780444881700. doi: 10.1016/S0070-4571(05)80030-5. URL `https://www.sciencedirect.com/science/article/pii/S0070457105800305`.

Ansari, H. Bayesian Inference , Applications in Persistent Scatterer Interferometric SAR Bayesian Inference , Applications in Persistent Scatterer Interferometric Synthetic Aperture Radar Homa Ansari Master ' s Thesis Earth Oriented Space Science and Technology – ES. (October 2013), 2014.

Baar, A. W., Boechat Albernaz, M., van Dijk, W. M., and Kleinhans, M. G. Critical dependence of morphodynamic models of fluvial and tidal systems on empirical downslope sediment transport. *Nature Communications*, 10(1), 2019. ISSN 20411723. doi: 10.1038/s41467-019-12753-x. URL `http://dx.doi.org/10.1038/s41467-019-12753-x`.

Bertino, L., Evensen, G., and Wackernagel, H. Sequential Data Assimilation Techniques in Oceanography. *International Statistical Review*, 71(2):223–241, 2007. ISSN 0306-7734. doi: 10.1111/j.1751-5823.2003.tb00194.x.

Bosboom, J. *Quantifying the quality of coastal morphological predictions*. 2020. ISBN 9789055841745. doi: 10.4233/uuid.

Bosboom, J., Reniers, A. J. H. M., and Luijendijk, A. P. On the perception of morphodynamic model skill. *Coastal Engineering*, 94(August):112–125, 2014. ISSN 03783839. doi: 10.1016/j.coastaleng.2014.08.008.

Bosboom, J. and Reniers, A. The Deceptive Simplicity of the Brier Skill Score. In *Handbook of Coastal and Ocean Engineering*, pages 1639–1661. 2018.

Chen, X., Chiew, Y., and Asce, M. Response of Velocity and Turbulence to Sudden Change of Bed Roughness in Open-Channel Flow. 129(January):35–43, 2003.

Cowell, P. and Thom, B. *Morphodynamics of coastal evolution*. Cambridge University Press, Cambridge, United Kingdom and New York, NY, USA, 1994.

de Boer, G. J. Application of a sand-mud model to the Friesche Zeegat. Influence of waves. Technical report, WL | Delft Hydraulics, 2002.

Dekking, F. M., Kraaikamp, C., Lopuhaä, H., and Meester, L. *A Modern Introduction to Probability and Statistics, Understanding Why and How*, chapter 3. Springer, 2005.

Deltares. Delft3D-FLOW - user manual, version 3.15. Technical report, Deltares, Delft, 2018.

Dissanayake, D. M. P. K., Roelvink, J. A., and van der Wegen, M. Modelled channel patterns in a schematized tidal inlet. *Coastal Engineering*, 56(11-12):1069–1083, 2009. ISSN 03783839. doi: 10.1016/j.coastaleng.2009.08.008. URL `http://dx.doi.org/10.1016/j.coastaleng.2009.08.008`.

Dobricic, S. and Pinardi, N. An oceanographic three-dimensional variational data assimilation scheme. *Ocean Modelling*, 22(3-4):89–105, 2008. ISSN 14635003. doi: 10.1016/j.ocemod.2008.01.004.

Elias, E. and Vermaas, T. Waddenzee Vaklodingen : Data op Orde. Technical report, Deltares, Delft, 2019.

Elias, E. P. L., Walstra, D. J. R., Roelvink, J. A., Stive, M. J. F., and Klein, M. D. Hydrodynamic validation of Delft3D with field measurements at Egmond. *Coastal Engineering 2000 - Proceedings of the 27th International Conference on Coastal Engineering, ICCE 2000*, 276(March), 2000. doi: 10.1061/40549(276)212.

Elias, E. P., Van Der Spek, A. J., Wang, Z. B., and De Ronde, J. Morphodynamic development and sediment budget of the Dutch Wadden Sea over the last century. *Geologie en Mijnbouw/Netherlands Journal of Geosciences*, 91(3):293–310, 2012. ISSN 00167746. doi: 10.1017/S0016774600000457.

Emerick, A. A. and Reynolds, A. C. Ensemble smoother with multiple data assimilation. *Computers and Geosciences*, 2013. ISSN 00983004. doi: 10.1016/j.cageo.2012.03.011.

Evensen, G. and van Leeuwen, P. An Ensemble Kalman Smoother for Nonlinear Dynamics. *Monthly Weather Review*, 128(6):1852–1867, 2002. ISSN 0027-0644. doi: 10.1175/1520-0493(2000)128<1852:aeksfn>2.0.co;2.

Fiechter, J., Steffen, K. L., Mooers, C. N. K., and Haus, B. K. Hydrodynamics and sediment transport in a southeast Florida tidal inlet. *Estuarine, Coastal and Shelf Science*, 2006. ISSN 02727714. doi: 10.1016/j.ecss.2006.06.021.

Fokker, P. A., Van Leijen, F. J., Orlic, B., Van Der Marel, H., and Hanssen, R. F. Subsidence in the Dutch Wadden Sea. *Geologie en Mijnbouw/Netherlands Journal of Geosciences*, 97(3):129–181, 2018. ISSN 15739708. doi: 10.1017/njg.2018.9.

Garcia, I. D., Serafy, G. E., Heemink, A., and Schuttelaars, H. Towards a data assimilation system for morphodynamic modeling: Bathymetric data assimilation for wave property estimation. *Ocean Dynamics*, 63(5):489–505, 2013. ISSN 16167341. doi: 10.1007/s10236-013-0606-4.

Ghil, M. and Malanotte-Rizzoli, P. Data Assimilation in Meteorology and Oceanography. *Advances in Geophysics*, 33:141–266, jan 1991. ISSN 0065-2687. doi: 10.1016/S0065-2687(08)60442-2. URL `https://www.sciencedirect.com/science/article/abs/pii/S0065268708604422`.

Giménez, R. and Govers, G. Interaction between bed roughness and flow hydraulics in eroding rills. *Water resources research*, 37(3):791–799, 2001.

Henderson, S. M. and Allen, J. S. Nearshore sandbar migration predicted by an eddy-diffusive boundary layer model. *Journal of Geophysical Research C: Oceans*, 109(6):1–15, 2004. ISSN 01480227. doi: 10.1029/2003JC002137.

Hersbach, H. The era5 atmospheric reanalysis. *American Geophysical Union, Fall Meeting 2016*, 2016.

Hsu, Y. L., Dykes, J. D., Allard, R. A., and Kaihatu, J. M. Evaluation of Delft3D performance in nearshore flows. *Naval Research Laboratory*, page 27, 2006.

Hsu, Y. L., Dykes, J. D., Allard, R. A., and Wang, D. W. Validation Test Report for Delft3D. *October*, pages 1–42, 2008.

Kirwan, M. L. and Megonigal, J. P. Tidal wetland stability in the face of human impacts and sea-level rise. *Nature*, 504(7478):53–60, 2013. ISSN 00280836. doi: 10.1038/nature12856.

Mol, M. B. The effective transport difference: A new concept for morphodynamic model validation, 2015.

Nakano, S., Ueno, G., and Higuchi, T. Merging particle filter for sequential data assimilation. Nonlinear Processes in Geophysics. *European Geosciences Union (EGU)*, 14(4):395–408, 2007.

Nichols, G. *Sedimentology and Stratigraphy*, chapter 4.2. Wiley-Blackwell, 9600 Garsington Road, Oxford, OX4 2DQ, UK, 2009a.

Nichols, G. *Sedimentology and Stratigraphy*, chapter 6.5. Wiley-Blackwell, 9600 Garsington Road, Oxford, OX4 2DQ, UK, 2009b.

Oertel, G. F. The barrier island system. *Marine Geology*, 1985. ISSN 00253227. doi: 10.1016/0025-3227(85)90077-5.

Oost, A. and de Haas, H. Het Friesche Zeegat: morfologisch-sedimentologische veranderingen in de periode 1970-1987: een getijde inlet systeem uit evenwicht. 1996.

Otvos, E. G. Coastal barriers - Nomenclature, processes, and classification issues, 2012. ISSN 0169555X.

Ruessink, B. G. and Kuriyama, Y. Numerical predictability experiments of cross-shore sandbar migration. *Geophysical Research Letters*, 35(1):1–5, 2008. ISSN 00948276. doi: 10.1029/2007GL032530.

Scott, T. R. and Mason, D. C. Data assimilation for a coastal area morphodynamic model: Morecambe Bay. *Coastal Engineering*, 54(2):91–109, 2007. ISSN 03783839. doi: 10.1016/j.coastaleng.2006.08.008.

Stanev, E. V., Wölff, J. O., Burchard, H., Bolding, K., and Flöser, G. On the circulation in the East Frisian Wadden Sea: Numerical modeling and data analysis. *Ocean Dynamics*, 53(1):27–51, 2003. ISSN 16167341. doi: 10.1007/s10236-002-0022-7.

Sutherland, J., Peet, A. H., and Soulsby, R. L. Evaluating the performance of morphological models. *Coastal Engineering*, 51(8-9):917–939, 2004. ISSN 03783839. doi: 10.1016/j.coastaleng.2004.07.015.

Townend, I., Wang, Z. B., Stive, M., and Zhou, Z. Development and extension of an aggregated scale model: Part 2 — Extensions to ASMITA. *China Ocean Engineering*, 30(5):651–670, 2016a. ISSN 0890-5487. doi: 10.1007/s13344-016-0042-6.

Townend, I., Wang, Z. B., Stive, M., and Zhou, Z. Development and extension of an aggregated scale model: Part 1 – Background to ASMITA. *China Ocean Engineering*, 30(4):483–504, 2016b. ISSN 08905487. doi: 10.1007/s13344-016-0030-x.

Trouw, K., Zimmermann, N., Mathys, M., Delgado, R., and Roelvink, D. Numerical modelling of hydrodynamics and sediment transport in the surf zone: A sensitivity study with different types of numerical models. *Proceedings of the Coastal Engineering Conference*, pages 1–12, 2012.

Tuan Pham, D., Verron, J., and Christine Roubaud, M. A singular evolutive extended Kalman filter for data assimilation in oceanography. *Journal of Marine Systems*, 16(3-4):323–340, 1998. ISSN 09247963. doi: 10.1016/S0924-7963(97)00109-7.

van de Kreeke, J. and Robaczewska, K. Tide-induced residual transport of coarse sediment; Application To the Ems Estuary. 31(3):209–220, 1993.

van de Kreeke, J., Brouwer, R. L., Zitman, T. J., and Schuttelaars, H. M. The effect of a topographic high on the morphological stability of a two-inlet bay system. *Coastal Engineering*, 2008. ISSN 03783839. doi: 10.1016/j.coastaleng.2007.11.010.

Van Der Wegen, M., Jaffe, B. E., and Roelvink, J. A. Process-based, morphodynamic hindcast of decadal deposition patterns in San Pablo Bay, California, 1856-1887. *Journal of Geophysical Research: Earth Surface*, 116 (2):1–22, 2011. ISSN 21699011. doi: 10.1029/2009JF001614.

van Dongeren, A., Plant, N., Cohen, A., Roelvink, D., Haller, M. C., and Catalán, P. Beach Wizard: Nearshore bathymetry estimation through assimilation of model computations and remote observations. *Coastal Engineering*, 2008. ISSN 03783839. doi: 10.1016/j.coastaleng.2008.04.011.

Van Goor, M. A., Zitman, T. J., Wang, Z. B., and Stive, M. J. F. Impact of sea-level rise on the morphological equilibrium state of tidal inlets. *Marine Geology*, 2003. ISSN 00253227. doi: 10.1016/S0025-3227(03)00262-7.

Van Leeuwen, P. J. Nonlinear data assimilation in geosciences: An extremely efficient particle filter. *Quarterly Journal of the Royal Meteorological Society*, 136(653):1991–1999, 2010. ISSN 00359009. doi: 10.1002/qj.699.

Van Leeuwen, P. Particle filtering in geophysical systems. *Monthly Weather Review*, 137(12):4089–4114, 2009. ISSN 00270644. doi: 10.1175/2009MWR2835.1.

Van Prooijen, B. C. and Wang, Z. B. A 1D model for tides waves and fine sediment in short tidal basins - Application to the Wadden Sea. *Ocean Dynamics*, 63(11-12):1233–1248, 2013. ISSN 16167341. doi: 10.1007/s10236-013-0648-7.

van Rijn, L. C., Wasltra, D. J. R., Grasmeijer, B., Sutherland, J., Pan, S., and Sierra, J. P. The predictability of cross-shore bed evolution of sandy beaches at the time scale of storms and seasons using process-based profile models. *Coastal Engineering*, 2003. ISSN 03783839. doi: 10.1016/S0378-3839(02)00120-5.

van Velzen, N., Altaf, M. U., and Verlaan, M. OpenDA-NEMO framework for ocean data assimilation. *Ocean Dynamics*, 66(5):691–702, 2016. ISSN 16167228. doi: 10.1007/s10236-016-0945-z. URL http://dx.doi.org/10.1007/s10236-016-0945-z.

Vermeersen, B. L., Slangen, A. B., Gerkema, T., Baart, F., Cohen, K. M., Dangendorf, S., Duran-Matute, M., Frederikse, T., Grinsted, A., Hijma, M. P., Jevrejeva, S., Kiden, P., Kleinherenbrink, M., Meijles, E. W., Palmer, M. D., Rietbroek, R., Riva, R. E., Schulz, E., Slobbe, D. C., Simpson, M. J., Sterlini, P., Stocchi, P., Van De Wal, R. S., and Van Der Wegen, M. Sea-level change in the Dutch Wadden Sea. *Geologie en Mijnbouw/Netherlands Journal of Geosciences*, 97(3):79–127, 2018. ISSN 15739708. doi: 10.1017/njg.2018.7.

Vossepoel, F. C. and van Leeuwen, P. J. Parameter estimation using a particle method: Inferring mixing coefficients from sea level observations. *Monthly Weather Review*, 135(3):1006–1020, 2007. ISSN 00270644. doi: 10.1175/MWR3328.1.

Wang, Z. B., Louters, T., and de Vriend, H. J. Morphodynamic modelling for a tidal inlet in the Wadden Sea. *Marine Geology*, 126(1-4):289–300, 1995. ISSN 00253227. doi: 10.1016/0025-3227(95)00083-B.

Wang, Z. B., Hoekstra, P., Burchard, H., Ridderinkhof, H., De Swart, H. E., and Stive, M. J. F. Morphodynamics of the Wadden Sea and its barrier island system. *Ocean and Coastal Management*, 68:39–57, 2012. ISSN 09645691. doi: 10.1016/j.ocecoaman.2011.12.022. URL http://dx.doi.org/10.1016/j.ocecoaman.2011.12.022.

Wang, Z. B., Elias, E. P., Van Der Spek, A. J., and Lodder, Q. J. Sediment budget and morphological development of the Dutch Wadden Sea: Impact of accelerated sea-level rise and subsidence until 2100. *Geologie en Mijnbouw/Netherlands Journal of Geosciences*, 97(3):183–214, 2018. ISSN 15739708. doi: 10.1017/njg.2018.8.

Wiberg, P. L. and Smith, J. D. Velocity distribution and bed roughness in high-gradient streams. *Water Resources Research*, 27(5):825–838, 1991. doi: 10.1029/90WR02770. URL https://agupubs.onlinelibrary.wiley.com/doi/abs/10.1029/90WR02770.

Wikle, C. K. and Berliner, L. M. A Bayesian tutorial for data assimilation. *Physica D: Nonlinear Phenomena*, 230(1-2):1–16, 2007. ISSN 01672789. doi: 10.1016/j.physd.2006.09.017.

Zhou, Z., Olabarrieta, M., Stefanon, L., d'Alpaos, A., Carniello, L., and Coco, G. Journal of Geophysical Research : Earth Surface A comparative study of physical and numerical modeling of tidal network ontogeny. pages 1–21, 2014. doi: 10.1002/2014JF003092.Received.

Zhou, Z., Coco, G., Townend, I., Olabarrieta, M., van der Wegen, M., Gong, Z., D'Alpaos, A., Gao, S., Jaffe, B. E., Gelfenbaum, G., He, Q., Wang, Y., Lanzoni, S., Wang, Z. B., Winterwerp, H., and Zhang, C. Is "Morphodynamic Equilibrium" an oxymoron?, 2017. ISSN 00128252.

A

Theory

A reason for the popularity of MSESS as a quality measure is the ease to apply it. However, there are also some disadvantages to using the MSESS on morphological results. Some important disadvantages of the MSESS as mentioned in Bosboom et al. [2014] and Bosboom and Reniers [2018] will be discussed.
The first disadvantage of MSESS is the "double penalty". This occurs when a morphological feature is present in the measurements and is also predicted in the simulation result but at the wrong location. In the left column in Figure A.1 three model predictions are shown: p_1, p_2 and p_3. In the middle column, the observation is shown. The colours in the figure indicate the bed level. In the observation, it is seen that there is one hill in the upper right corner of 1 meter. In the first prediction, nothing but a flat surface is predicted. The right column shows that one error of -1 meter is found. In the second and third predictions there is a hill predicted, but in the wrong location. In the right column of the second and third predictions, it is seen that this leads to a double error.
The first error is at the location where the feature is simulated, but should not be. The second error is at the location where the feature is not simulated, but should have been. This double penalty occurs as soon as the predicted bar and the observed bar do not overlap. A consequence of this double penalty is a higher value for the MSESS for the simulation that did not predict the feature. However, a morphologist might judge that the simulation that predicted the feature at the wrong location is better [Bosboom et al., 2014]. The result is that the MSESS rewards a simulation that underpredicts the variance in bed level.

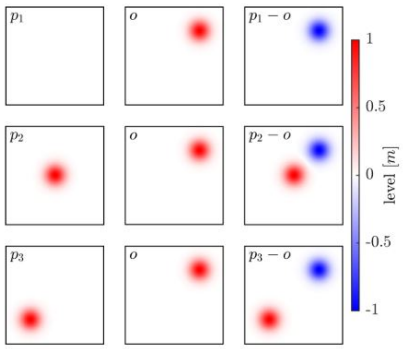

Figure A.1: Counter intuitive behaviour of the (R)MSE: double penalty effect and location errors, from [Mol, 2015]

A second pitfall in the use of the MSESS is the fact that it uses a zero change model as a reference. The bed level change from the start of a simulation to the evaluation time must represent the difficulty of predictions. For example, take a bar migrating over the sea bed from location A to location B. In the first simulation it migrates from A to B, whereas in the second simulation it migrates from A, via location C, to B. The cumulative bed changes do not take into account what processes take place during the simulation time. However, the detour via location C makes it more difficult for a model to make a correct prediction and this should be taken

in to account in the MSESS.
Furthermore, a combination of larger, persistent scales and smaller, intermittent scales in the cumulative bed changes can result in an increase of skill with time. At the start of a simulation, the small spatial scale processes are often dominant. On small spatial scales, the skill scores are often bad. Over time the relative contribution of these small scales to the cumulative change decreases. This results in higher skill scores when the simulation time is longer, even though the predictions on these scales are not getting more skilful with time.

In Bosboom [2020] another error metric is suggested, the RMSTE. In previous researches, this is not yet used, since it is just introduced. The RMSTE is a measure that takes into account the distance that the sediment needs to travel to be in the correct place. A result is that using the RMSTE makes it possible to discriminate between simulations that predicted a morphological feature at different distances from where it was observed. The reward of underestimates is also avoided by using the RMSTE [Bosboom, 2020]. When the sediment needs to be moved over large distances, the RMSTE will be larger than when it has to move over a smaller distance to end up in the observed location. So, in Figure A.1 the prediction p_2 will receive a smaller penalty than prediction p_3.

Results

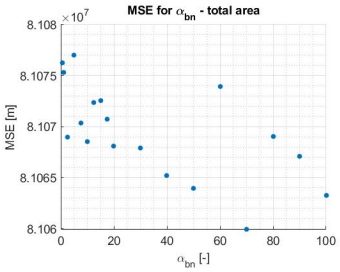

(a) MSE α_{bn} - total area

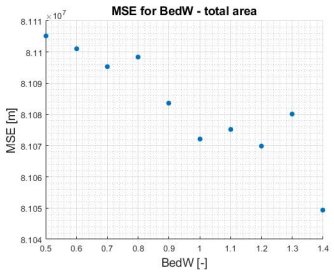

(b) MSE BedW - total area

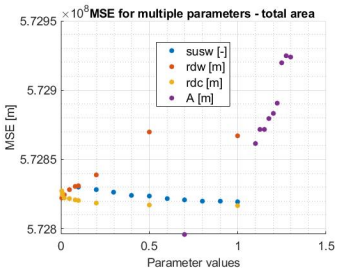

(c) MSE parameters - total area

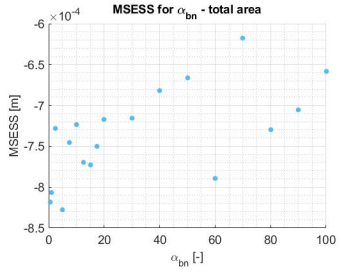

(a) MSESS α_{bn} - total area

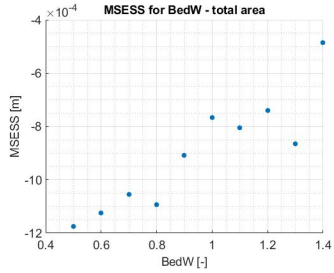

(b) MSESS BedW - total area

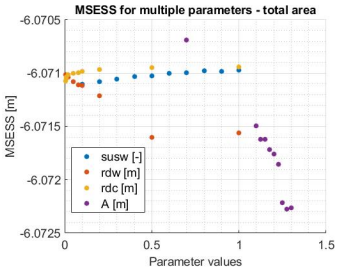

(c) MSESS parameters - total area

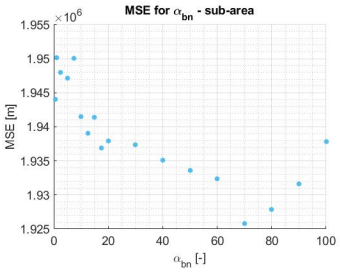

(a) MSE α_{bn} - sub-area

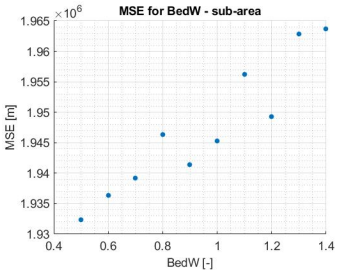

(b) MSE BedW - sub-area

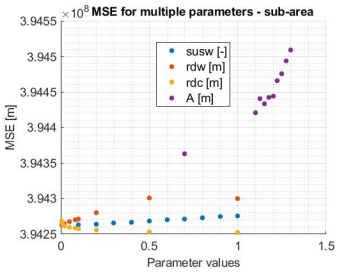

(c) MSE parameters - sub-area

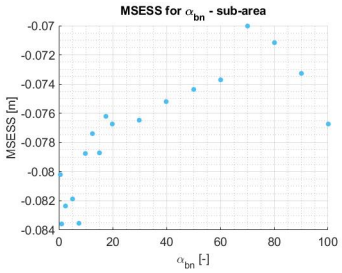

(a) MSESS α_{bn} - sub-area

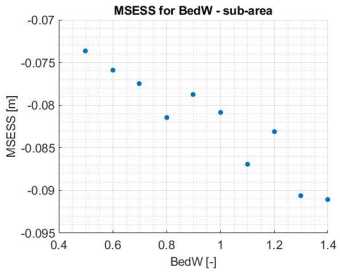

(b) MSESS BedW - sub-area

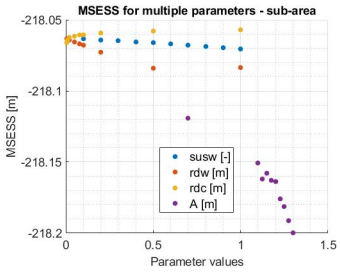

(c) MSESS parameters - sub-area

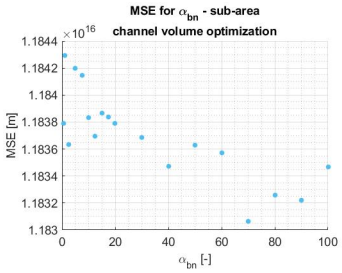

(a) MSE α_{bn} - channel volume

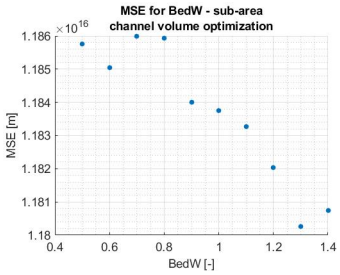

(b) MSE BedW - channel volume

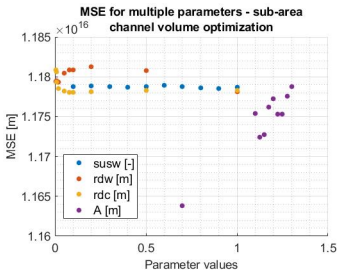

(c) MSE parameters - channel volume

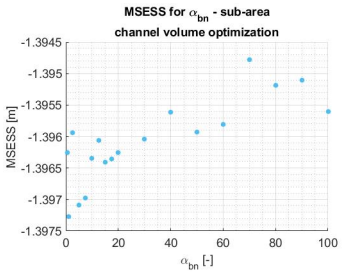

(a) MSESS α_{bn} - channel volume

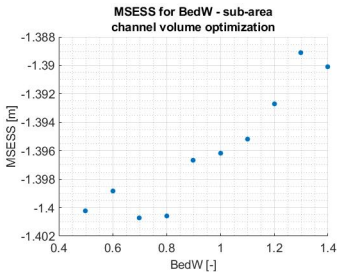

(b) MSESS BedW - channel volume

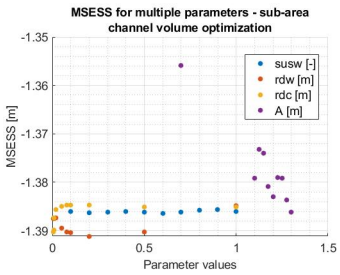

(c) MSESS parameters - channel volume

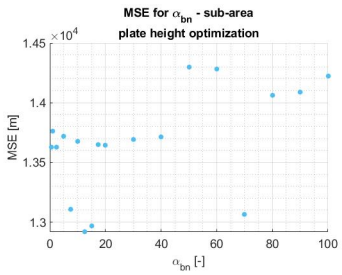

(a) MSE α_{bn} - plate height

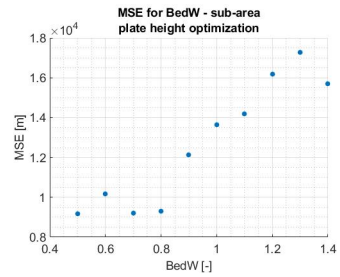

(b) MSE BedW - plate height

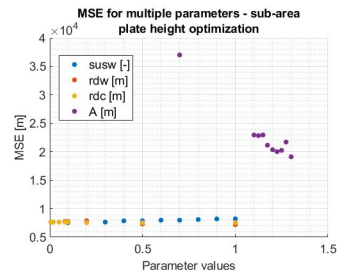

(c) MSE parameters - plate height

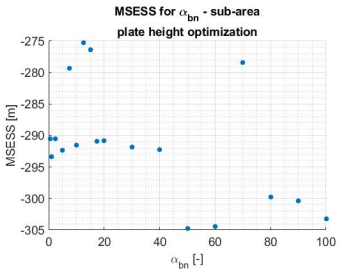

(a) MSESS α_{bn} - plate height

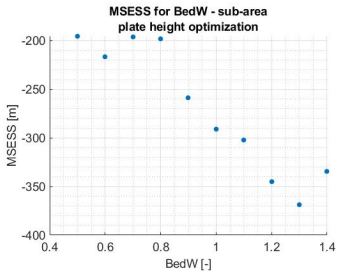

(b) MSESS BedW - plate height

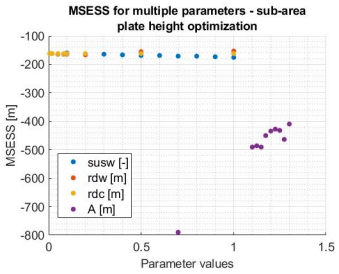

(c) MSESS parameters - plate height

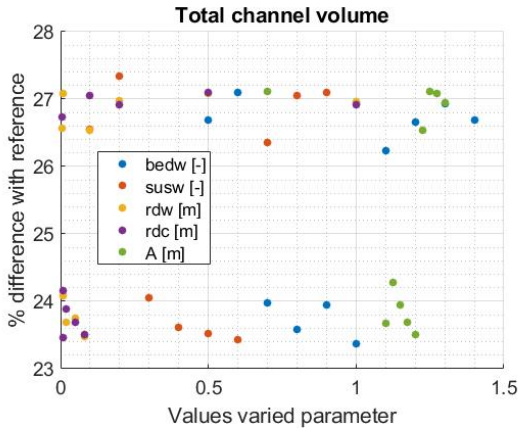

(a) Difference multiple parameters - total channel volume

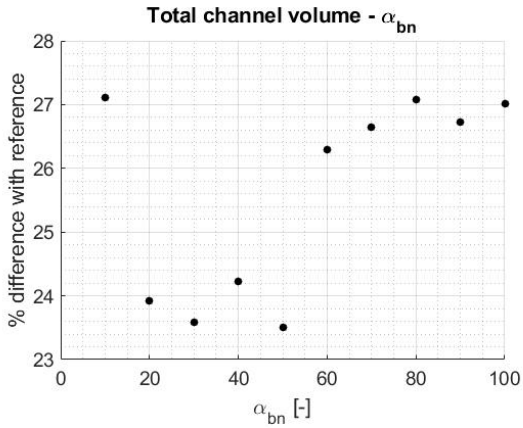

(b) Difference α_{bn} - total channel volume

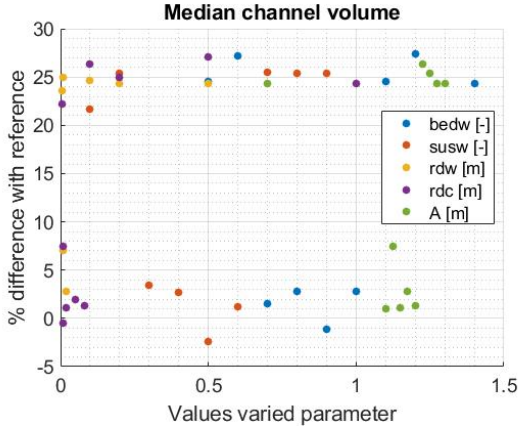

(a) Difference multiple parameters - median channel volume

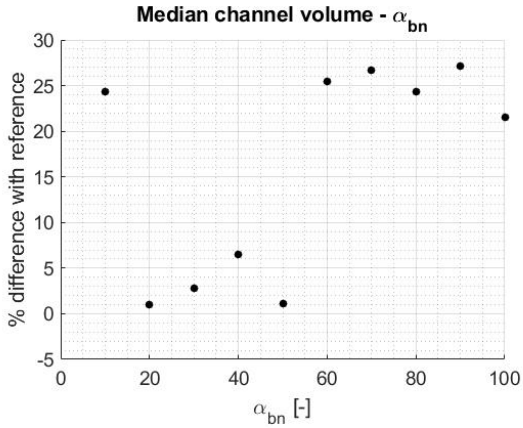

(b) Difference α_{bn} - median channel volume

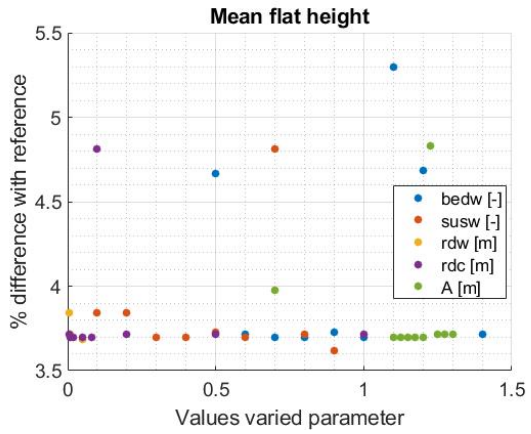

(a) Difference multiple parameters - mean plate height

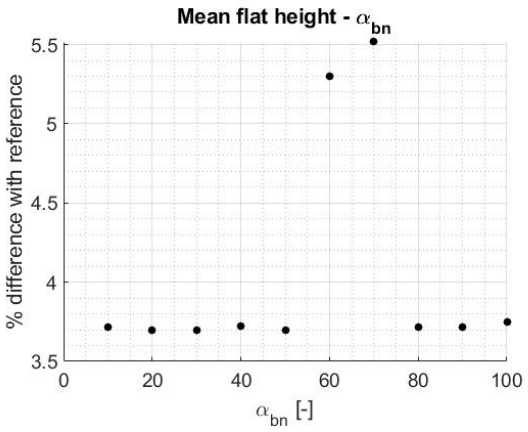

(b) Difference α_{bn} - mean plate height

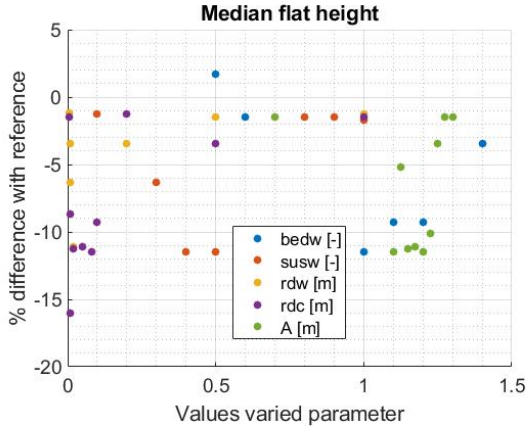

(a) Difference multiple parameters - median plate height

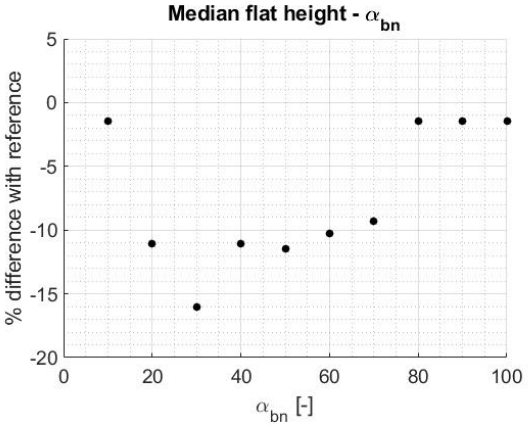

(b) Difference α_{bn} - median plate height

B

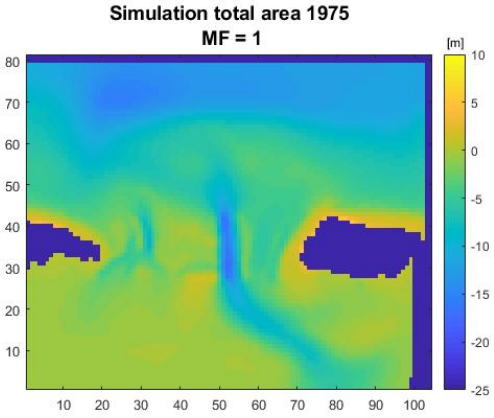

(a) MF=1, total area

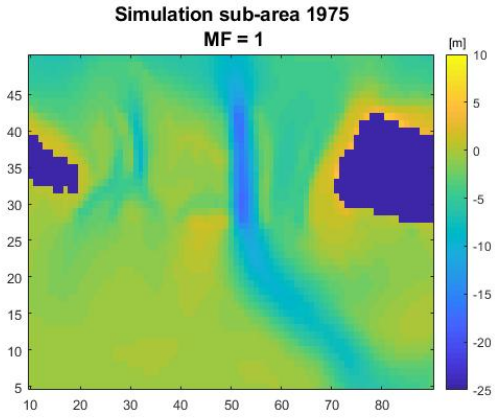

(b) MF=1, sub-area

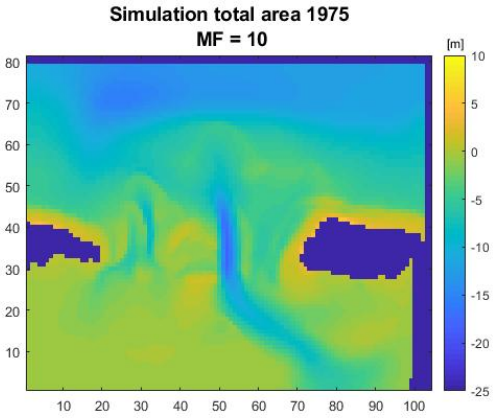

(a) MF=10, total area

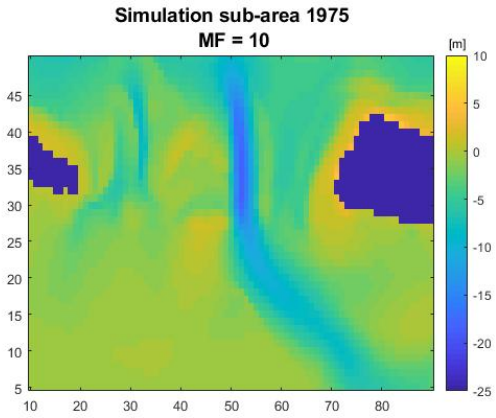

(b) MF=10, sub-area

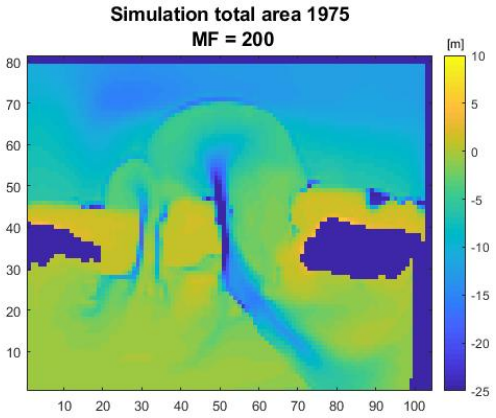

(a) MF=200, total area

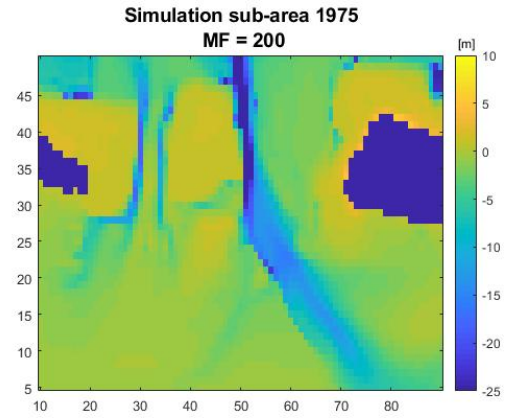

(b) MF=200, sub-area

C

Name	Abbreviation	Reference run	Range
Current related roughness	RDC	0.01	0.005 0.008 0.01 0.02 0.05 0.08 0.1 0.2 0.5 1
Wave related roughness	RDW	0.02	0.005 0.008 0.01 0.02 0.05 0.08 0.1 0.2 0.5 1
Tidal amplitude	A	1.237 m	0.7 m 1.0999 m 1.125 m 1.15 m 1.175 m 1.2 m 1.225 m 1.25 m 1.275 m 1.2999 m

Table C.1: Parameter names and their abbreviations (1/2)

Name	Abbreviation	Reference run	Range
Wave-related suspended load sediment transport factor	SusW	0.3	0.1 0.2 0.3 0.4 0.5 0.6 0.7 0.8 0.9 1
Wave-related bedload sediment transport factor	BedW	1	0.5 0.6 0.7 0.8 0.9 1 1.1 1.2 1.3 1.4
Transverse bedload slope	αb_n	1.5	0.5 1 2.5 5 7.5 10 12.5 15 17.5 20 30 40 50 60 70 80 90 100

Table C.2: Parameter names and their abbreviations (2/2)